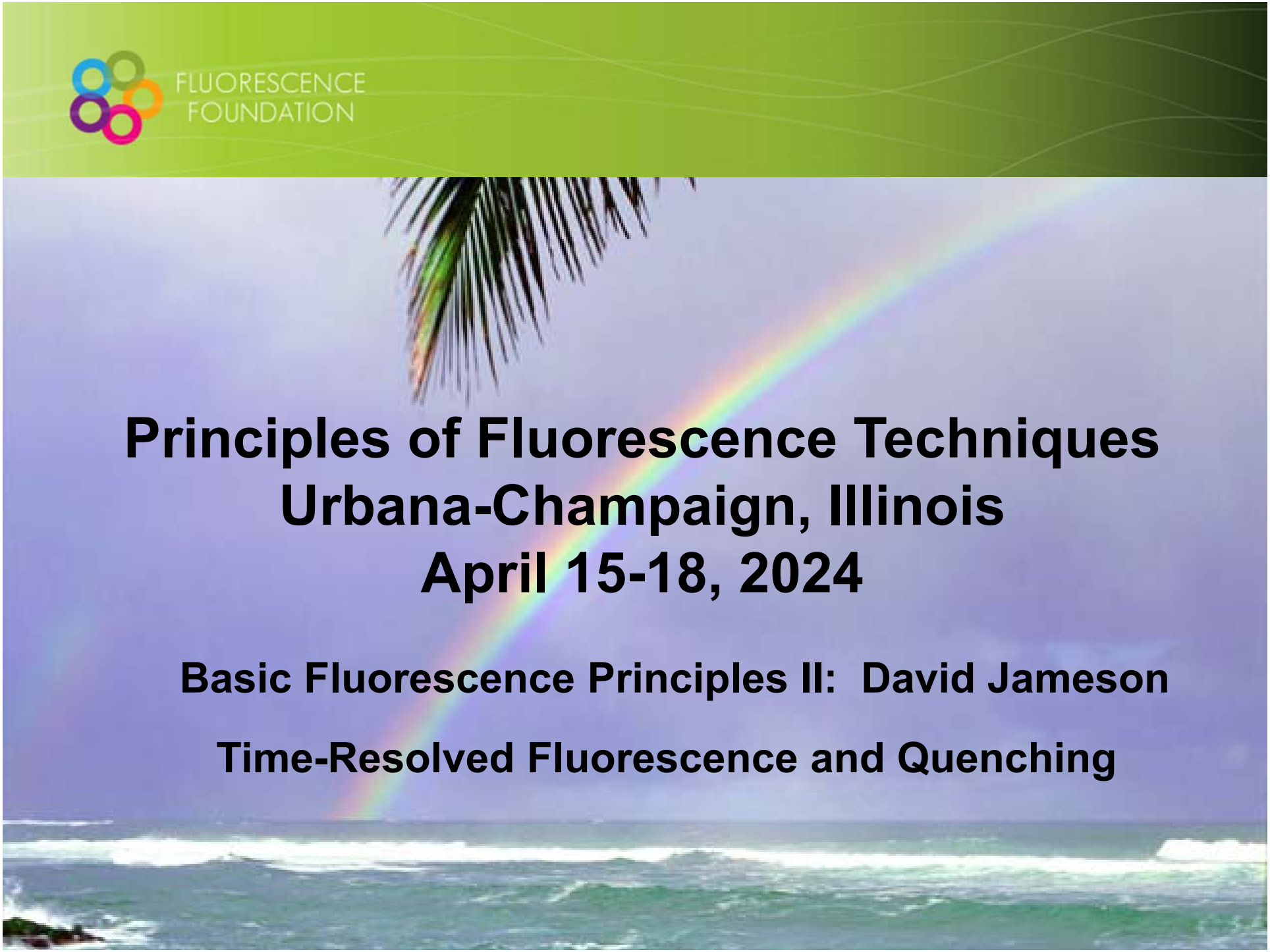


# Principles of Fluorescence Techniques
# Urbana-Champaign, Illinois
# April 15-18, 2024

## Basic Fluorescence Principles II: David Jameson

## Time-Resolved Fluorescence and Quenching

# Why do lifetime measurements?

Fluorescence intensity measurements are “extensive” which means that they depend upon instrumentation parameters and the concentration of the fluorophore.

Fluorescence lifetimes are “intensive” which means that they do not depend on instrumentation parameters or the concentration of the fluorophore.

This “intensive” property is extremely important for many *in vivo* measurements as you will learn.

Many fluorescence intensity based assays, e.g., for calcium ions, pH, etc require ratiometric determinations (intensities at two different excitation or emission wavelengths) for quantification. Lifetime data can be used at a single excitation/emission wavelength.

Lifetimes are required to quantify certain types of fluorescence measurements such as anisotropy/polarization, quenching and Förster Resonance Energy Transfer (FRET).

At a more fundamental level, lifetime determinations are often required to understand the photophysics of fluorophores in diverse environments.

**FIGURE 1.6** Painting of George Gabriel Stokes, 1891, by Hubert von Herkomer, from the Royal Society Collection. Downloaded on March 29, 2013 from: http://www.bbc.co.uk/arts/yourpaintings/paintings/george-stokes-18191903-216241/

**Since the seminal paper by Stokes, which contained the first true understanding of the fluorescence phenomenon, there has been curiosity about the duration of fluorescence, i.e., the fluorescence lifetime.**

XXX. *On the Change of Refrangibility of Light.* *By* G. G. Stokes, *M.A., F.R.S., Fellow of Pembroke College, and Lucasian Professor of Mathematics in the University of Cambridge.*

Received May 11,—Read May 27, 1852.

224. But by far the most striking point of contrast between the two phenomena, consists in the apparently instantaneous commencement and cessation of the illumination, in the case of internal dispersion, when the active light is admitted and cut off. There is nothing to create the least suspicion of any appreciable duration in the effect. When internal dispersion is exhibited by means of an electric spark, it appears no less momentary than the illumination of a landscape by a flash of lightning. I have not attempted to determine whether any appreciable duration could be made out by means of a revolving mirror.

*The Time Interval between Absorption and Emission of Light in Fluorescence.*

By R. W. Wood, For. Mem. R.S., Johns Hopkins University, Baltimore.

(Received June 12, 1921.)

Some experiments were then made at the University of Wisconsin, in collaboration with Prof. C. E. Mendenhall, during my visit to Madison in December. We used a high pressure, six-cylinder pump, and obtained a jet velocity of about 200 metres per second, with a fine glass nozzle about 0·2 mm. in diameter. More recently, Prof. Mendenhall has increased the velocity to 230 metres per second, and, by blackening one side of the jet tube, leaving a small clear space for the entrance of the sunlight, has assured himself that there is no displacement as great as 0·1 mm. (observing the fluorescent patch with a short-focus lens). This means that the duration of the fluorescence is less than 1/2,300,000 second.

*The Time Interval between Absorption and Emission of Light in Fluorescence.*

lem. R.S., Johns Hopkins University, Baltimore.

(Received June 12, 1921.)

Some experiments were niversity of Wisconsin, in collaboration with Prof. C. ng my visit to Madison in December. We used a high der pump, and obtained a jet velocity of about 200 metres h a fine glass nozzle about 0·2 mm. in diameter. More re lendenhall has increased the velocity to 230 metres per seco blackening one side of the jet tube, leaving a small clear spac ntrance of the sunlight, has assured himself that there is no di as great as 0·1 mm. (observing the fluorescent patch with a short-f ). This means that the duration of the fluorescence is less than 1/2,3 second.

*The Time Interval between Absorption and Emission of Light in Fluorescence.*

By R. W. Wood, For. Mem. R.S., Johns Hopkins University, Baltimore.

(Received June 12, 1921.)

Some experiments were then made at the University of Wisconsin, in collaboration with Prof. C. E. Mendenhall, during my visit to Madison in December. We used a high pressure, six-cylinder pump, and obtained a jet velocity of about 200 metres per second, with a fine glass nozzle about 0·2 mm. in diameter. More recently, Prof. Mendenhall has increased the velocity to 230 metres per second, and, by blackening one side of the jet tube, leaving a small clear space for the entrance of the sunlight, has assured himself that there is no displacement as great as 0·1 mm. (observing the fluorescent patch with a short-focus lens). This means that the duration of the fluorescence is less than 1/2,300,000 second.

i.e. < 435ns

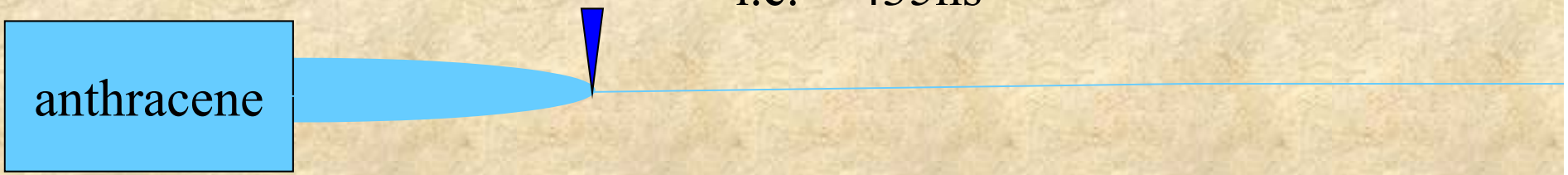

This work was followed by a report by Philip Gottling in 1923 who used a Kerr Cell – as originally suggested by Lord Rayleigh in 1905.

# THE DETERMINATION OF THE TIME BETWEEN EXCITATION AND EMISSION FOR CERTAIN FLUORESCENT SOLIDS

By Philip F. Gottling

Abstract

**Time lag between excitation and emission of fluorescence by barium platino-cyanide and rhodamine.**—The work begun in 1921 by R. W. Wood on the measurement of fluorescent intervals and phosphorescent times has been continued. The method of Abraham and Lemoine, somewhat modified, was used for determining the very short periods of time involved. The fluorescent light is polarized and then passed through a condenser, containing nitrobenzene as dielectric, which had begun to be discharged when the illuminating spark started. The later the light arrives the lower the average field of the condenser and the smaller the angular setting of the analyzing nicol to match the two images produced by a double image prism. The apparatus was calibrated by means of light reflected from a mirror at different distances from the spark. The interval of time between the occurrence of a spark and the emission of the fluorescent light excited by that spark, was found to be $(2.12 \pm .01) \times 10^{-7}$ sec. for barium platino-cyanide and $(2.11 \pm .14) \times 10^{-8}$ sec. for rhodamine.

He found 21.1 ns for a solution of rhodamine in acetone, acetic acid and glycerol. Possibly he was observing a combination of fluorescence and phosphorescence

Enrique Gaviola

## Ein Fluorometer.
## Apparat zur Messung von Fluoreszenzabklingungszeiten.

Von **E. Gaviola** in Berlin.

Mit 9 Abbildungen. (Eingegangen am 24. März 1927.)

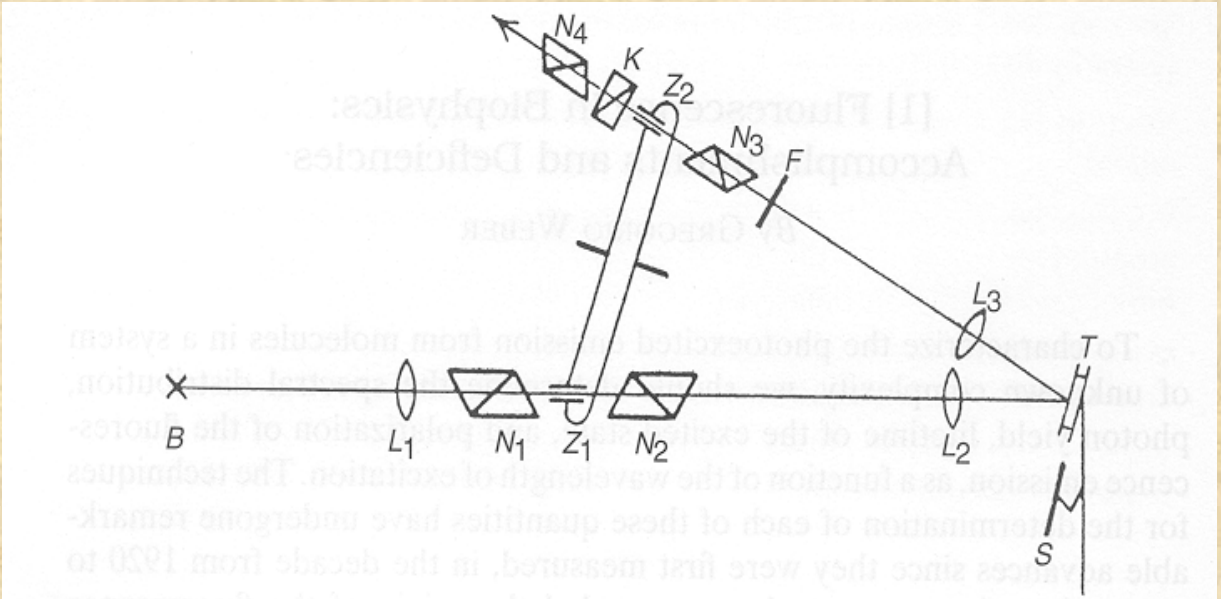


FIG. 1. Original apparatus of Gaviola[1] for the measurement of fluorescence lifetimes, described in text. *B*, Source of exciting light; *T*, cuvette containing the fluorescent solution; *S*, mirror.

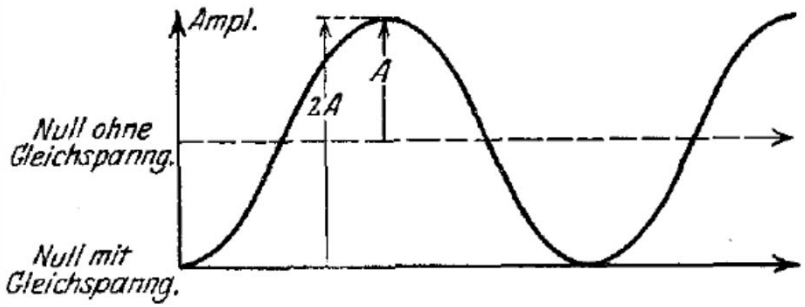


Fig. 7.

| Farbstoff | Abklingungszeiten | | |
|---|---|---|---|
| | in Wasser Sekunden | in Glycerin Sekunden | in Meth.-Alkohol Sekunden |
| Uranin | $4{,}5 \cdot 10^{-9}$ | $4{,}4 \cdot 10^{-9}$ | — |
| Fluorescein | — | — | $5{,}0 \cdot 10^{-9}$ |
| Rhodamin B | $2{,}0 \cdot 10^{-9}$ | $4{,}2 \cdot 10^{-9}$ | — |
| Rhodulin Orange | 2,7 | 4,3 | — |
| Erythrosin | 1,8 | 2,4 | $2{,}6 \cdot 10^{-9}$ |
| Tetrajodfluor. Na | 1,0 | 2,0 | 2,2 |
| Eosin 5 B | 1,9 | — | 3,4 |
| Uranylsulfat | — | — | 1,3 |
| Uranylsulfat in Schwefelsäure | — | — | 1,9 |
| Chinisarin in Pentan | — | — | 2,9 |
| Uranglas | — | — | $>15{,}0$ |
| Rubinkristall | — | — | $>15{,}0$ |

## What is meant by the “lifetime” of a fluorophore???

Although we often speak of the properties of fluorophores as if they are studied in isolation, such is not usually the case.

Absorption and emission processes are almost always studied on *populations* of molecules and the properties of the supposed typical members of the population are deduced from the macroscopic properties of the process.

In general, the behavior of an excited population of fluorophores is described by a familiar rate equation:

$$\frac{dn^*}{dt} = -n^* \Gamma + f(t)$$

where $n^*$ is the number of excited elements at time t, $\Gamma$ is the rate constant of emission and f(t) is an arbitrary function of the time, describing the time course of the excitation . The dimensions of $\Gamma$ are $sec^{-1}$ (transitions per molecule per unit time).

If excitation occurs at t = 0, the last equation, takes the form:

$$\frac{dn^*}{dt} = -n^* \Gamma$$

and describes the decrease in excited molecules at all further times. Integration gives:

$$n^*(t) = n^*(0)\exp(-\Gamma t)$$

The lifetime, $\tau$, is equal to $\Gamma^{-1}$

If a population of fluorophores are excited, the lifetime is the time it takes for the number of excited molecules to decay to 1/e or 36.8% of the original population according to:

$$\frac{n^*(t)}{n^*(0)} = e^{-t/\tau}$$

In pictorial form:

$$\frac{n^*(t)}{n^*(0)} = e^{-t/\tau}$$

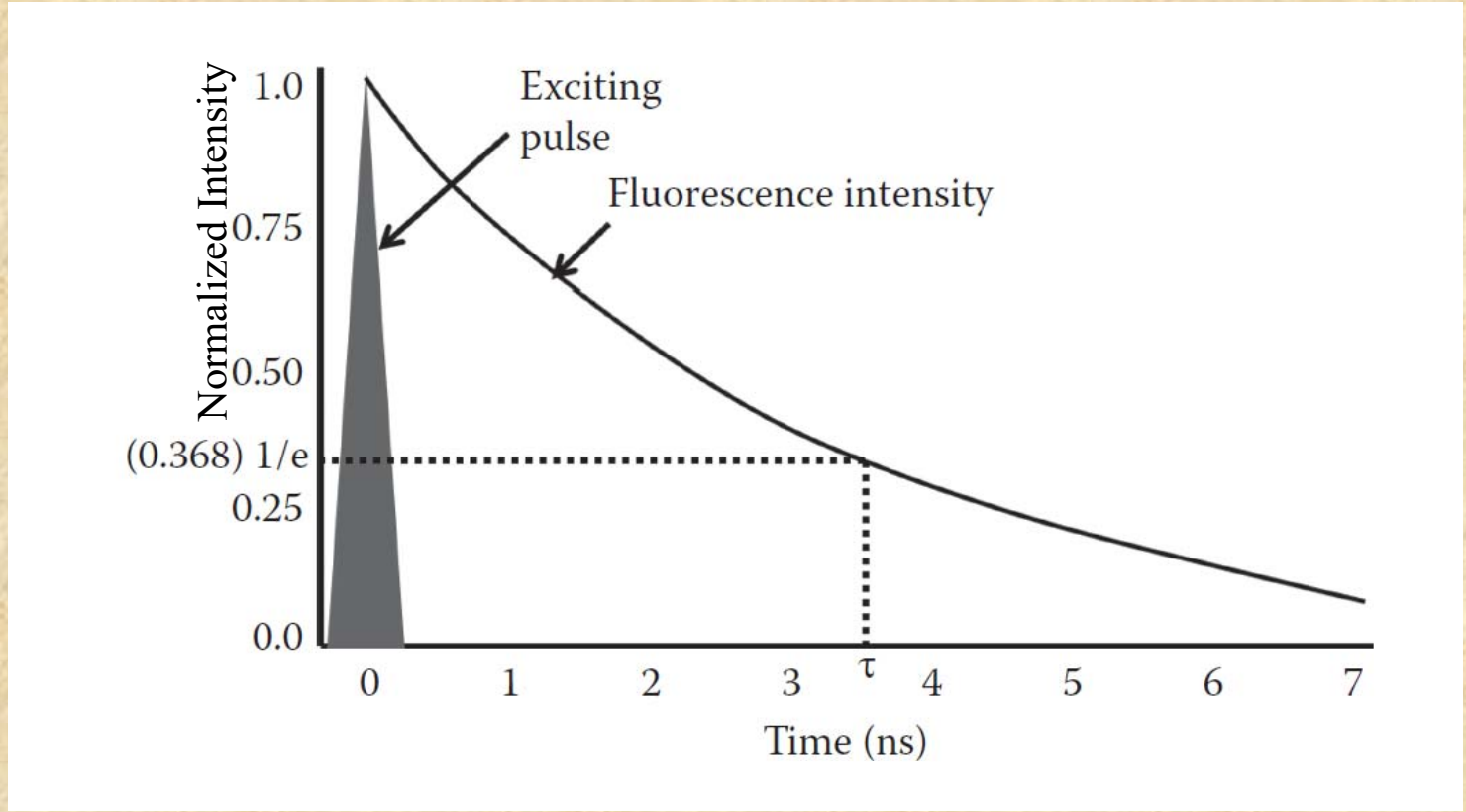

The lifetime and quantum yield for a given fluorophore is often dramatically affected by its environment.

Examples of this fact would be NADH, which in water has a lifetime of ~0.4 ns but bound to dehydrogenases can be a long as 9 ns.

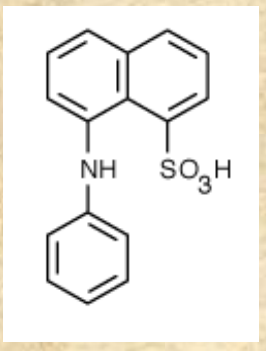


ANS in water is ~100 picoseconds but can be 15 – 20 ns bound to proteins

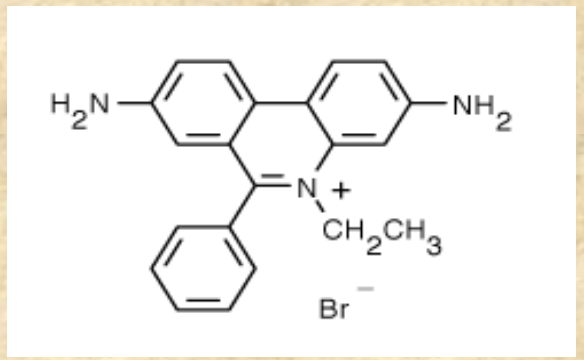


Ethidium bromide is 1.8 ns in water, 22 ns bound to DNA and 27ns bound to tRNA

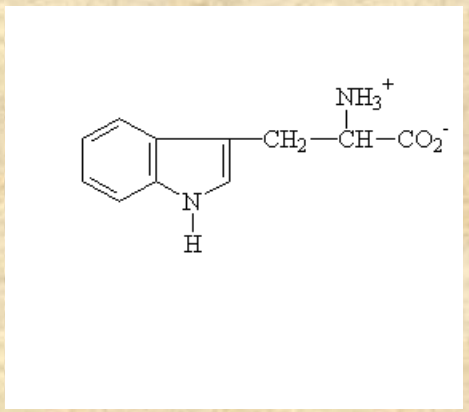


The lifetime of tryptophan in proteins ranges from ~0.1 ns up to ~8 ns

Excited state lifetimes have traditionally been measured using either the *impulse* response or the *harmonic* response method. In principle both methods have the same information content. These methods are also referred to as either the "time domain" method or the "frequency domain" method.

In the *impulse (*or pulse) method, the sample is illuminated with a short pulse of light and the intensity of the emission versus time is recorded. Originally these short light pulses were generated using *flashlamps* which had widths on the order of several nanoseconds. Modern laser sources can now routinely generate pulses with widths on the order of picoseconds or shorter.

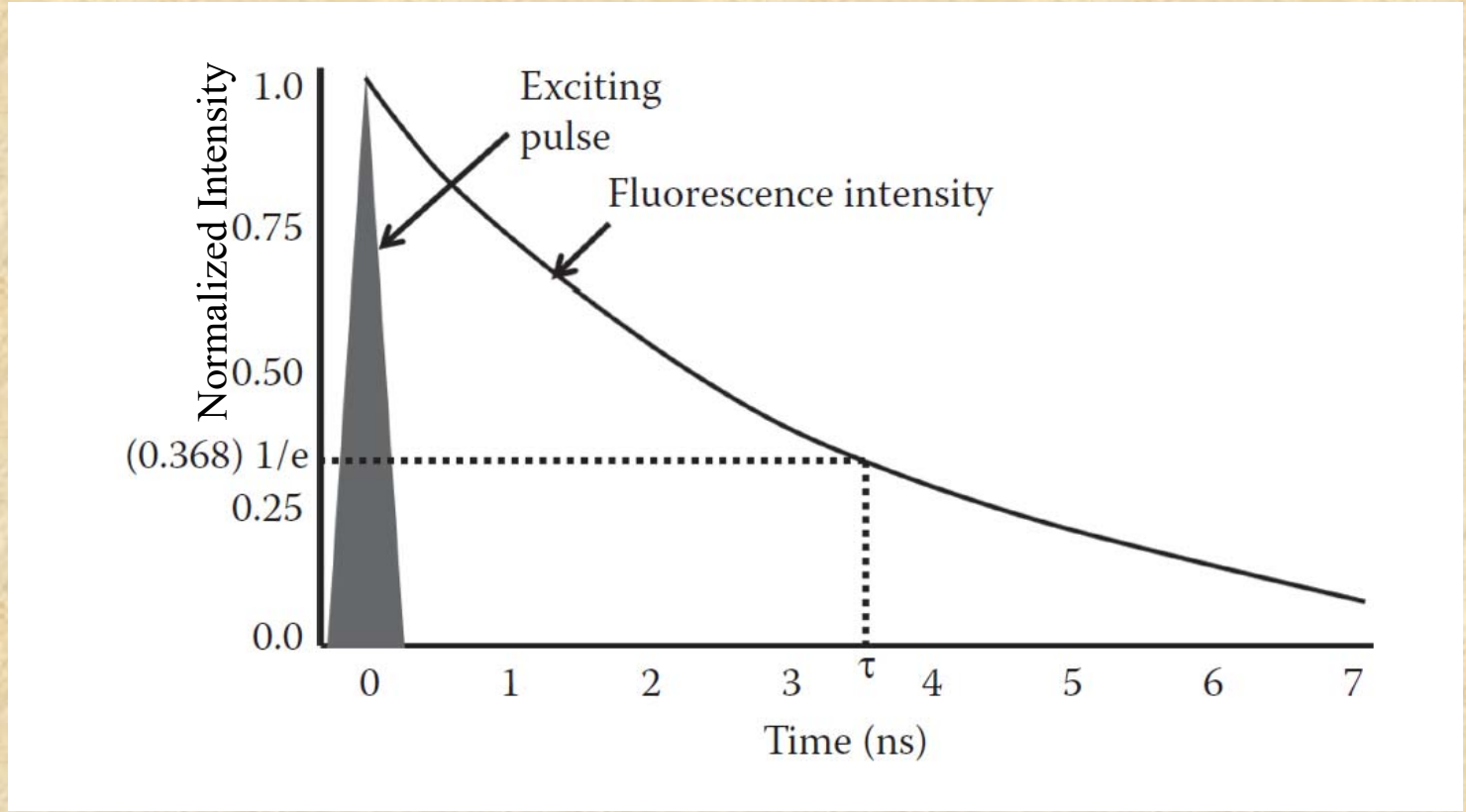

As shown in the intensity decay figure, the *fluorescence* lifetime, t , is the time at which the intensity has decayed to 1/e of the original value. The decay of the intensity with time is given by the relation:

$$I_t = \alpha e^{-t/\tau}$$

Where $I_t$ is the intensity at time t, $\alpha$ is a normalization term (the pre-exponential factor) and $\tau$ is the lifetime.

It is more common to plot the fluorescence decay data using a logarithmic scale as shown here.

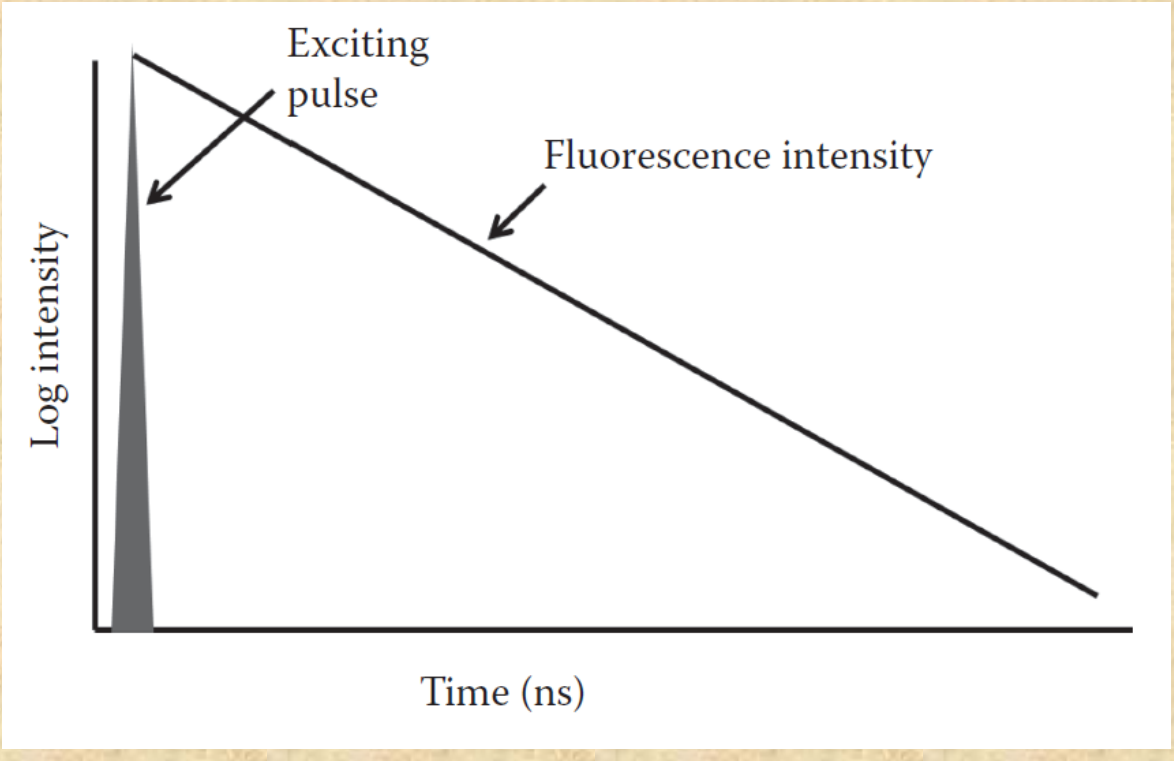

If the decay is a single exponential and if the lifetime is long compared to the exciting light then the lifetime can be determined directly from the slope of the curve.

If the lifetime and the excitation pulse width are comparable some type of *deconvolution* method must be used to extract the lifetime.

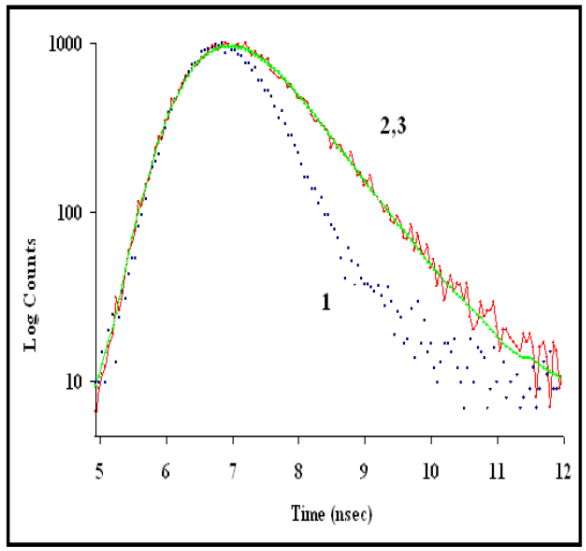


**Figure-3:** Fluorescence decay curves: $H_2$ flash lamp (1), 1H-Benzimidazole (2) and theoretical curve fit (3), in acetonitrile solution.

INTERNATIONAL JOURNAL OF SCIENTIFIC & TECHNOLOGY RESEARCH VOLUME 2, ISSUE 10, OCTOBER 2013

Yaser A. Yousef

Great effort has been expended on developing mathematical methods to “deconvolve” the effect of the exciting pulse shape on the observed fluorescence decay.

With the advent of very fast laser pulses these deconvolution procedures became less important for most lifetime determinations, although they are still required whenever the lifetime is of comparable duration to the light pulse.

If the decay is multiexponential, the relation between the intensity and time after excitation is given by:

$$I(t) = \sum_i \alpha_i e^{-t/\tau_i}$$

One may then observe data such as those sketched below:

Here we can discern at least two lifetime components indicated as $\tau_1$ and $\tau_2$ . This presentation is oversimplified but illustrates the point.

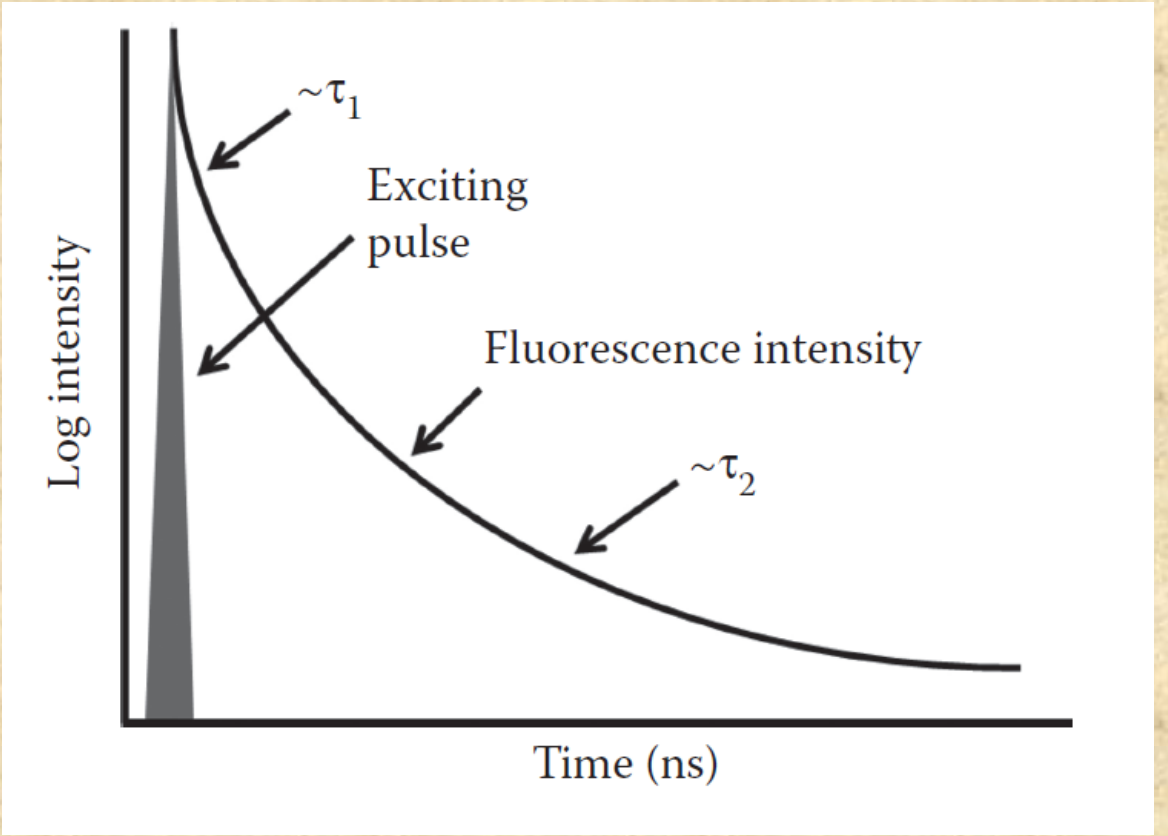

Here are pulse decay data on anthracene in cyclohexane taken on an IBH 5000U Time-correlated single photon counting instrument equipped with an LED short pulse diode excitation source.

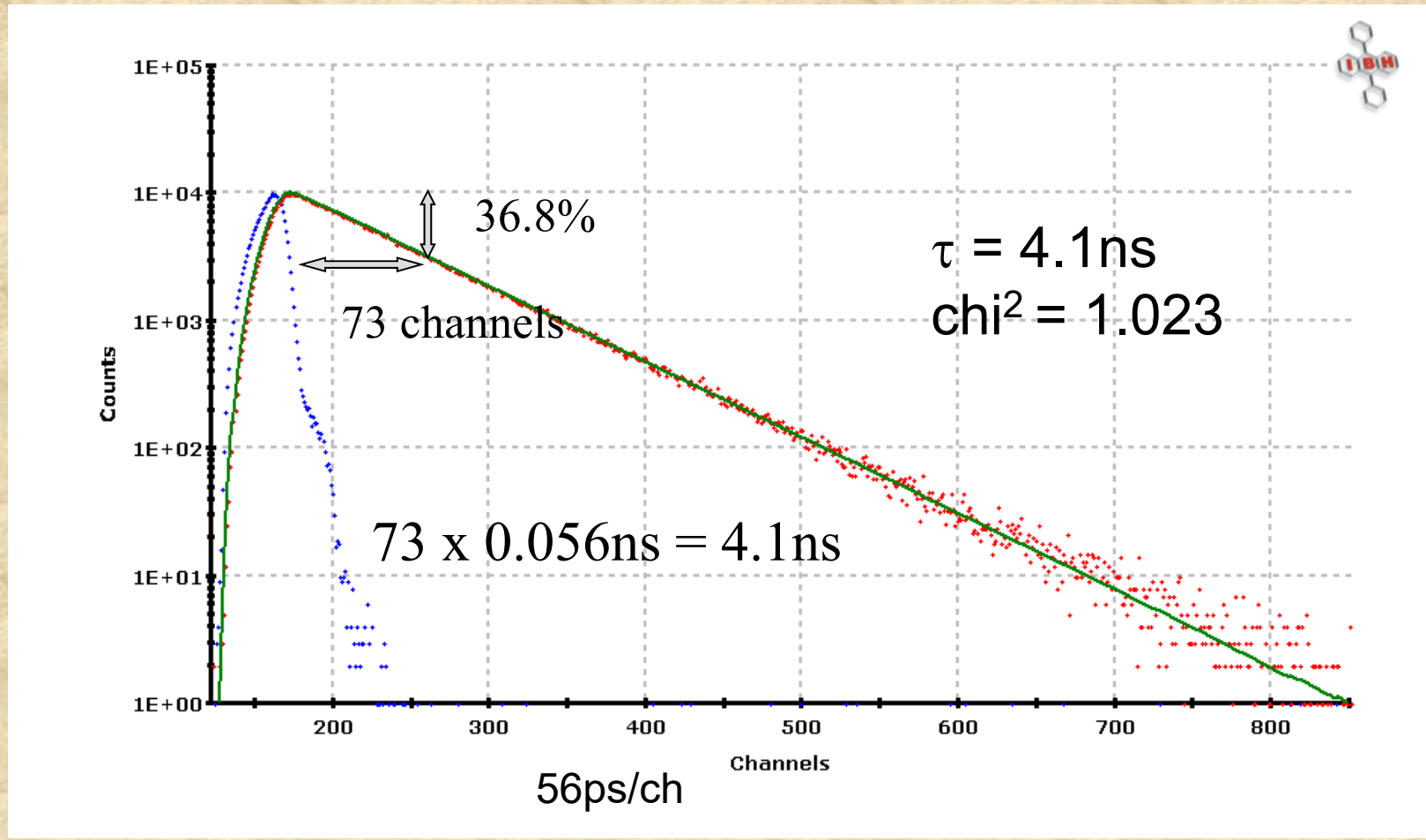


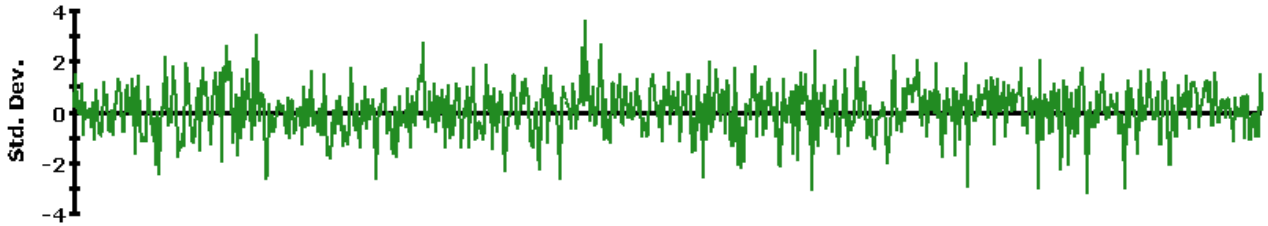

In the harmonic method (also known as the phase and modulation or frequency domain method) a continuous light source is utilized, such as a laser or xenon arc, and the intensity of this light source is modulated sinusoidally at high frequency as depicted below. Typically, an *electro-optic* device, such as a *Pockels cell* is used to modulate a continuous light source, such as a CW laser or a xenon arc lamp. Alternatively, LEDs or laser diodes can be directly modulated.

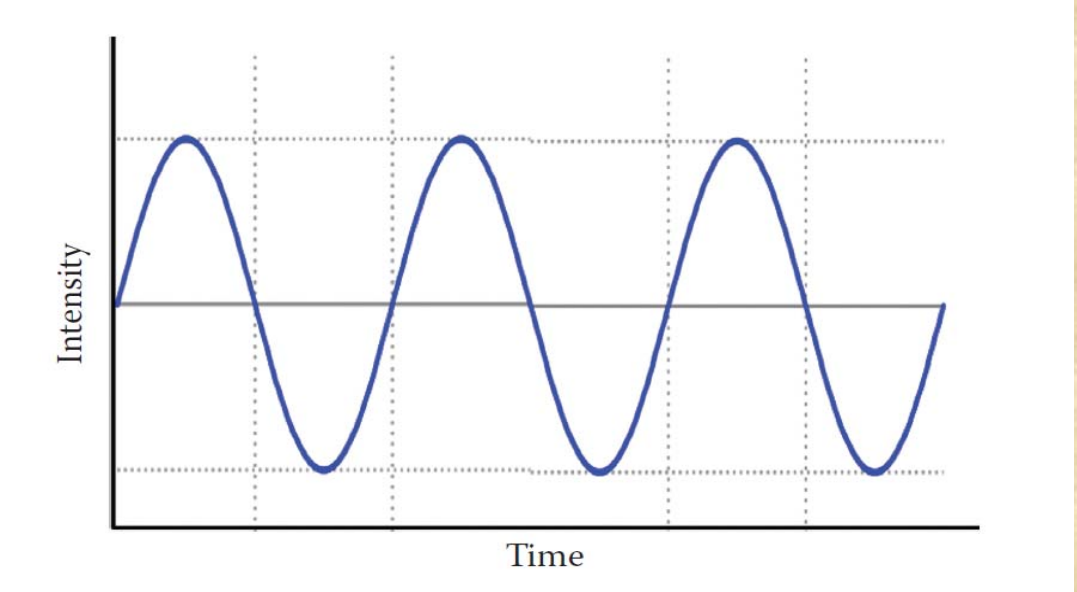


In such a case, the excitation frequency is described by:

$$E(t) = Eo\,[1 + M_E \sin \omega t]$$

E(t) and Eo are the intensities at time t and o, $M_E$ is the modulation factor which is related to the ratio of the AC and DC parts of the signal and $\omega$ is the angular modulation frequency.

$\omega = 2\pi f$ where f is the linear modulation frequency

Due to the persistence of the excited state, fluorophores subjected to such an excitation will give rise to a modulated emission which is shifted in phase relative to the exciting light as depicted below.

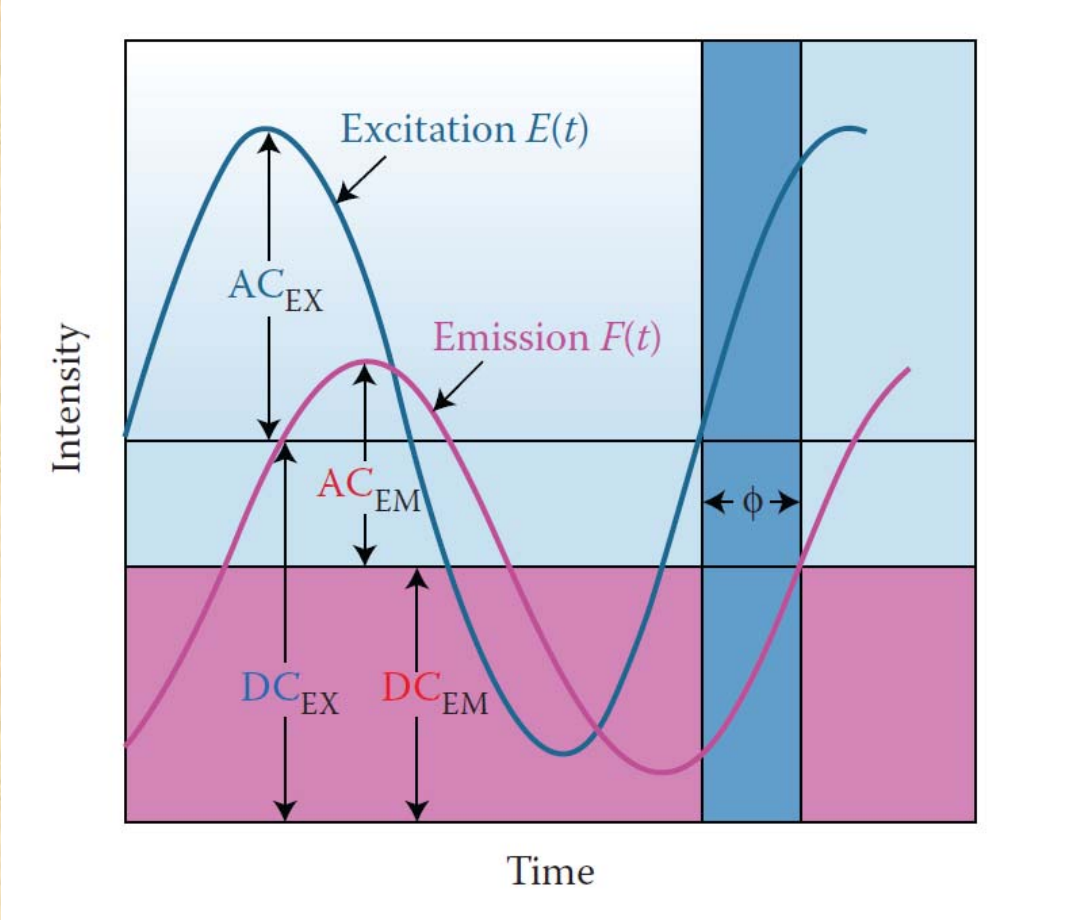


This sketch illustrates the phase delay ($\phi$) between the excitation, E(t), and the emission, F(t). Also shown are the AC and DC levels associated with the excitation and emission waveforms.

One can demonstrate that:

$$\mathbf{F(t) = Fo\,[1 + M_F \sin(\omega t + \phi)]}$$

This relationship signifies that measurement of the phase delay, $\phi$, forms the basis of one measurement of the lifetime, $\tau$. In particular one can demonstrate that:

$$\mathbf{\tan \phi = \omega\tau}$$

The *modulations* of the excitation ($M_E$) and the emission ($M_F$) are given by:

$$M_E = \left(\frac{AC}{DC}\right)_E \quad \text{and} \quad M_F = \left(\frac{AC}{DC}\right)_F$$

The *relative modulation*, M, of the emission is then:

$$M = \frac{(AC/DC)_F}{(AC/DC)_E}$$

$\tau$ can also be determined from M according to the relation: $M = \dfrac{1}{\sqrt{1+(\omega\tau)^2}}$

Using the *phase shift* and *relative modulation* one can thus determine a *phase lifetime* ($\tau_P$) and a *modulation lifetime* ($\tau_M$).

If the fluorescence decay is a single exponential, then $\tau_P$ and $\tau_M$ will be equal at all modulation frequencies.

If, however, the fluorescence decay is multiexponential then $\tau_P < \tau_M$ and, moreover, the values of both $\tau_P$ and $\tau_M$ will depend upon the modulation frequency, i.e.,

$$\tau_P(\omega_1) < \tau_P(\omega_2) \quad \text{if} \quad \omega_1 > \omega_2$$

To get a feeling for typical phase and modulation data, consider the following data set.

| Frequency (MHz) | $\tau_P$ (ns) | $\tau_M$ (ns) |
|---|---|---|
| 5 | 6.76 | 10.24 |
| 10 | 6.02 | 9.70 |
| 30 | 3.17 | 6.87 |
| 70 | 1.93 | 4.27 |

These differences between $\tau_P$ and $\tau_M$ and their frequency dependence form the basis of the methods used to analyze for lifetime heterogeneity, i.e., the component lifetimes and amplitudes.

In the case just shown, the actual system being measured was a mixture of two fluorophores with lifetimes of 12.08 ns and 1.38 ns, with relative contributions to the total intensity of 53% and 47% respectively.

Here must must be careful to distinguish the term *fractional contribution to the total intensity* (usually designated as f) from $\alpha$, the pre-exponential term referred to earlier. The relation between these two terms is given by:

$$f_i = \frac{\alpha_i \tau_i}{\sum_j \alpha_j \tau_j}$$

where j represents the sum of all components. In the case just given then, the ratio of the pre-exponential factors corresponding to the 12.08 ns and 1.38 ns components is approximately 1/8. In other words, there are eight times as many molecules in solution with the 1.38 ns lifetime as there are molecules with the 12.08 ns lifetime.

Multifrequency phase and modulation data are usually presented as shown below:

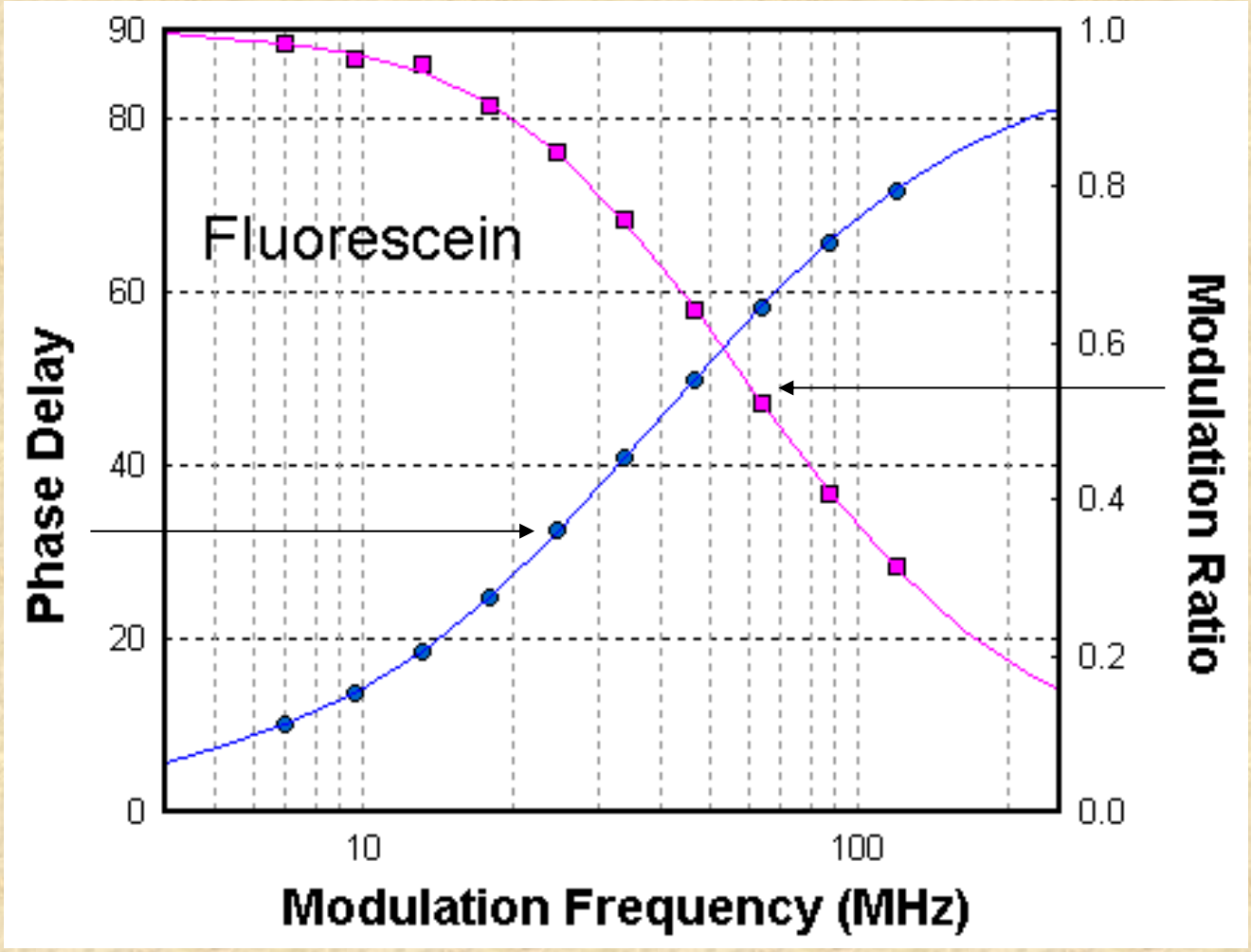


The plot shows the frequency response curve (phase and modulation) of Fluorescein in phosphate buffer pH 7.4 acquired on an ISS Chronos using a 470 nm LED. The emission was collected through a 530 high pass filter. The data is best fitted by a single exponential decay time of 4 ns.

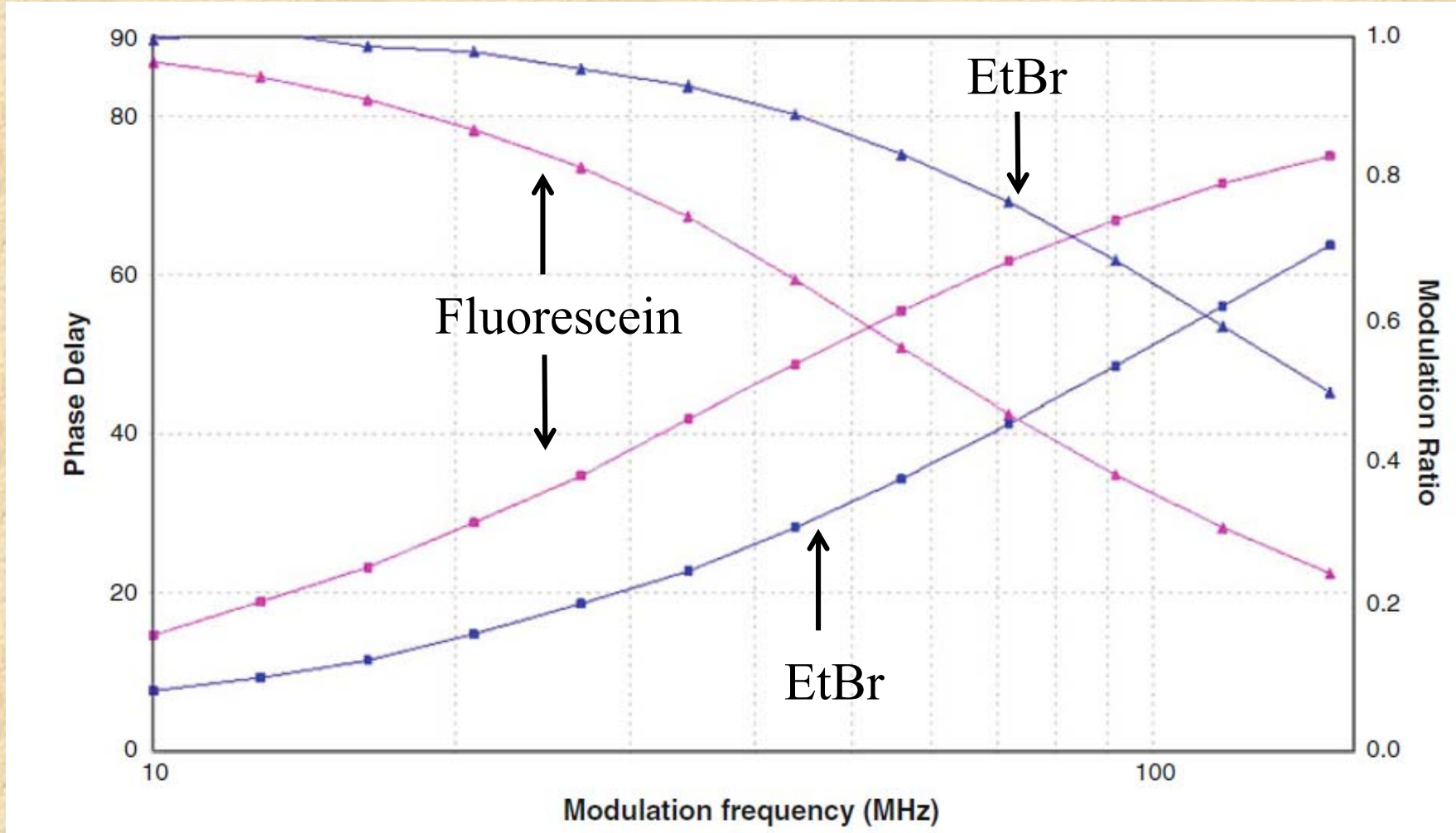


**Fig. 4** Phase (*square*) and modulation (*triangle*) plot of fluorescein and ethidium bromide

Fluorescein (NaOH) – 4.05 ns Ethidium Bromide (water) – 1.71 ns

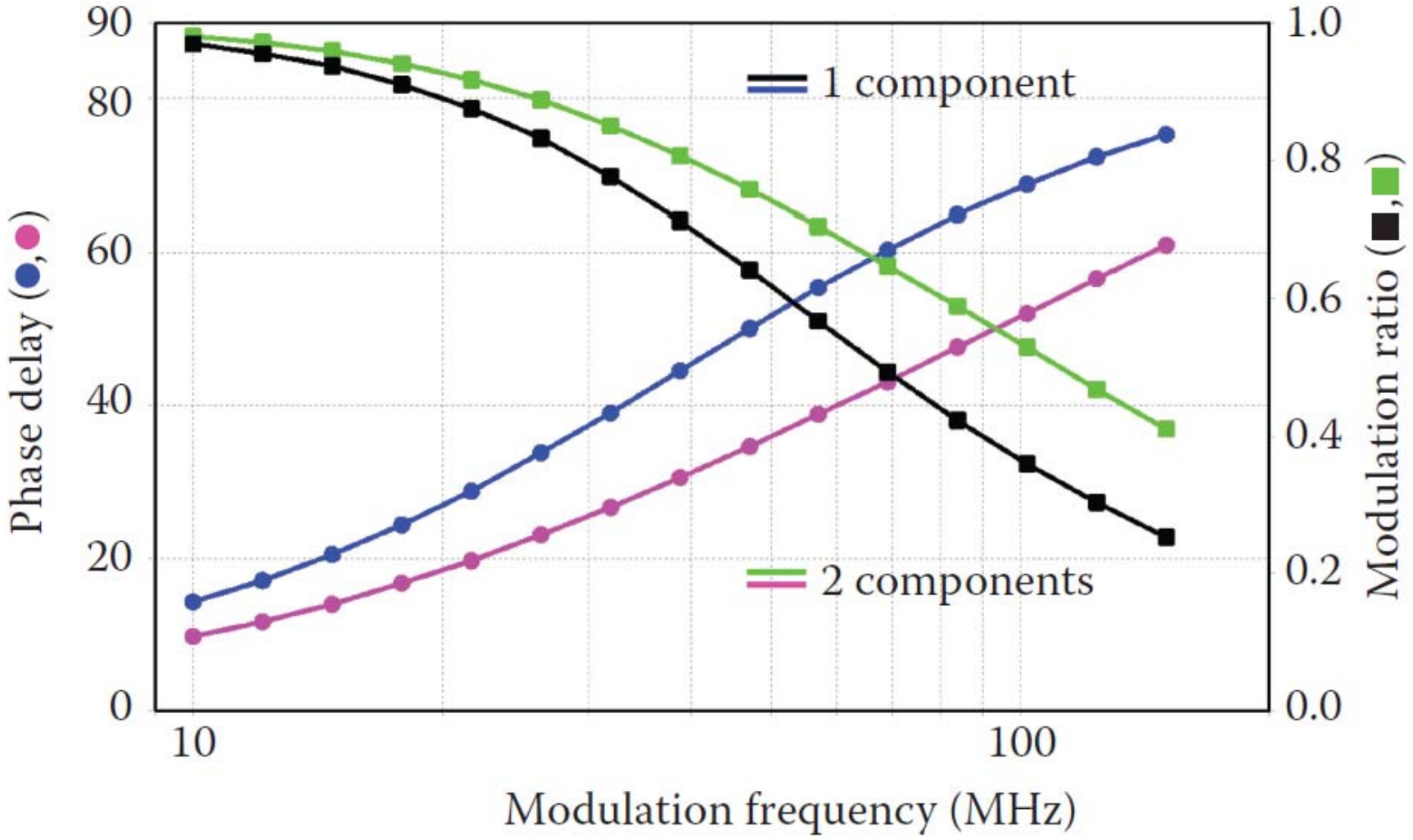


**FIGURE 6.8** Simulation of phase and modulation data for a one-component system ($\tau = 4.05$ ns) and a two-component system ($\tau_1 = 4.05$ ns, $f_1 = 0.5$; $\tau_2 = 1.0$ ns, $f_2 = 0.5$). (I thank Carissa Vetromile for this figure.)

# Frequency domain data can also be acquired using the harmonic content of pulsed sources

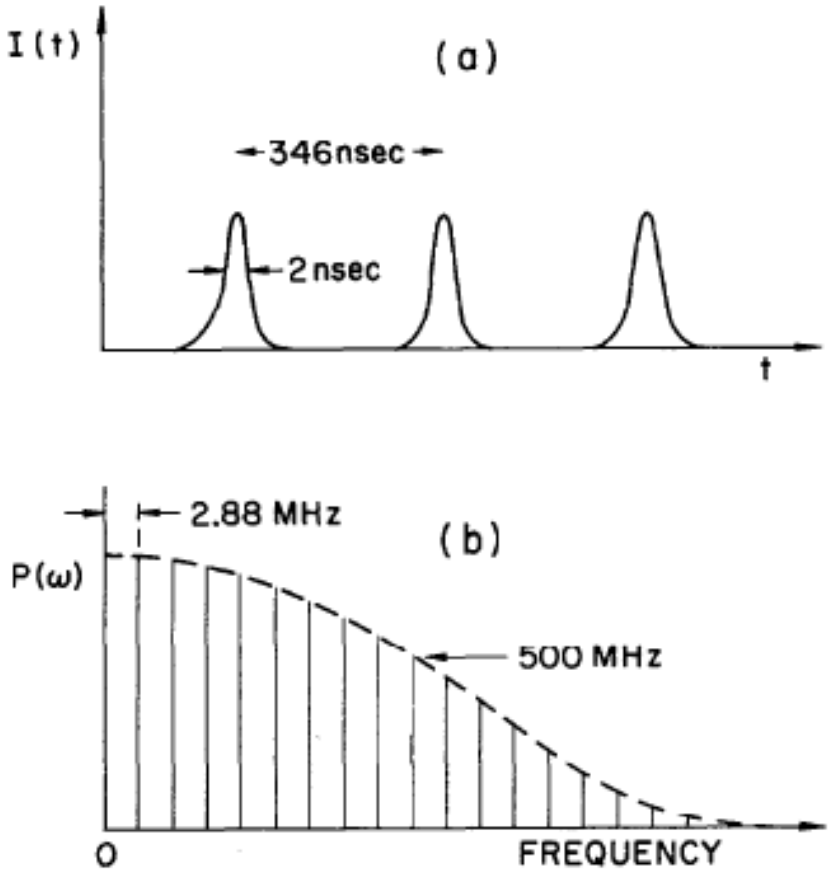


FIG. 2. (a) Schematic representation of the light pulses emitted by the storage ring operating in the single-bunch mode. (b) The power spectrum of the pulse train shown in (a).

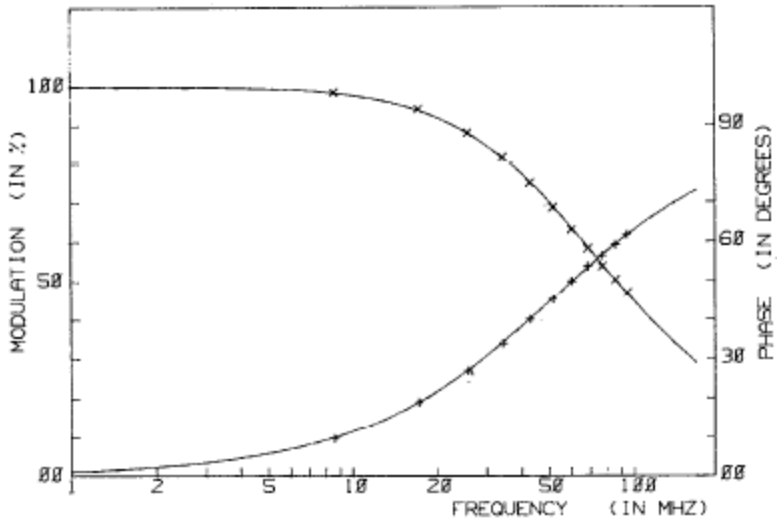


FIG. 9. Multifrequency phase (+) and modulation (×) data for tryptophan at 20°C $p$H = 6.9. Solid lines correspond to the best fit using two exponential components: $\tau_1 = 3.106 \pm 0.013$ ns, $\tau_2 = 9.00$ ns, and $f_1 = 0.968 \pm 0.005$.

Rev. Sci. Instrum. 55 (4), April 1984

N. Boens, W. Qin, N. Basarić, J. Hofkens, M. Ameloot, J. Pouget, J.P. Lefèvre et al. 2007 Fluorescence lifetime standards for time and frequency domain fluorescence spectroscopy. *Anal Chem.* 79: 2137–2149.

| Fluorophore | Solvent | FD Lifetime (ns) | TD Lifetime (ns) |
|---|---|---|---|
| Anthracene | MeOH | 5.00 | 5.20 |
| | Cyclohexane | 5.32 | 5.32 |
| 9-Cyanoanthracene | MeOH | 15.29 | 16.27 |
| | Cyclohexane | 12.39 | 13.47 |
| 9,10-Diphenylanthracene | MeOH | 8.71 | 8.77 |
| | Cyclohexane | 7.17 | 7.76 |
| *N*-methylcarbazole | Cyclohexane | 14.06 | 14.15 |
| Coumarin 153 | MeOH | 4.18 | 4.33 |
| Erythrosine B | Water | 0.090 | 0.089 |
| | MeOH | 0.45 | 0.48 |
| NATA | Water | 3.14 | 3.01 |
| POPOP | Cyclohexane | 1.12 | 1.12 |
| PPO | MeOH | 1.63 | 1.66 |
| | Cyclohexane | 1.35 | 1.38 |
| Rhodamine B | Water | 1.73 | 1.75 |
| | MeOH | 2.48 | 2.44 |
| Rubrene | MeOH | 9.79 | 9.97 |
| *N*-(3-sulfopropyl) acridinium | Water | 30.90 | 31.37 |
| *p*-Terphenyl | MeOH | 1.10 | 1.20 |
| | Cyclohexane | 0.96 | 1.00 |

In addition to decay analysis using discrete exponential decay models, one may also choose to fit the data to *distribution* models. In this case, it is assumed that the excited state decay characteristics of the emitting species actually results in a large number of lifetime components. Shown below is a typical lifetime distribution plot for the case of single tryptophan containing protein – human serum albumin.

The distribution shown here is Lorentzian but depending on the system different types of distributions, e.g., Gaussian or asymmetric distributions, may be utilized. This approach to lifetime analysis is described in: Alcala, J. R., E. Gratton and F. G. Prendergast. Fluorescence lifetime distributions in proteins. *Biophys. J. 51*, 597-604 (1987).

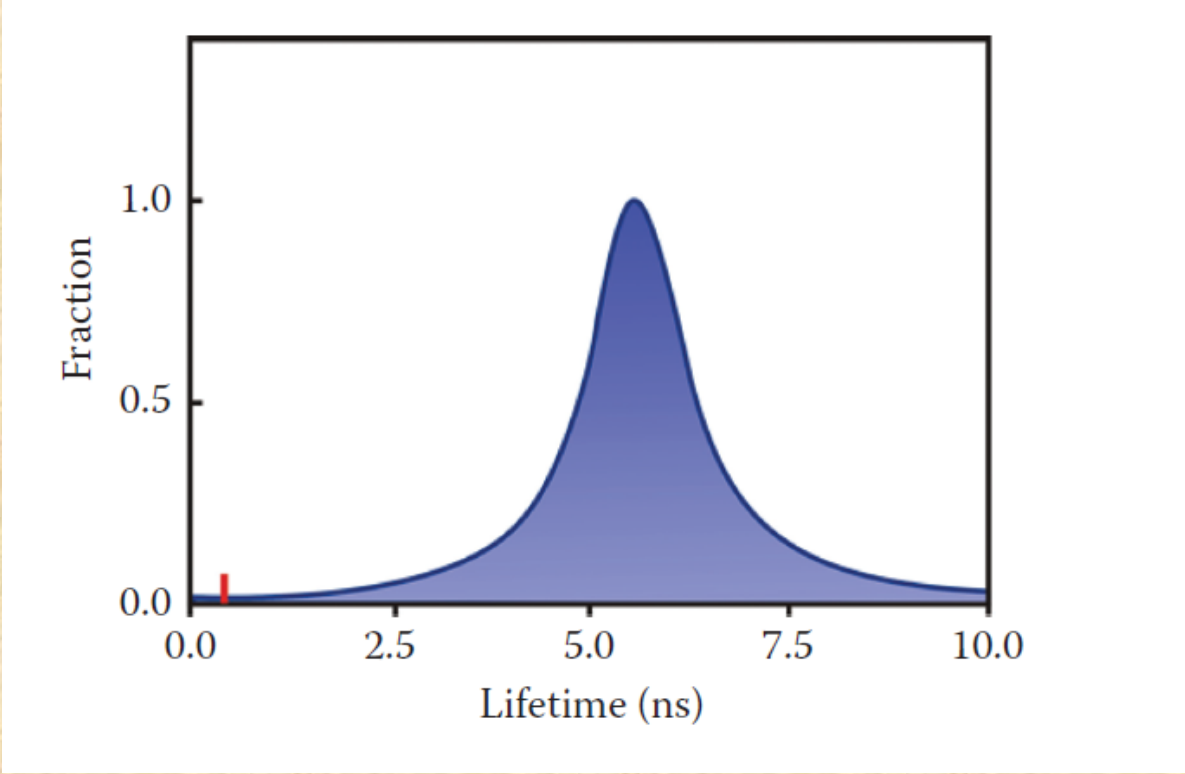

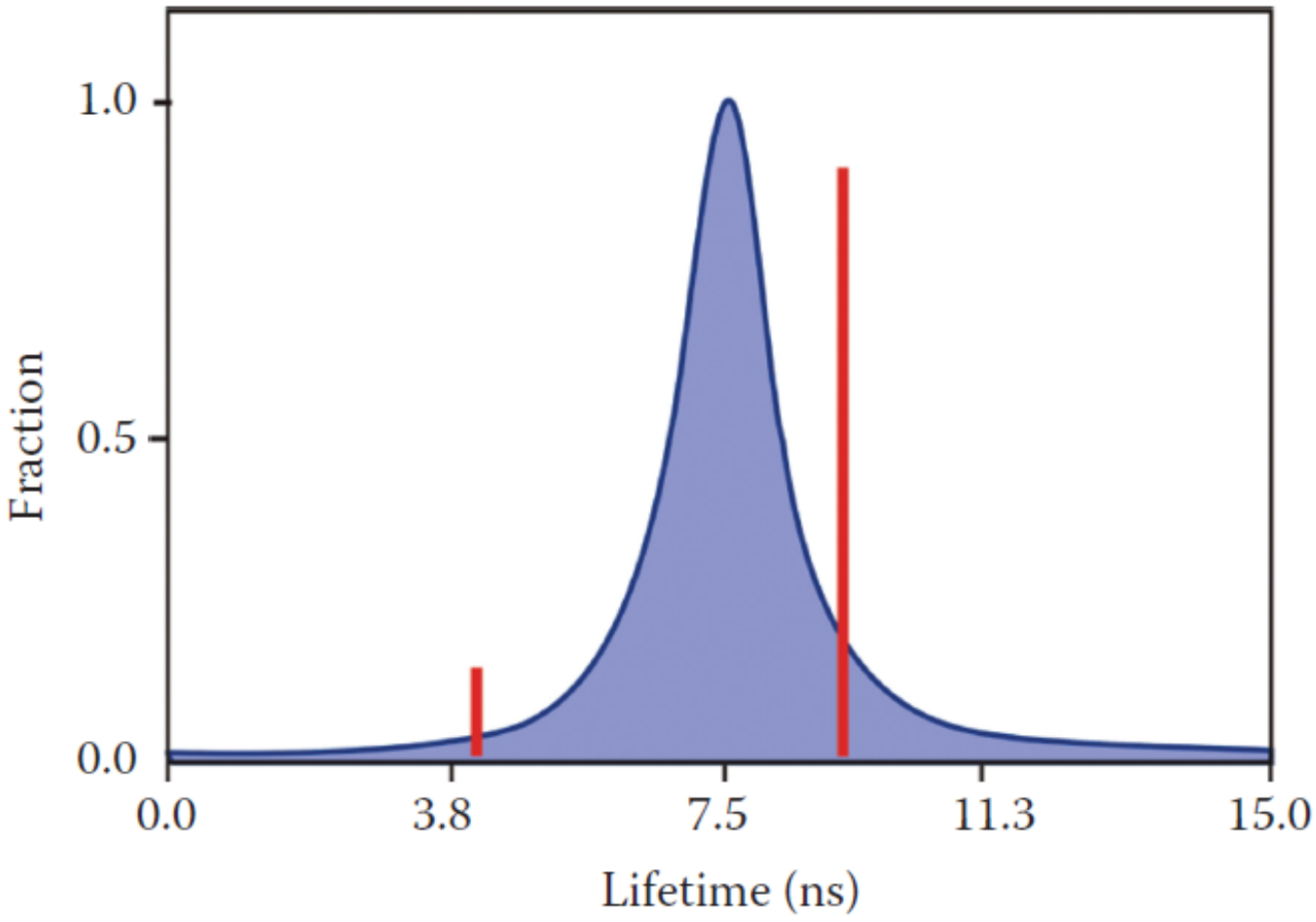


**FIGURE 6.10** Comparison of discrete (red) and distribution (blue) lifetime analyses for mant-GDP bound to N-Ras protein P21. Both approaches give similar chi-square values. (Modified from D.M. Jameson and T.L. Hazlett 1991. *Biophysical and Biochemical Aspects of Fluorescence Spectroscopy*, pp. 105–133. Plenum Press, New York.)

Another popular lifetime analysis method – based on Information Theory - is the *Maximum Entropy Method* (MEM). In this method no *a priori* intensity decay model is assumed.

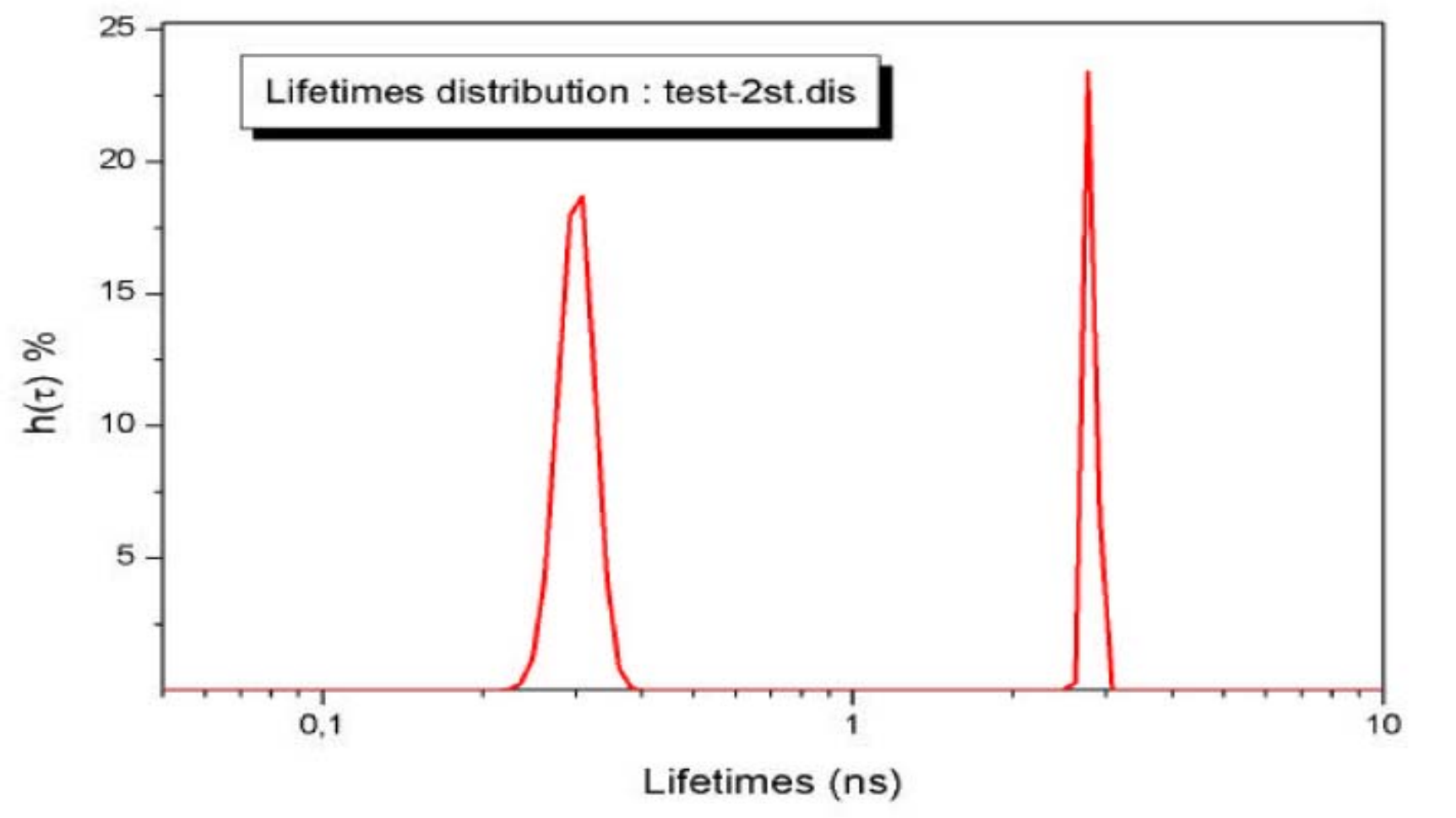


Jean-Claude Brochon
Maximum entropy method of data analysis in time-resolved spectroscopy.
Methods Enzymol. 1994;240:262-311.

Wavelength dependent lifetime data can be used to resolve individual spectra in a mixture

Gratton, E. and Jameson, D.M. (1985) *Anal. Chem. 57*:1694-1697. New Approach to Phase and Modulation Resolved Spectra.

Mixture: Lifetimes were 10.8ns, 4.3ns and 0.9ns

Spectra of individual components

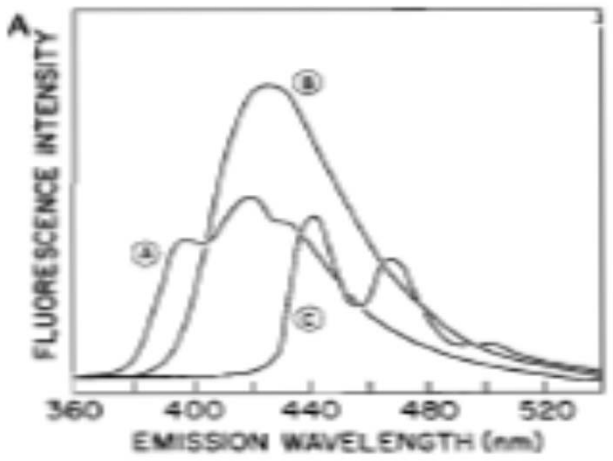


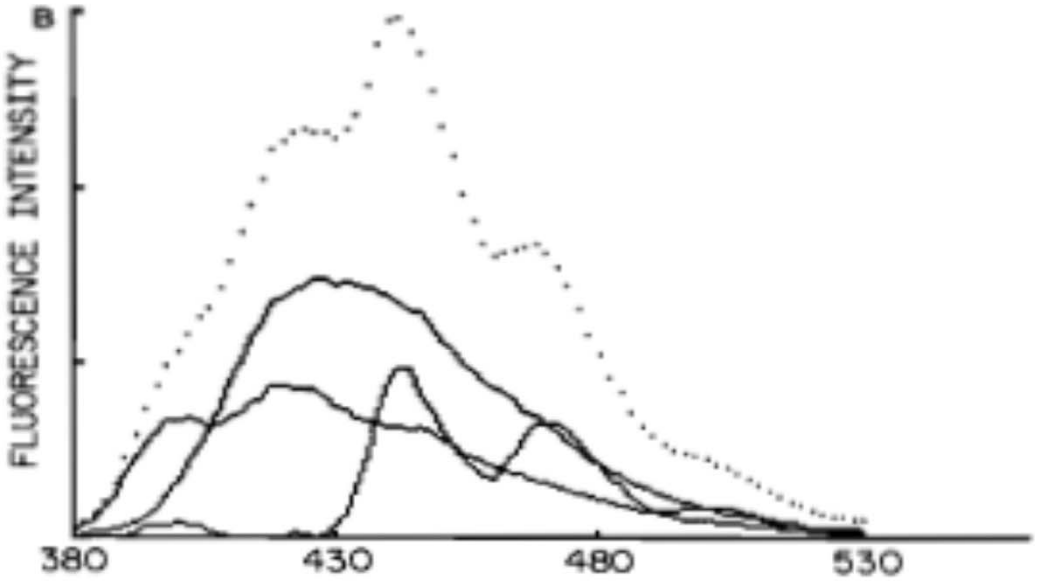


**Figure 3.** (A) Intensity spectra of individual components, POPOP (A), DENS (B), and perylene (C) in ethanol (not degassed). (B) Intensity (dotted line) and phase resolved spectra (solid lines) for the ternary mixture in A.

# Global Analysis

In Global Analysis one can link decay parameters across many data sets which often allows for a more robust analysis

**Example of the application of Global Analysis**

## Binding of Ethidium-Bromide to Transfer RNA

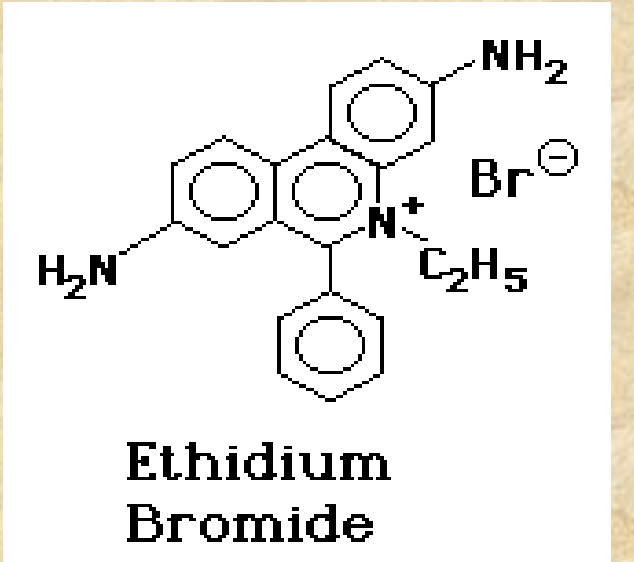


Ethidium Bromide

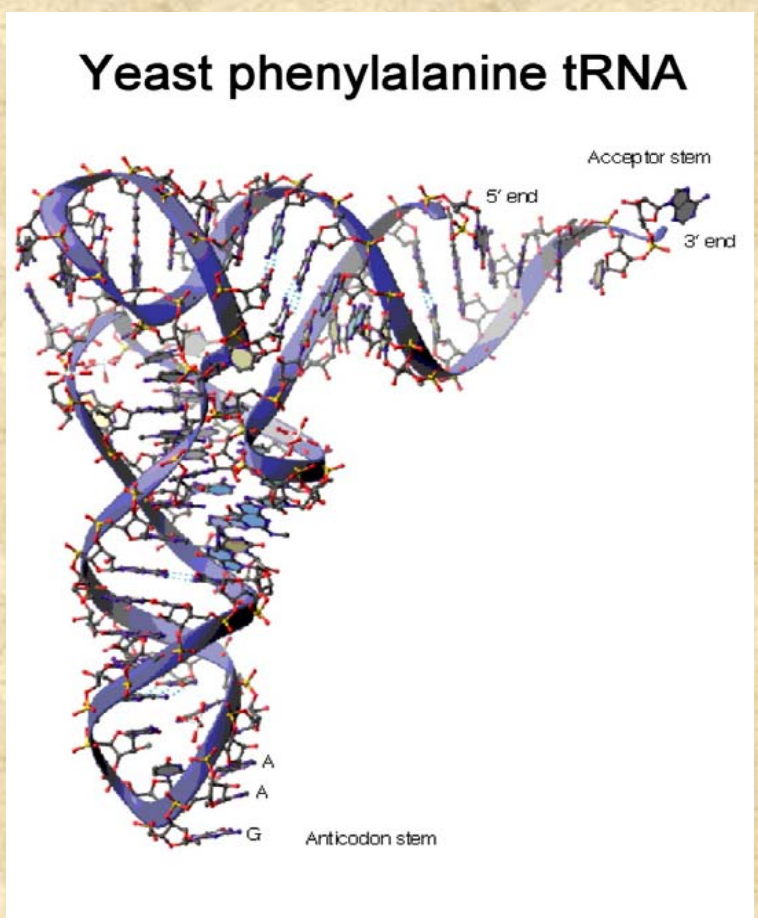

Ethidium bromide can intercalate into nucleic acid structures
It binds well to both DNA and RNA

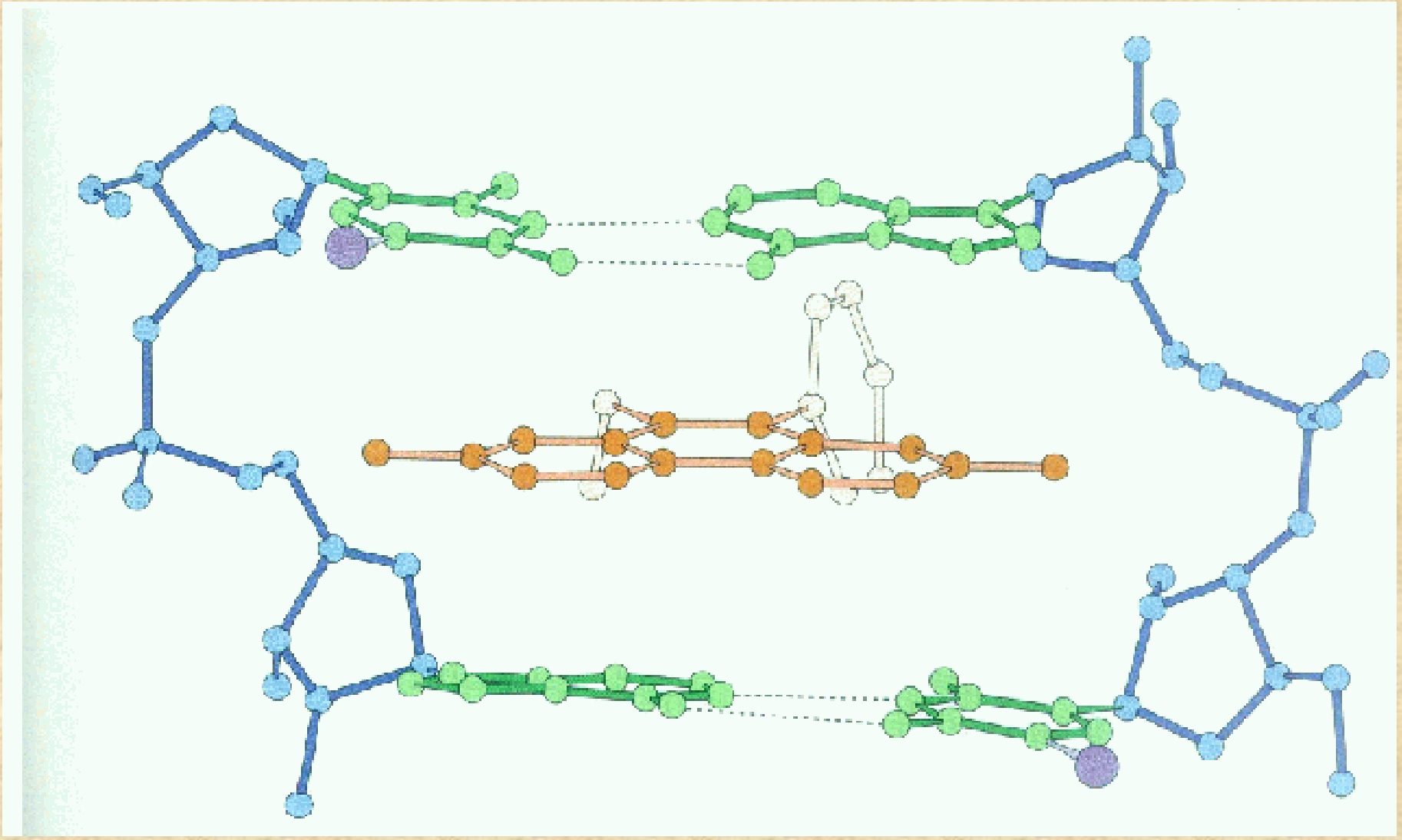

Fluorescence investigations of EB - tRNA interactions, carried out for more than 30 years, have indicated a “strong” binding site and one or more “weak, non-specific” binding sites.

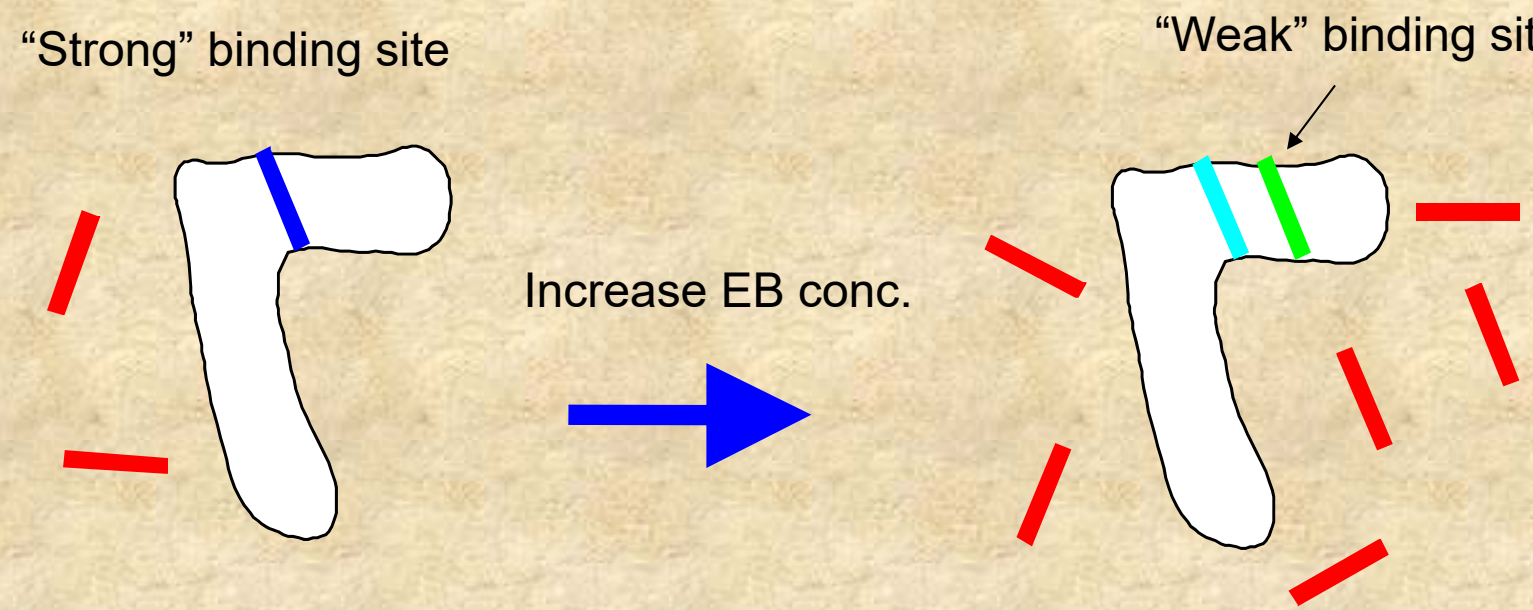


Question: What are the lifetimes of the strong and the weak binding sites???

If the tRNA is in excess only one EB will bind to the “strong” binding site which has a $K_d$ of around 1 micromolar (under these conditions a single exponential decay of 27ns is observed). If the EB/tRNA ratio is increased, one or more additional EB’s will bind and the question is: What are the lifetimes of EB bound to different sites on tRNA?” Shown below are phase and modulation data for a solution containing 124 μM yeast $tRNA^{phe}$ and 480 μM EB

The phase and modulation data were first fit to a single exponential component shown as the solid lines in the top plot. The residuals for this fit are shown in the bottom plot.

In this case $\tau$ = 18.49 ns and the $\chi^2$ value was 250.

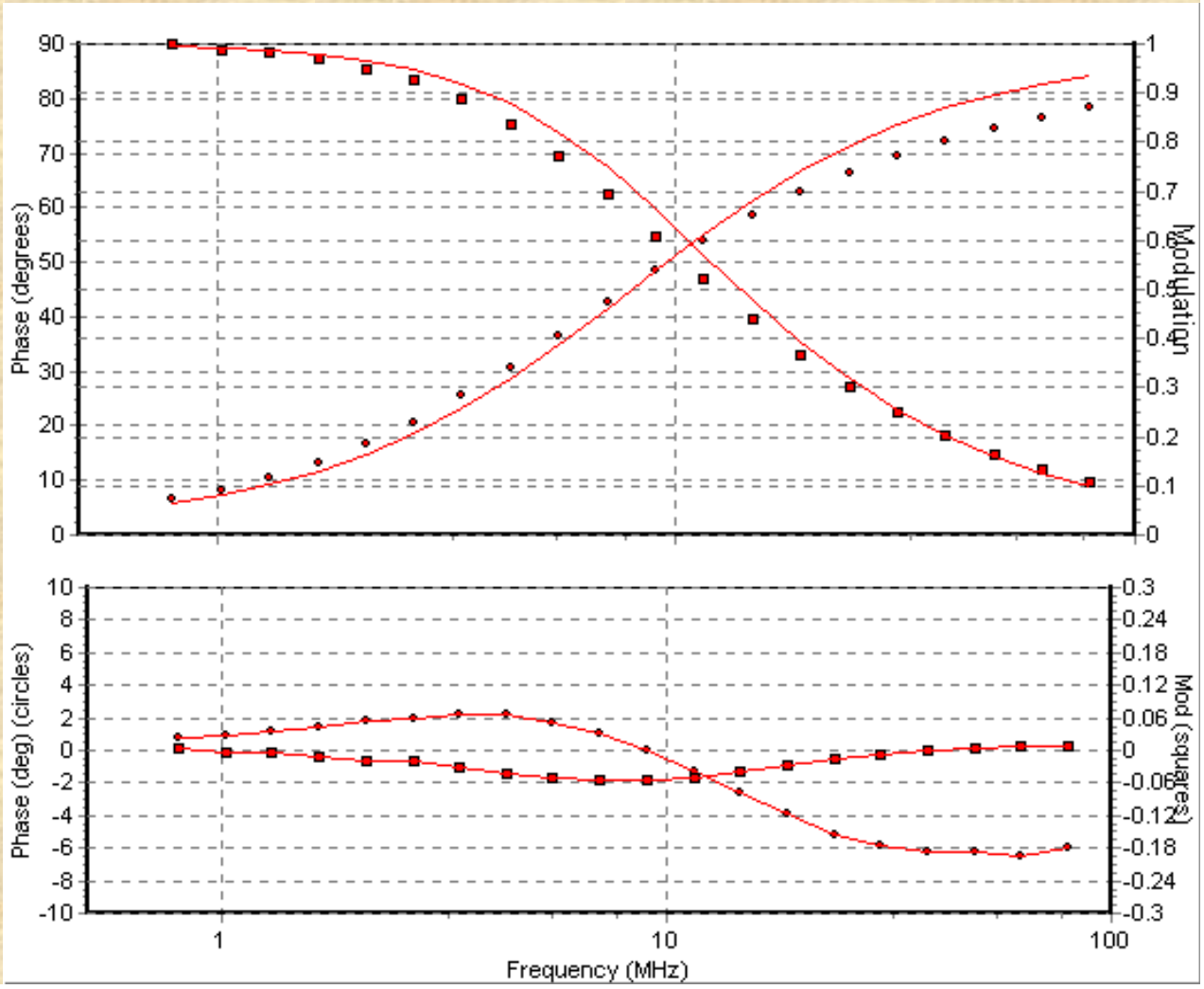

The data were then fit to a 2-component model shown here  In this case the two lifetime components were 22.71 ns with a fractional intensity of 0.911 and 3.99 ns with a fractional intensity of 0.089.

The $\chi^2$ for this fit was 3.06 (note the change in scale for the residual plot compared to the first case shown).

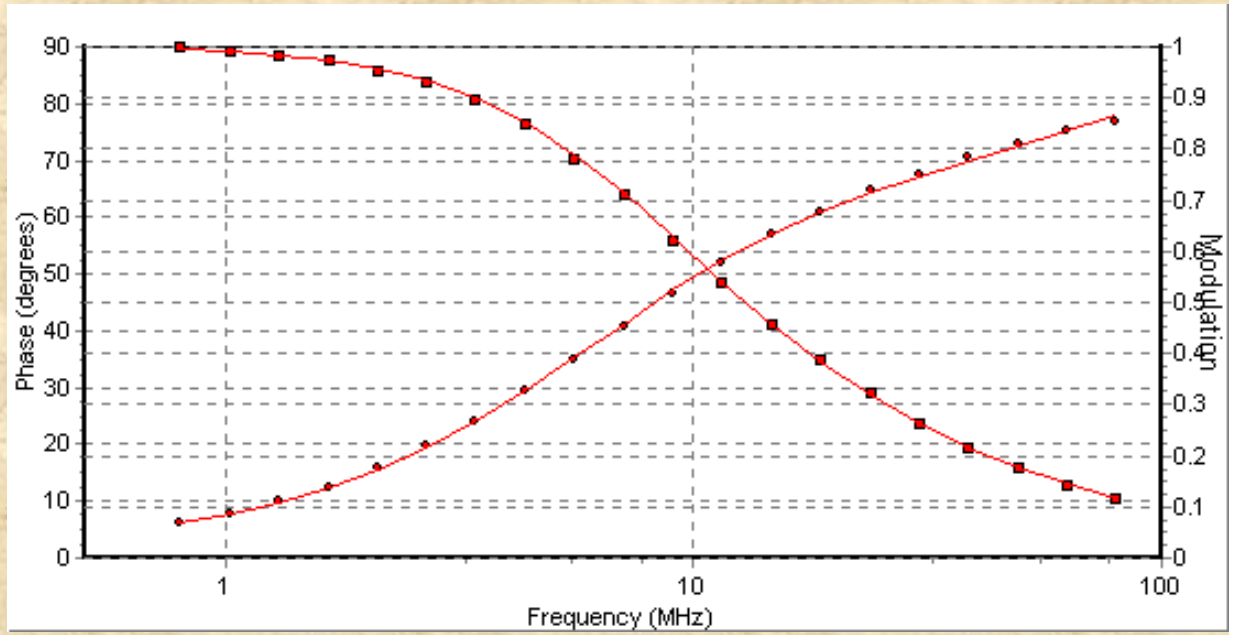


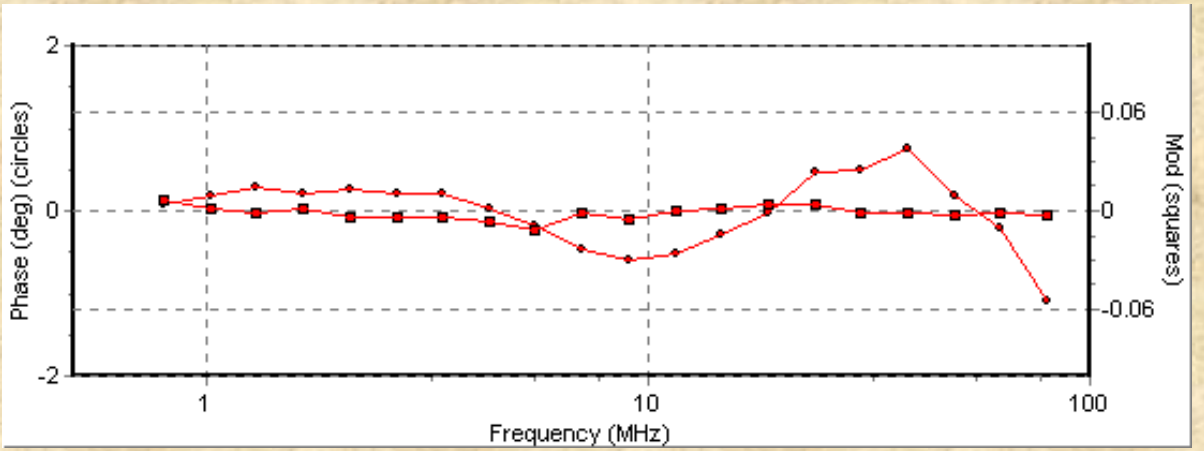

A 3-component model improves the fit still more. In this case

$\tau_1$ = 24.25 ns, $f_1$ = 0.83

$\tau_2$ = 8.79 ns, $f_2$ = 0.14

$\tau_3$ = 2.09 ns, $f_3$ = 0.03

$\chi^2$ = 0.39.

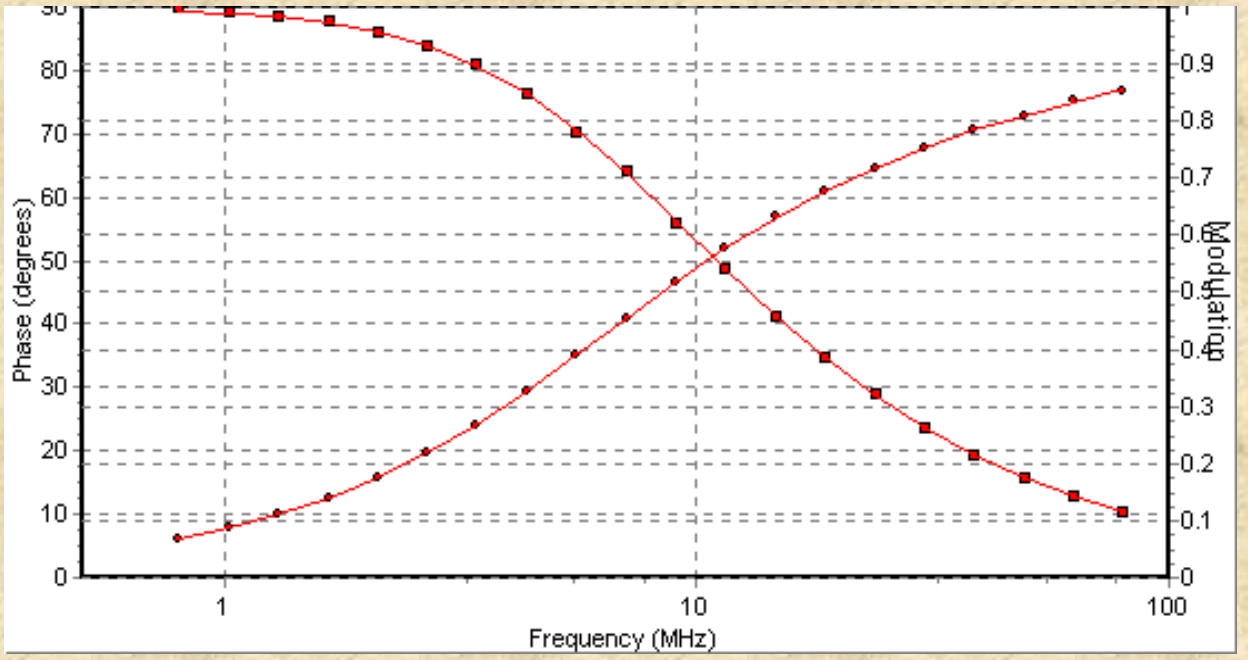


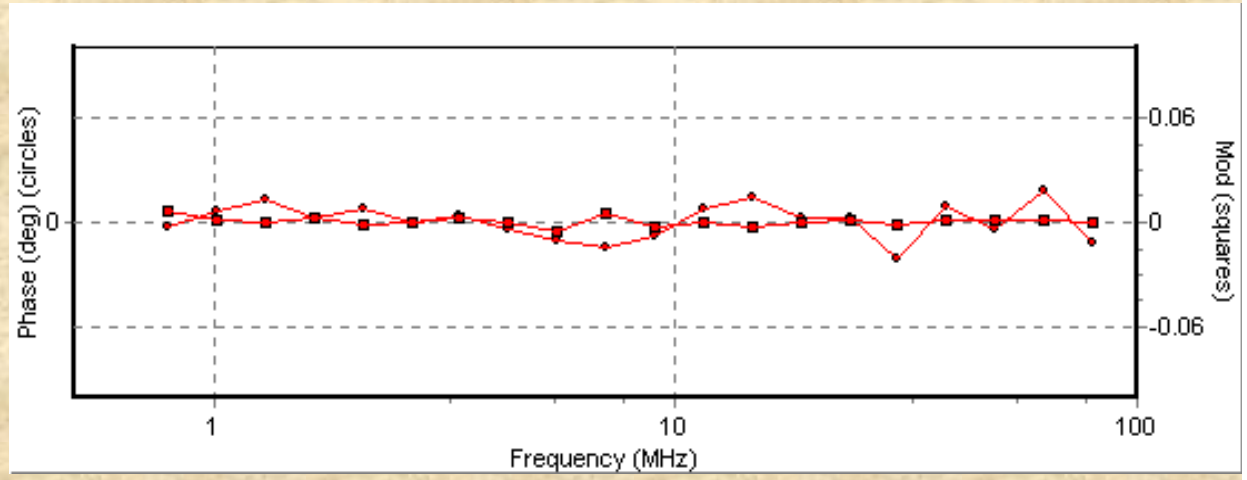

Adding a fourth component – with all parameters free to vary - does not lead to a significant improvement in the $\chi^2$. In this case one finds 4 components of 24.80 ns (0.776), 12.13ns (0.163), 4.17 ns (0.53) and 0.88 ns (0.008).

But we are not using all of our information! We can actually fix some of the components in this case. We know that **free EB** has a lifetime of **1.84 ns** and we also know that the lifetime of **EB bound to the "strong" tRNA binding site** is **27 ns**. So we can fix these in the analysis. The results are four lifetime components of 27 ns (0.612), 18.33 ns (0.311), 5.85 ns (0.061) and 1.84 ns (0.016). The $\chi^2$ improves to 0.16.

We can then go one step better and carry out **"Global Analysis"**.
In Global Analysis, multiple data sets are analyzed simultaneously and different parameters (such as lifetimes) can be "linked" across the data sets. The important concept in this particular experiment is that the lifetimes of the components stay the same and only their fractional contributions change as more ethidioum bromide binds.

In this system, 8 data sets, with increasing EB/tRNA ratios, were analyzed. Some of the data are shown below for EB/tRNA ratios of 0.27 (circles), 1.34 (squares), 2.41 (triangles) and 4.05 (inverted triangles).

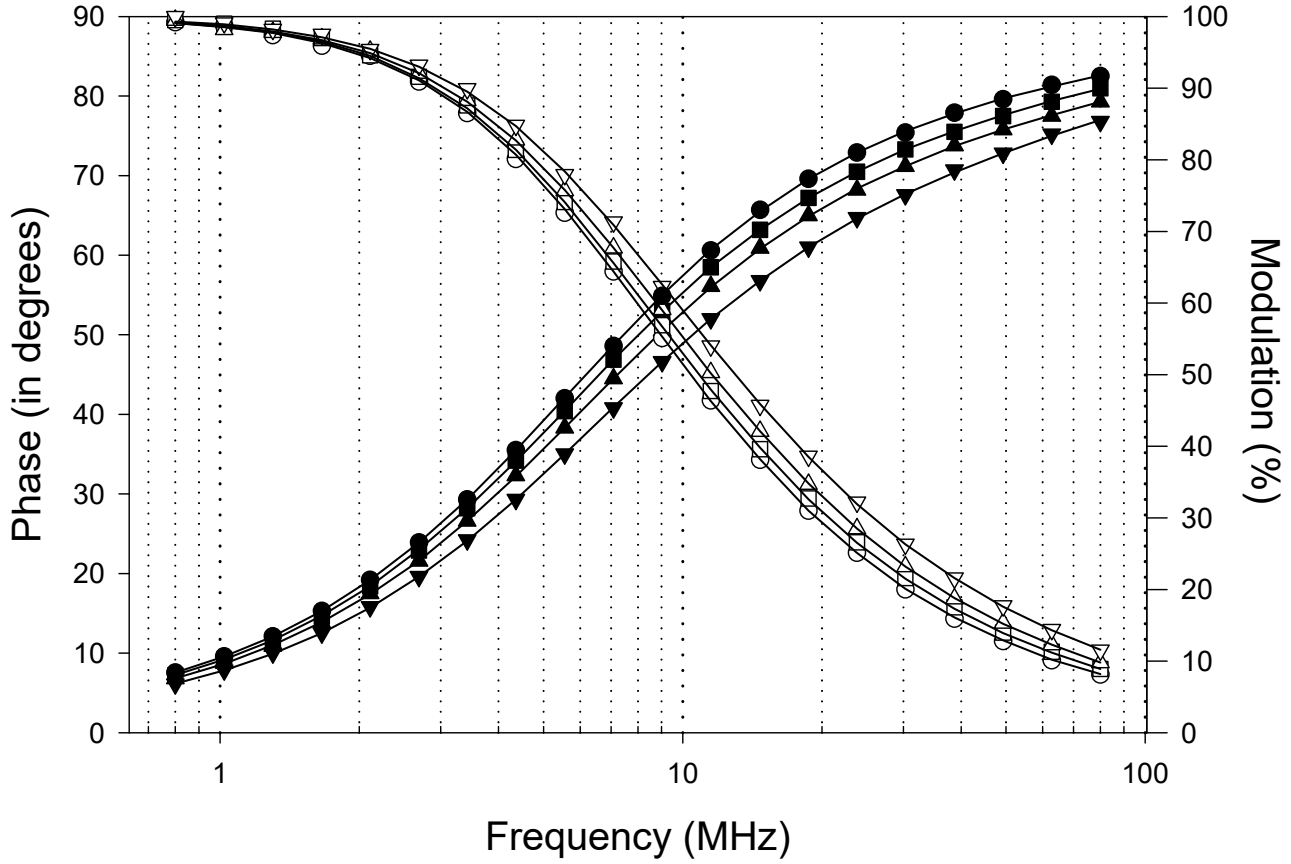

Global Analysis on seven data sets fit best to the 4 component model with two fixed components of 27ns and 1.84ns and two other components of 17.7ns and 5.4ns.

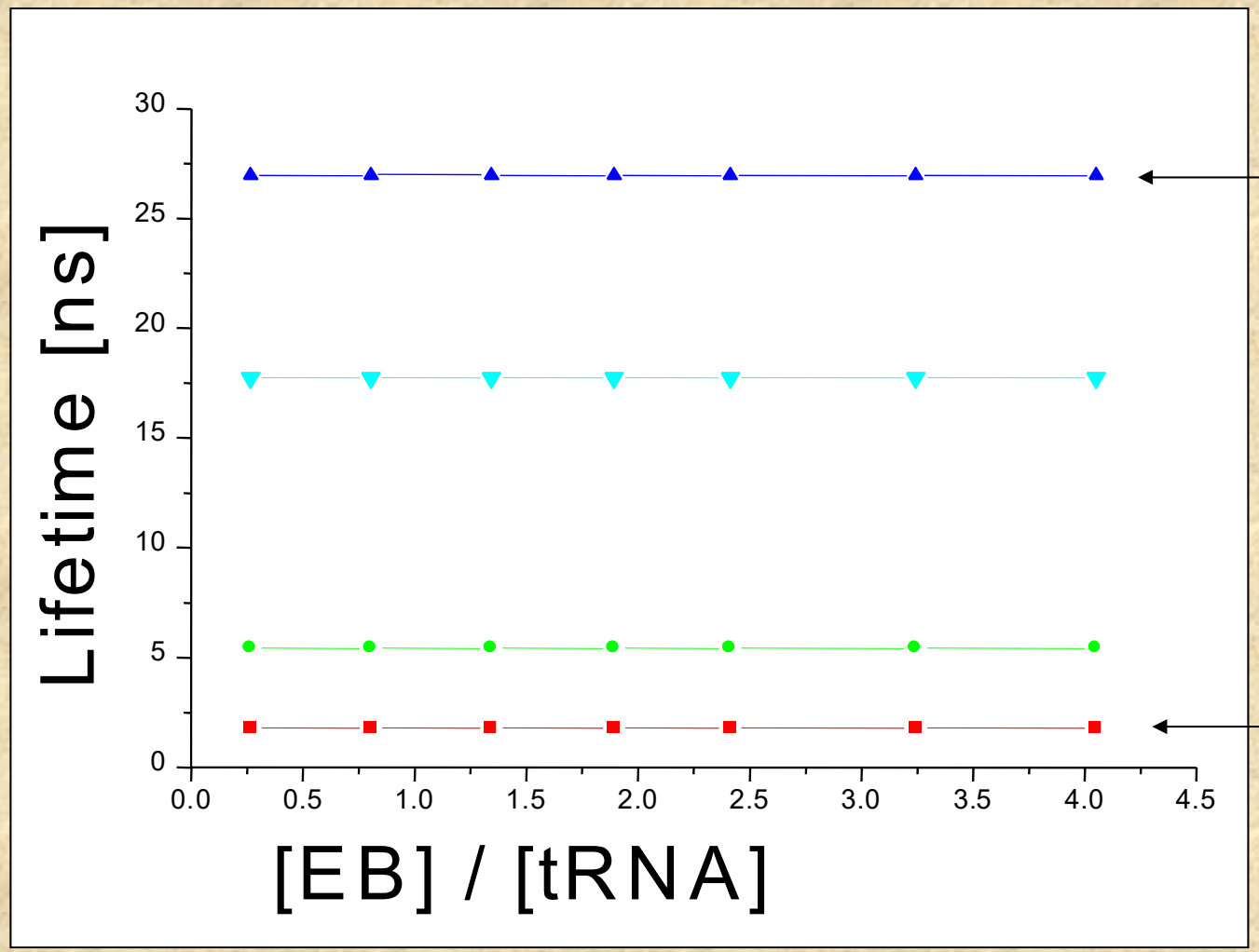

As shown in the plot below, as the EB/tRNA ratio increases the fractional contribution of the 27ns component decreases while the fractional contributions of the 17.7ns and 5.4ns components increase.

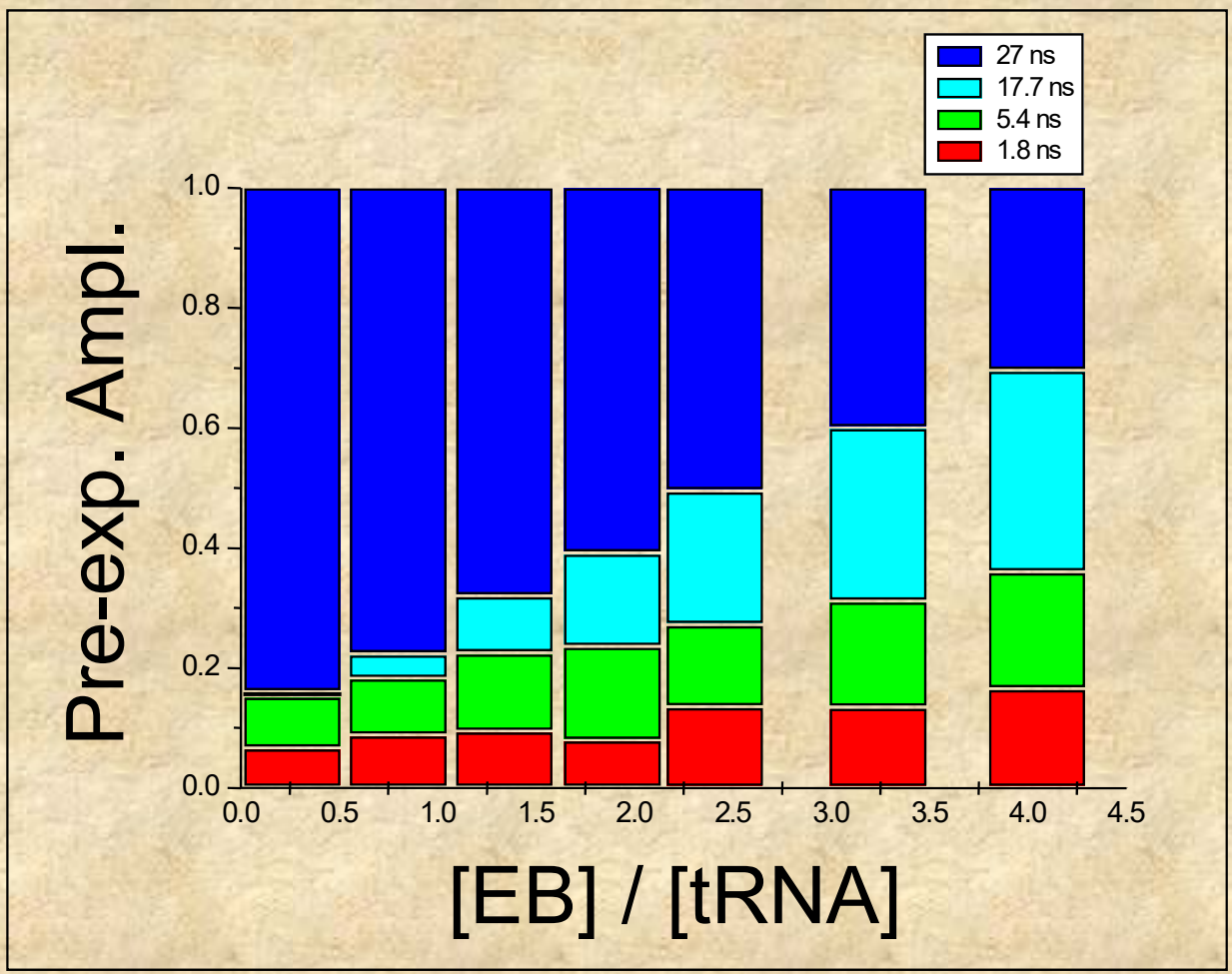

# The Model

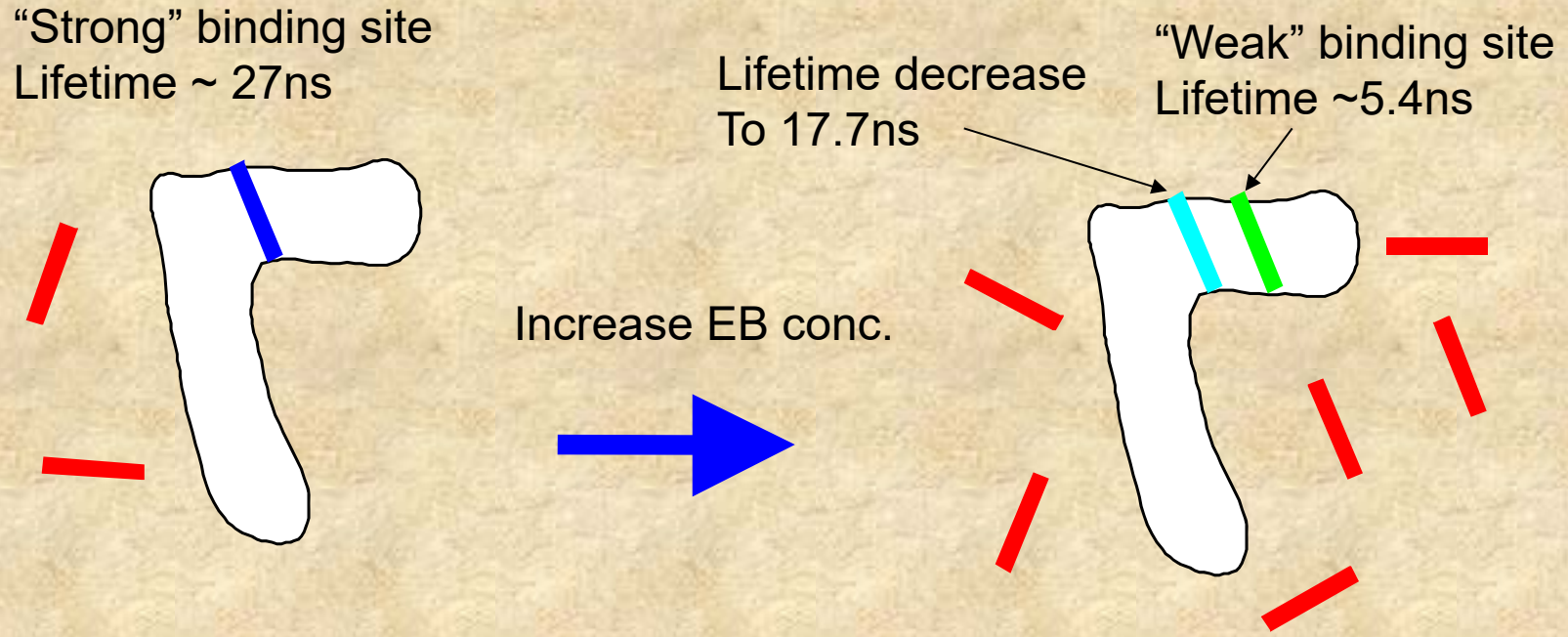


Question:
Is the drop in the lifetime of the "strong" binding site due to a change in tRNA conformation or energy transfer???

Answer: ???

Later in this workshop you'll learn about Fluorescence Lifetime Imaging or FLIM

In FLIM, lifetime data are obtained through a microscope - lifetime data is acquired at each pixel in the image

Lifetime data is more robust than intensity since it does not depend on how many fluorescent molecules are present

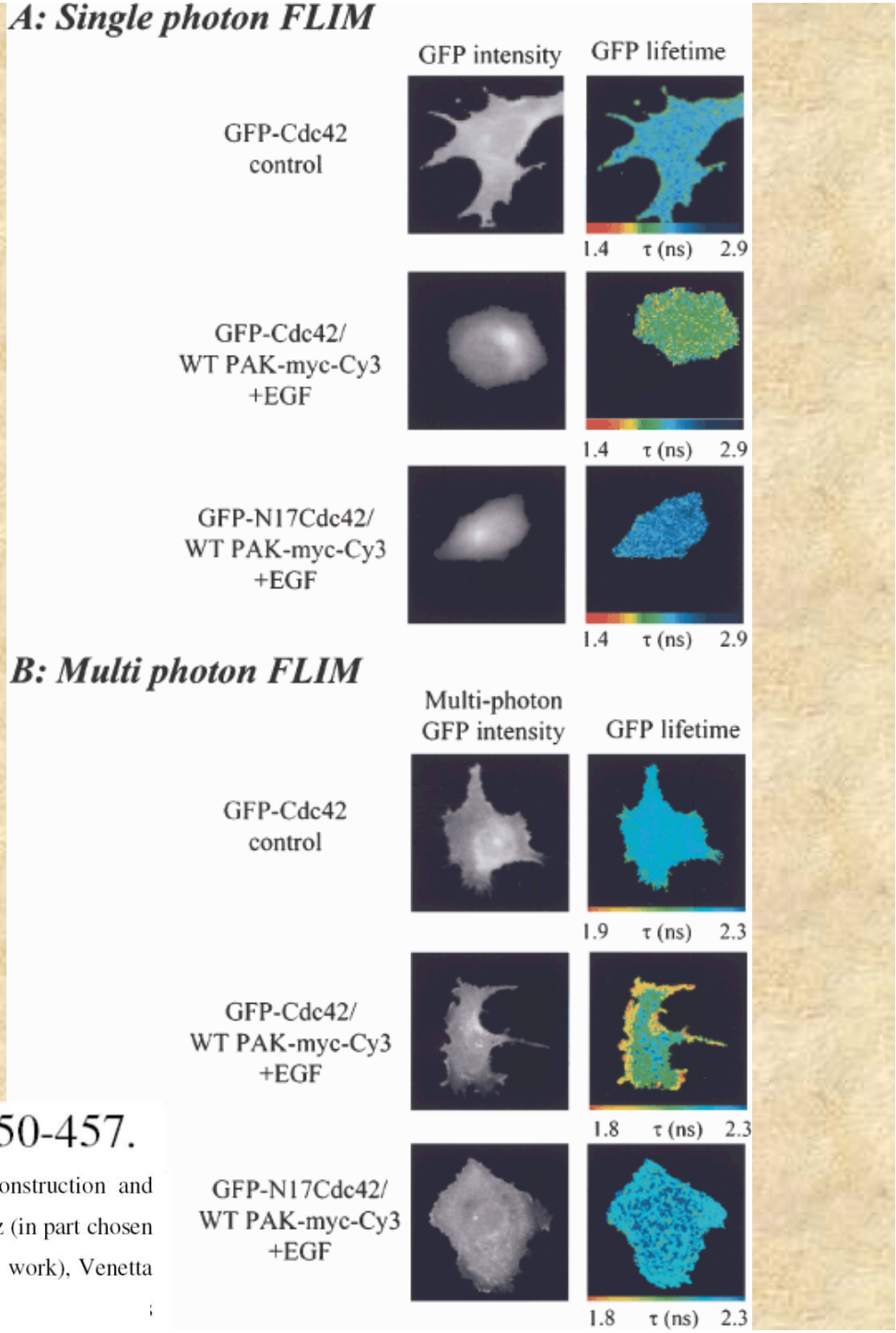


B. D. Venetta, *Rev. Sci. Instrum.*, 1959, **30**, 450-457.

In 1959 Venetta[4] described the construction and operation of a phase fluorometer coupled to a microscope. Using a frequency of 5.8 MHz (in part chosen due to the availability of FM transformers in televisions which could be salvaged for this work), Venetta was able to measure a lifetime of 2.7 ns for proflavin bound to the nuclei of tumor cells.

# Introduction to Phasors

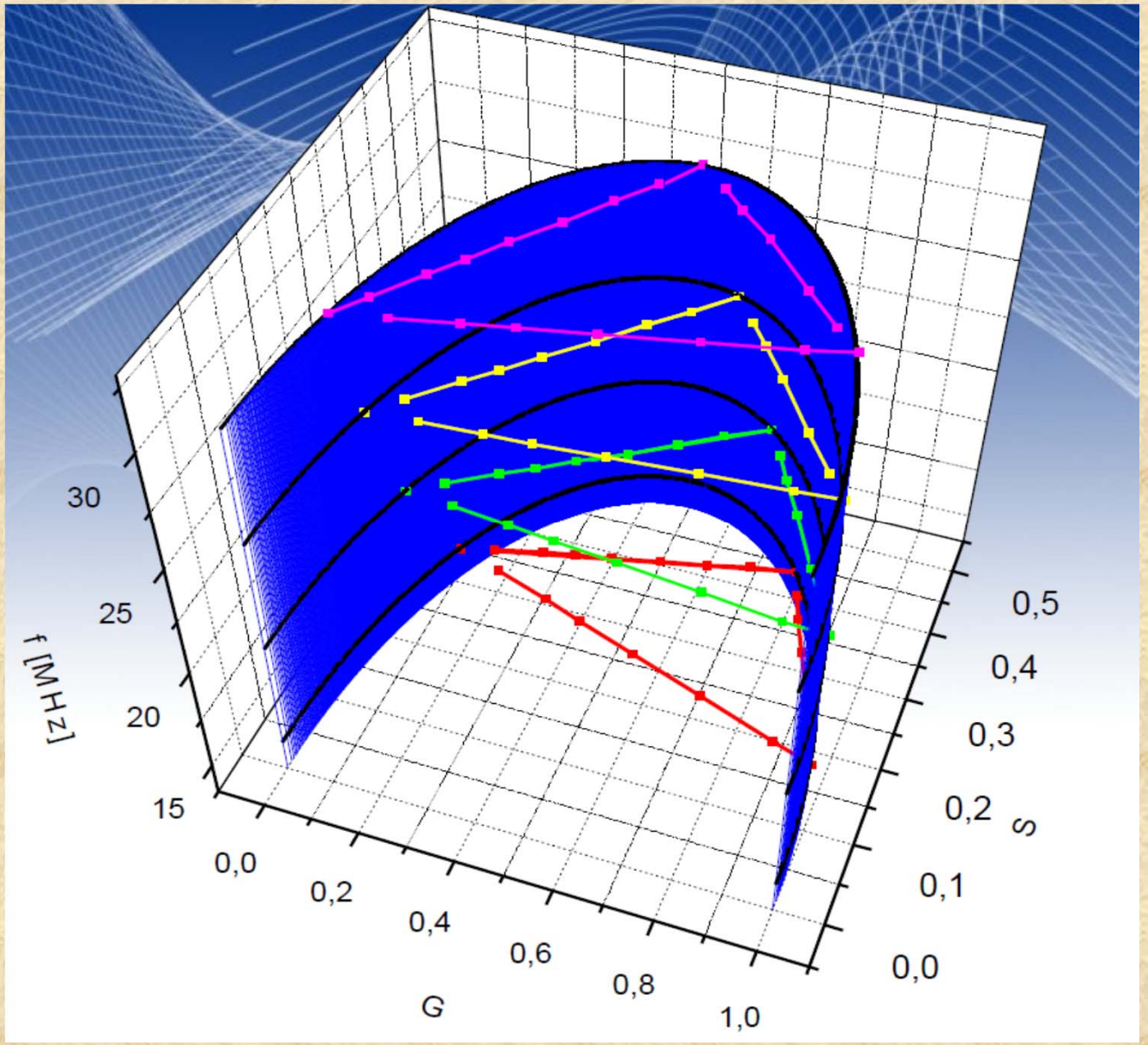

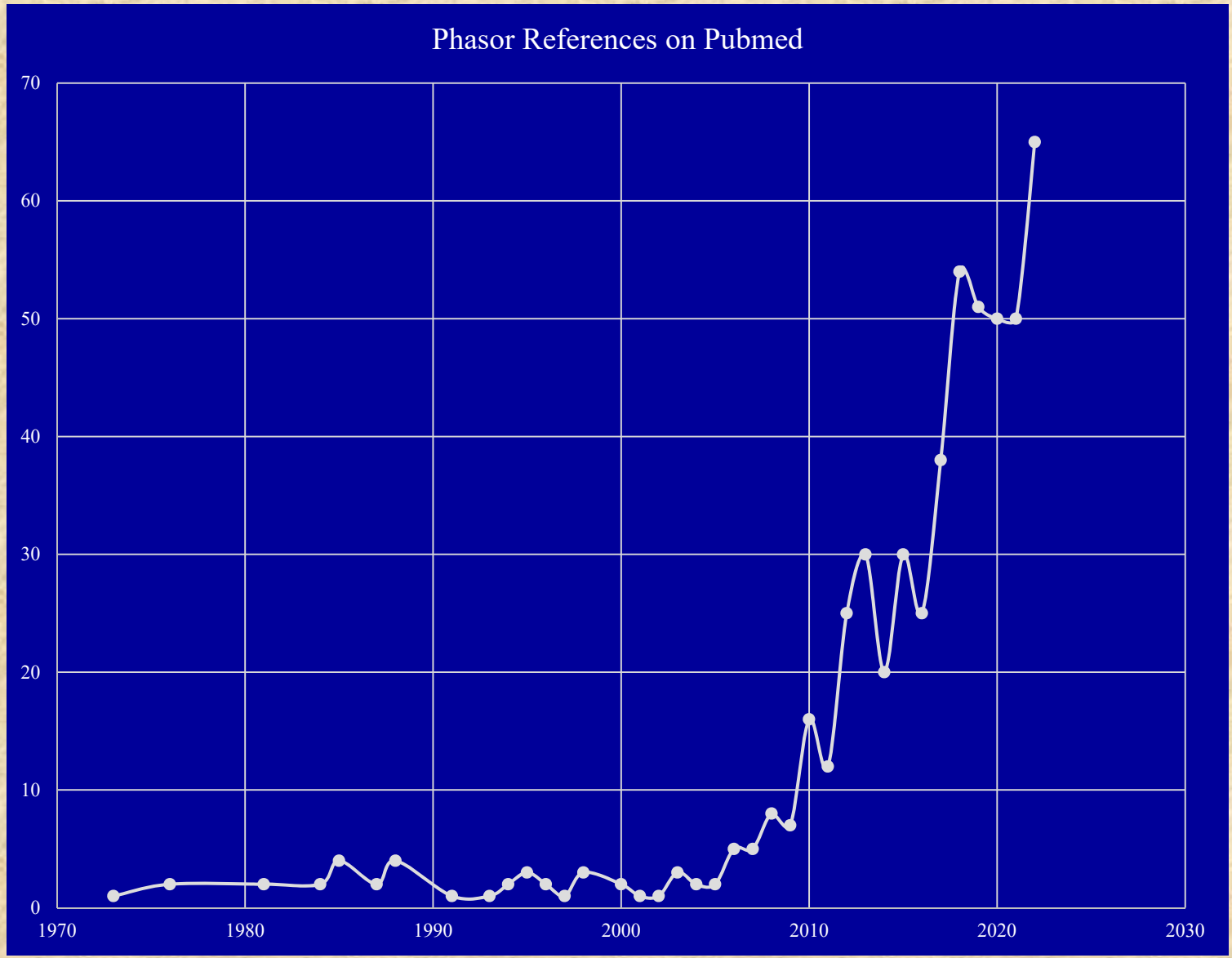
Phasor References on Pubmed
70
60
50
40
30
20
10
0
1970
1980
1990
2000
2010
2020
2030

# Phasors

The concept of phasors has been around a long time

The original phasor transform was an invention of Charles Proteus Steinmetz, a mathematician and engineer born in 1865.

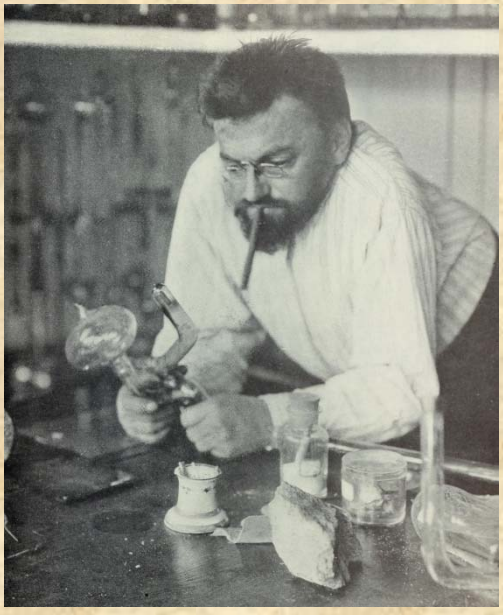

Steinmetz was a famous figure in science and technology near the turn of the century and made many significant contributions to electrical engineering.

Steinmetz introduced the concept of **phase vectors** (which he named "**phasors**") in a paper published in 1893*

Specifically, his phasor transforms greatly facilitated analysis of RLC circuits by allowing one to use algebraic equations in the phasor space instead of differential equations in the time domain.

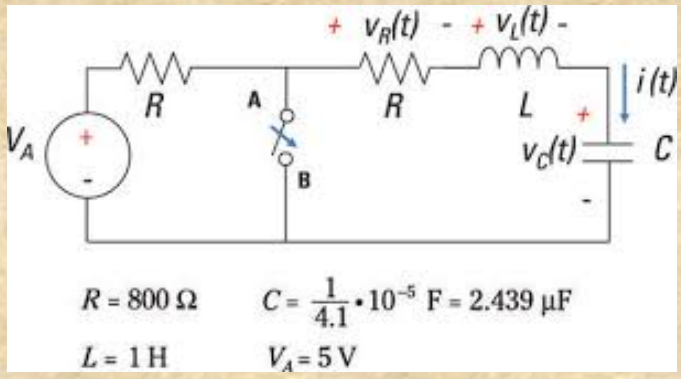


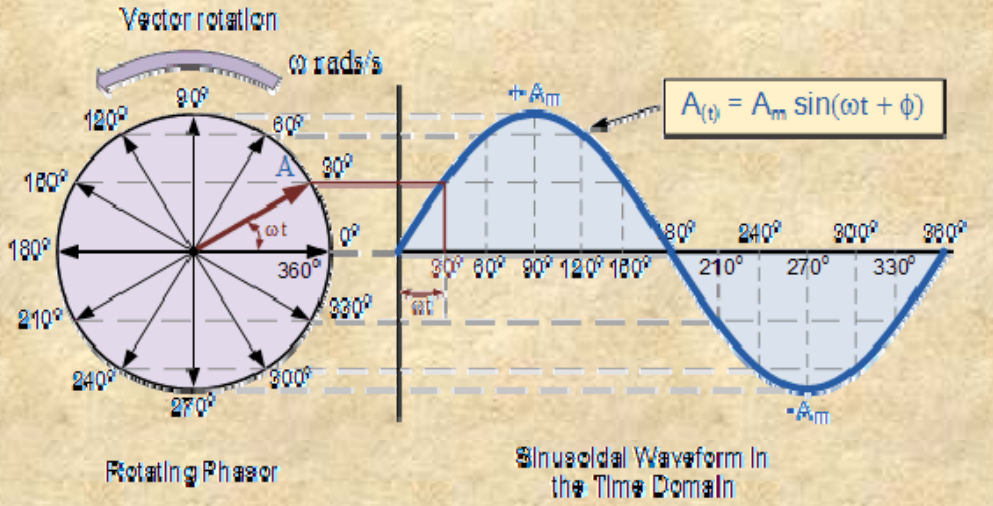


* Steinmetz, C. P. (1893). Complex quantities and their use in electrical engineering. Proceedings of the International Electrical Congress, Conference of the AIEE : American Institute of Electrical EngineersProceedings, Chicago (pp. 33–74), Chicago: AIEE.

Reprinted from The Journal of Physical Chemistry, 1981, 85, 040.


# Resolution of the Fluorescence Lifetimes in a Heterogeneous System by Phase and Modulation Measurements

**Gregorio Weber**

*Department of Biochemistry, School of Chemical Sciences, University of Illinois, Urbana, Illinois 61801* *(Received: August 12, 1980)*

A closed-form procedure is described for the determination of the decay constants and the relative contributing intensities of the $N$ independent components of a heterogeneous fluorescence emission employing measurements of the phase shift and relative modulation of the total fluorescence at $N$ appropriate harmonic excitation frequencies. At each frequency the phase and modulation measurements yield the real part of the Fourier transform of the fluorescence impulse response, $G$, and its imaginary part, $S$. It is shown that the moments of a distribution of the lifetimes are linear combinations of the $G$s (zero and even moments) or the $S$s (odd moments), and the rule for the construction of the coefficients of $G$ and $S$ in these linear combinations is derived. The classical de Prony method is used to obtain the lifetimes and fractional contributions of the components from the moments. For binary and ternary mixtures the numerical computations required are trivial. In the present state of the art, the lifetimes of the components of a binary mixture should be derivable with a loss in precision somewhat smaller than 1 order of magnitude with respect to the overall measured lifetimes.

$$G_r = M_r \cos \Phi_r = [(1 + (\omega_r \tau_r^{P})^2)(1 + (\omega_r \tau_r^{M})^2)]^{-1/2} \quad (9)$$

$$S_r = M_r \sin \Phi_r = G_r \omega_r \tau_r^{P} \quad (10)$$

Time domain

$$G(\omega) = \int_0^\infty I(t) \cos \omega t \, dt$$

$$S(\omega) = -\int_0^\infty I(t) \sin \omega t \, dt \quad (55)$$

Frequency Domain

APPLIED SPECTROSCOPY REVIEWS, 20(1), 55-106 (1984)

# The Measurement and Analysis of Heterogeneous Emissions by Multifrequency Phase and Modulation Fluorometry

DAVID M. JAMESON
Department of Pharmacology
The University of Texas Health Science Center at Dallas
Dallas, Texas 75235

ENRICO GRATTON
Department of Physics
University of Illinois at Urbana-Champaign
Urbana, Illinois 61801

ROBERT D. HALL
Laboratory of Molecular Biophysics
National Institute of Environmental Health Sciences
Research Triangle Park
North Carolina 27709



## APPENDIX 2. PHASE AND MODULATION LIFETIME RELATIONS

We have asserted that a heterogeneous emitting population, in the absence of excited state reaction, will demonstrate a phase lifetime which is always less than the modulation lifetime. The algebraic demonstration of this fact is somewhat cumbersome [11, 68]. We present here a brief and more intuitive demonstration of the phenomenon.

One may make a simple geometrical representation of the phase delay and relative modulation as shown in Fig. 11. Here we depict a vector of length M making an angle $\phi$ with the x-axis where $\phi$ represents the phase delay and M the relative modulation. Since for a single exponential decay we have the relation $M = \cos \phi$, the endpoint of the vector is constrained to be on the circle of radius 1/2 with a center at (1/2, 0). The intercept of the extension of this vector with the line through x = 1 equals $\omega t$ (since $\tan \phi = \omega t$). This circle is universal for single exponential systems irrespective of the lifetime or modulation frequency. We note that the X and Y intercepts of the vector correspond to our previously defined G and S functions (since $G = M \cos \phi$ and $S = M \sin \phi$).

Figure 12 represents the case of two exponential decays with phase delays and relative modulations of $\phi_1$, $\phi_2$ and $M_1$, $M_2$, respectively. These decays contribute to the total emission intensity decay with fractional weights of $f_1$ and $f_2$, respectively. The total fluorescence observed is represented by the vector sum, M, of the two components and gives an observed phase delay of $\phi$. Again we see that the intercept of the extension of the M vector with the x = 1 line corresponds to $\omega\tau^P$ (since $\tan \phi = \omega\tau^P$). The value of $\omega\tau^M$, however, corresponds to the line segment BD. This observation follows from the fact that the triangle OAB,

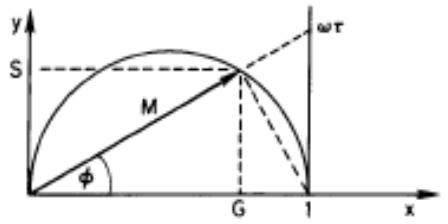


FIG. 11. Geometrical representation of phase delay ($\phi$) and modulation ratio ($M$) for a single exponential decay.

What was the first use of fluorescence phasors in the lab?

# Why was this work done?

*Journal of Fluorescence, Vol. 1, No. 3, 1991*

## A Method for On-Line Background Subtraction in Frequency Domain Fluorometry

**Gregory D. Reinhart,[1,2] Pasquina Marzola,[3] David M. Jameson,[2,4] and Enrico Gratton[5,6]**

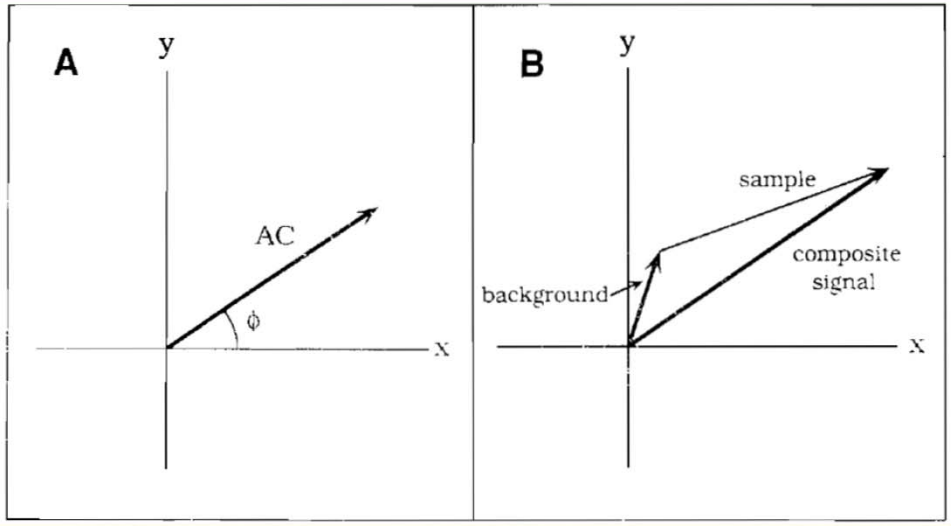


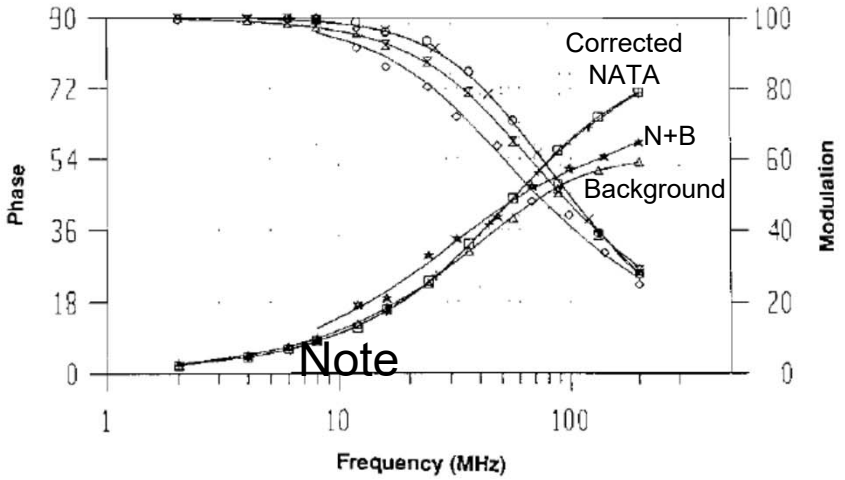

Actually a “phasor” approach was utilized in 1993 by Lenny Brand’s lab applied to calcium binding probes

They had not seen our 1984 review nor the 1991 paper so their work was independent

ANALYTICAL BIOCHEMISTRY **209**, 209–218 (1993)

# Dynamic Fluorescence Measurements of Two-State Systems: Applications to Calcium-Chelating Probes

Kim Marie Hirshfield,[1] Dmitri Toptygin,[2] Beverly S. Packard,* and Ludwig Brand[2,3]
*Department of Biology, The Johns Hopkins University, Baltimore, Maryland 21218;*
*and *Division of Cytokine Biology, CBER, FDA, Bethesda, Maryland 20892*

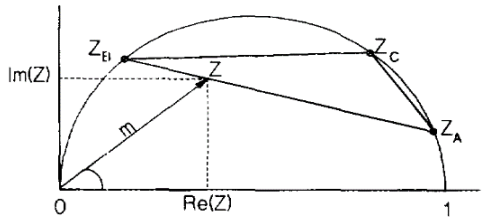


**FIG. 2.** Representation of the complex plane formed by the axes Re $Z$ and Im $Z$. Graph demonstrates the relationship of $Z(\omega)$ on the dynamic parameters of phase angle, $\phi$, and modulation, $m$, for a given frequency. At a single frequency, the points $Z_A$, $Z_B$, and $Z_C$ correspond to contribution from 100% A, 100% B, or 100% C, respectively.

They never named their plot

Nothing then appeared to happen in the phasor field until this paper in 2004

*Journal of Microscopy, Vol. 213, Pt 1 January 2004, pp. 1–5*
*Received 20 March 2003; accepted 4 September 2003*

SHORT COMMUNICATION

# Graphical representation and multicomponent analysis of single-frequency fluorescence lifetime imaging microscopy data

A. H. A. CLAYTON*, Q. S. HANLEY† & P. J. VERVEER‡
*Ludwig Institute for Cancer Research, PO Box 2008, Royal Melbourne Hospital, Parkville, Victoria 3050, Australia
†Department of Biological and Chemical Sciences, University of the West Indies, Cave Hill Campus, St. Michael, Barbados
‡Cell Biology and Cell Biophysics Program, European Molecular Biology Laboratory, Meyerhofstraße 1, D-69117 Heidelberg, Germany*


The point of Clayton et al., was to resolve two lifetime components in a FLIM image given only one light modulation frequency. To do this operation the authors used Weber's 1981 algorithm

In 2005, Hanley and Clayton published a paper explicitly naming their approach the "AB Plot." Interestingly, in this paper Hanley and Clayton presented several AB plots which used data from previous FLIM publications to resolve mixtures of fluorophores. No actual FLIM images were presented.

In 2005 Redford and Clegg published an overview of what they termed a "Polar Plot". Although they did not present any FLIM images, they wrote "We have been applying this method in the last few years to our FLIM data, and it has given us unique insights and has aided us in interpretation [8,9]." They references they added were both to abstracts presented at the 2003 Biophysical Society Meeting.

Bob Clegg

*Journal of Fluorescence, Vol. 15, No. 5, September 2005 (© 2005)*

## Polar Plot Representation for Frequency-Domain Analysis of Fluorescence Lifetimes

**Glen I. Redford[1] and Robert M. Clegg[1,2]**

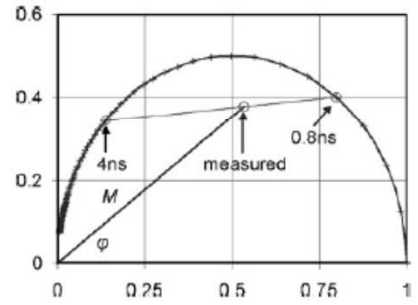


**Fig. 1.** A simulated plot of lifetime locations measured at 100 MHz. The semicircle is the single lifetime curve. The location {1,0} represents 0 lifetime. The location {0,0} represents infinite lifetime. Lifetimes increase counter-clockwise to the left. In this coordinate system the measured value is the intensity-weighted average of the two component lifetimes. All different ratios of the two lifetime components would fall on the line between them. For example, as shown, components with lifetimes of 4 and 0.8 ns (here the short lifetime has two-thirds the probability/intensity of the long lifetime), the measured lifetime is, phase: 1.1, and modulation: 1.8 ns.

The really BIG surge forward in phasor development, though, also came in 2005

Enrico introduced Phasors during his lecture at the 2005 Principles of Fluorescence Course in Genoa (sponsored by ISS)

Enrico introduced Phasors during his lecture at the 2005 Principles of Fluorescence Course in Genoa (sponsored by ISS)

# Lecture 10
# RICS and FLIM


## Enrico Gratton

**Laboratory for Fluorescence Dynamics**
**University of Illinois at Urbana-Champaign**


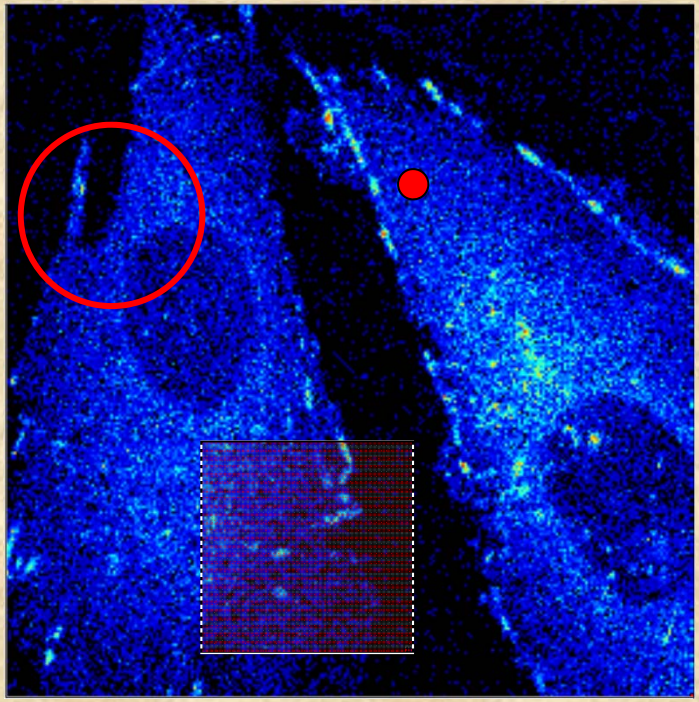

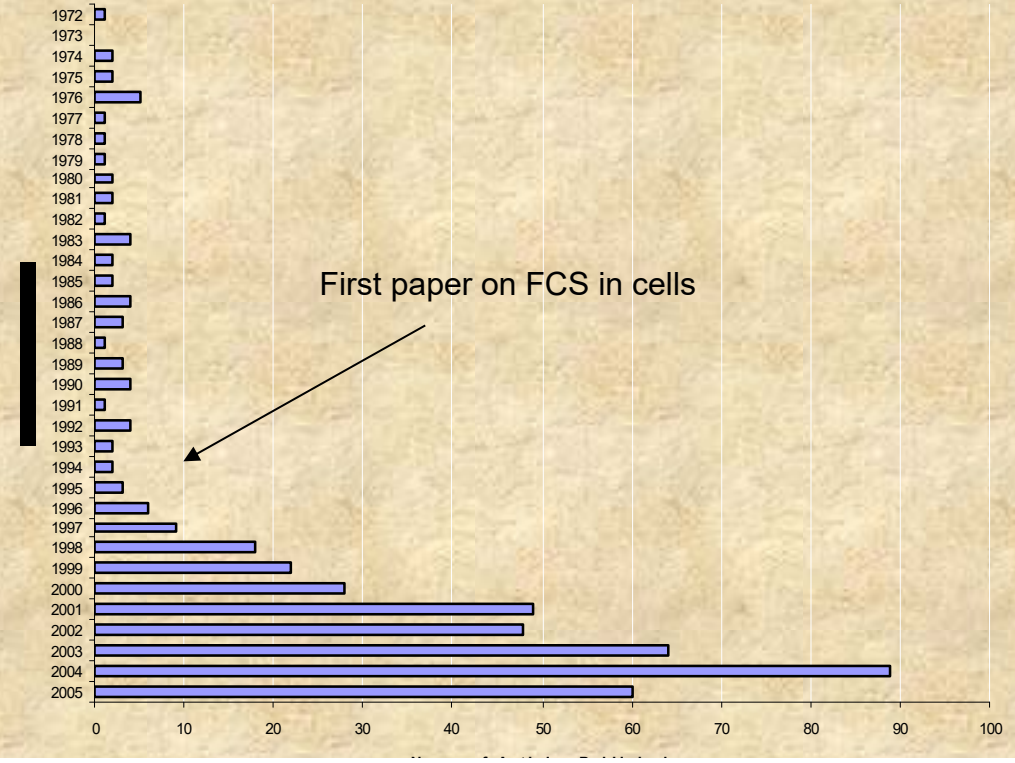

# The algebra of phasors

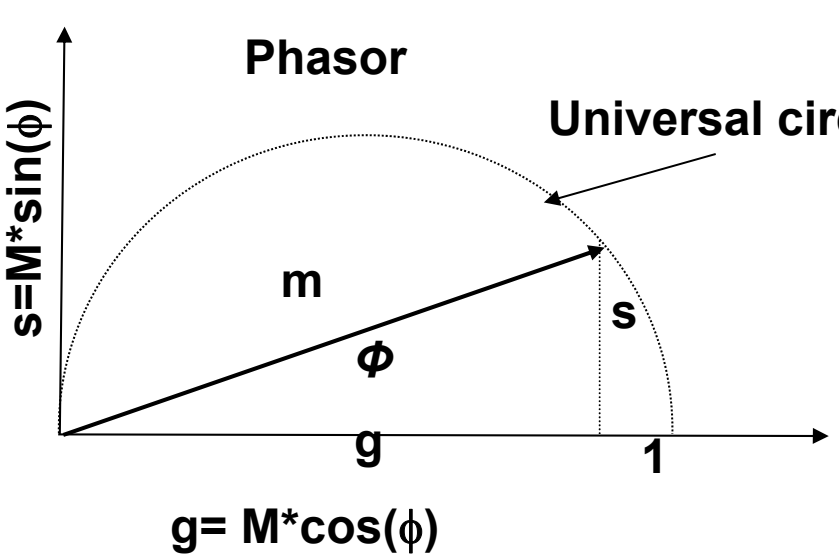


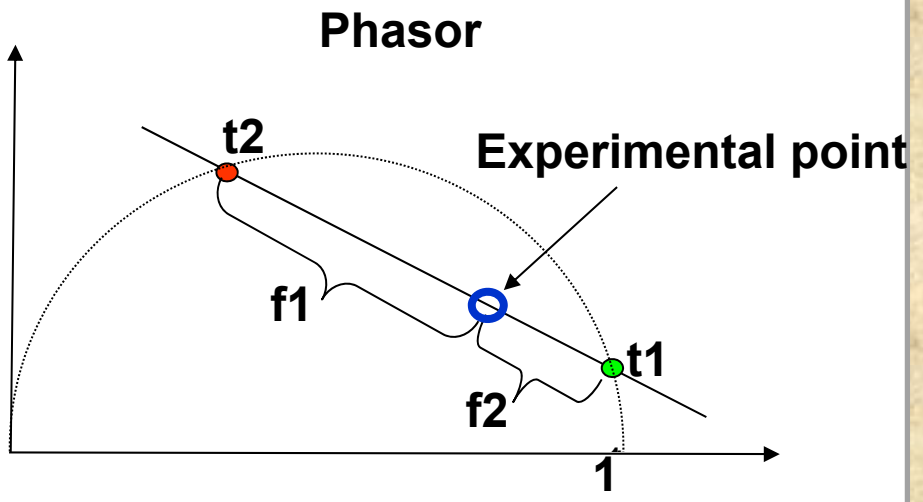


Simple rules to the Phasor plot:

1) All single exponential lifetimes lie on the “universal circle”
2) Multi-exponential lifetimes are a linear combination of their components
3) The ratio of the linear combination determines the fraction of the components

Slide from Enrico

# Phasor Linear Combination (Lifetime)

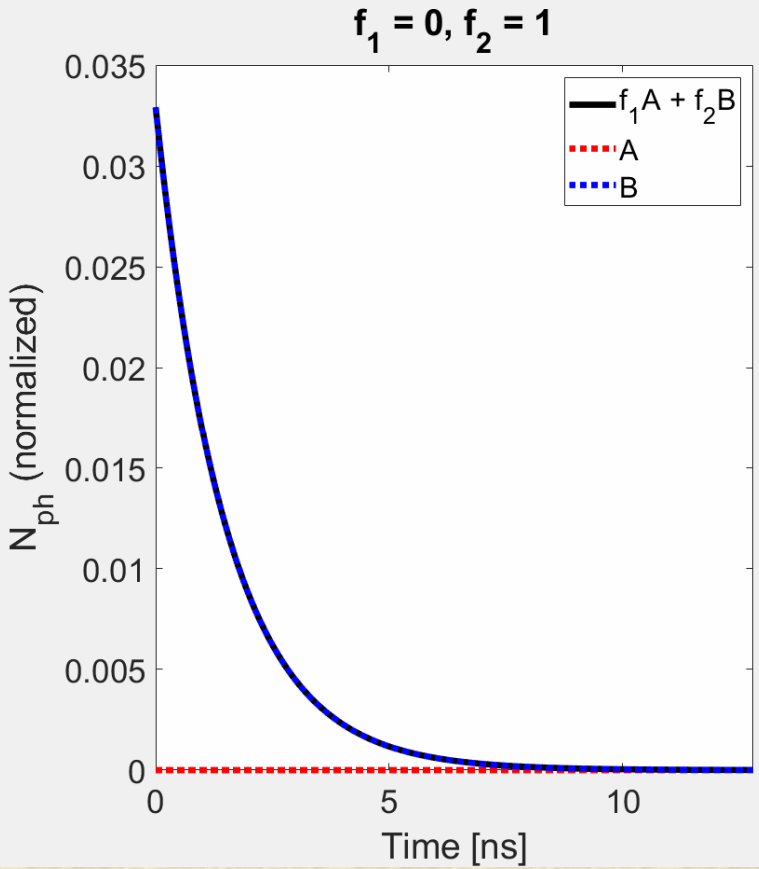


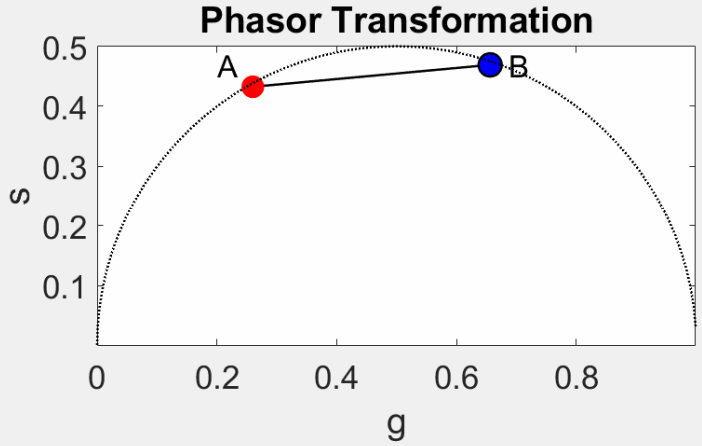


Digman MA, Caiolfa VR, Zamai M, Gratton E. **The phasor approach to fluorescence lifetime imaging analysis**. Biophys J. 2008;94(2):L14–L16. doi:10.1529/biophysj.107.120154

# Methodological measurements I

- Map the position of the mixture of three different single-exponential dyes (Rhodamine B, AEDANS, DENS)

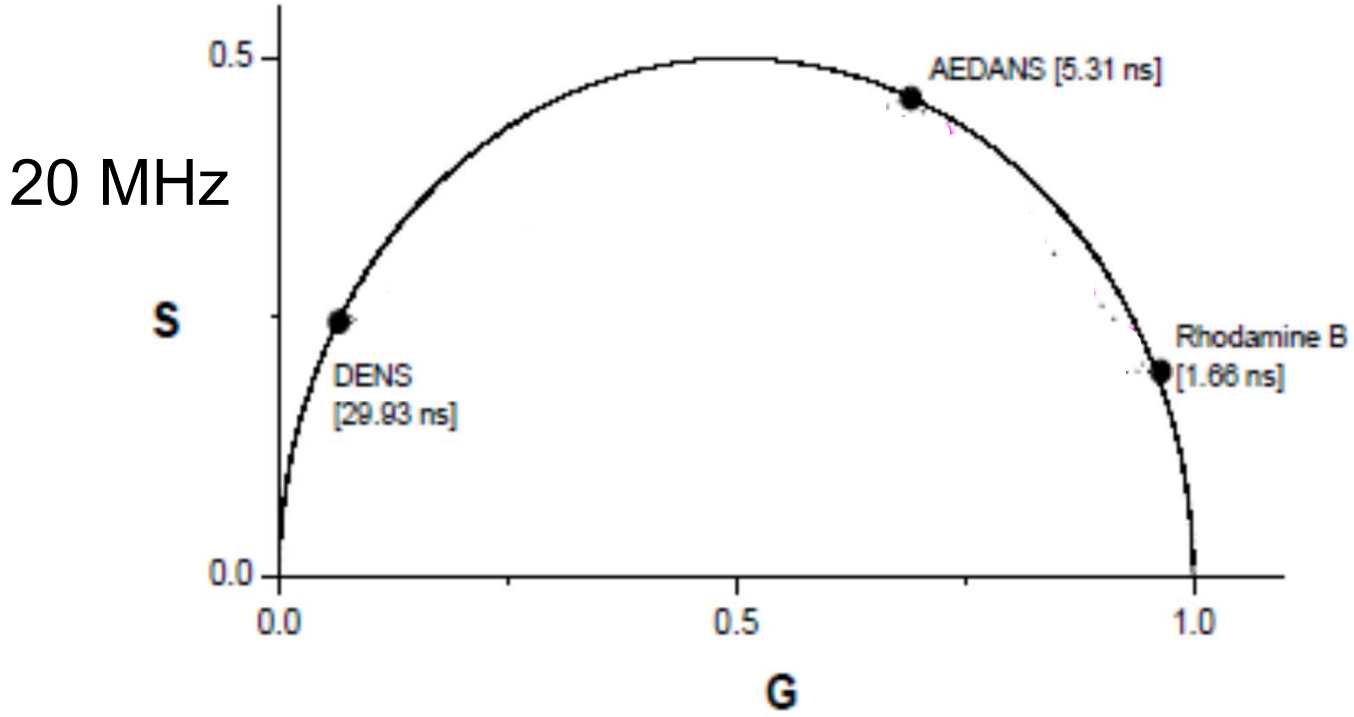

# Methodological measurements I

- Map the position of the mixture of three different single-exponential dyes (Rhodamine B, AEDANS, DENS)
- The mixture lies inside the hypothetical triangle
- When some of the dye is added to the mixture – the point is moved towards the appropriate triangle vertex

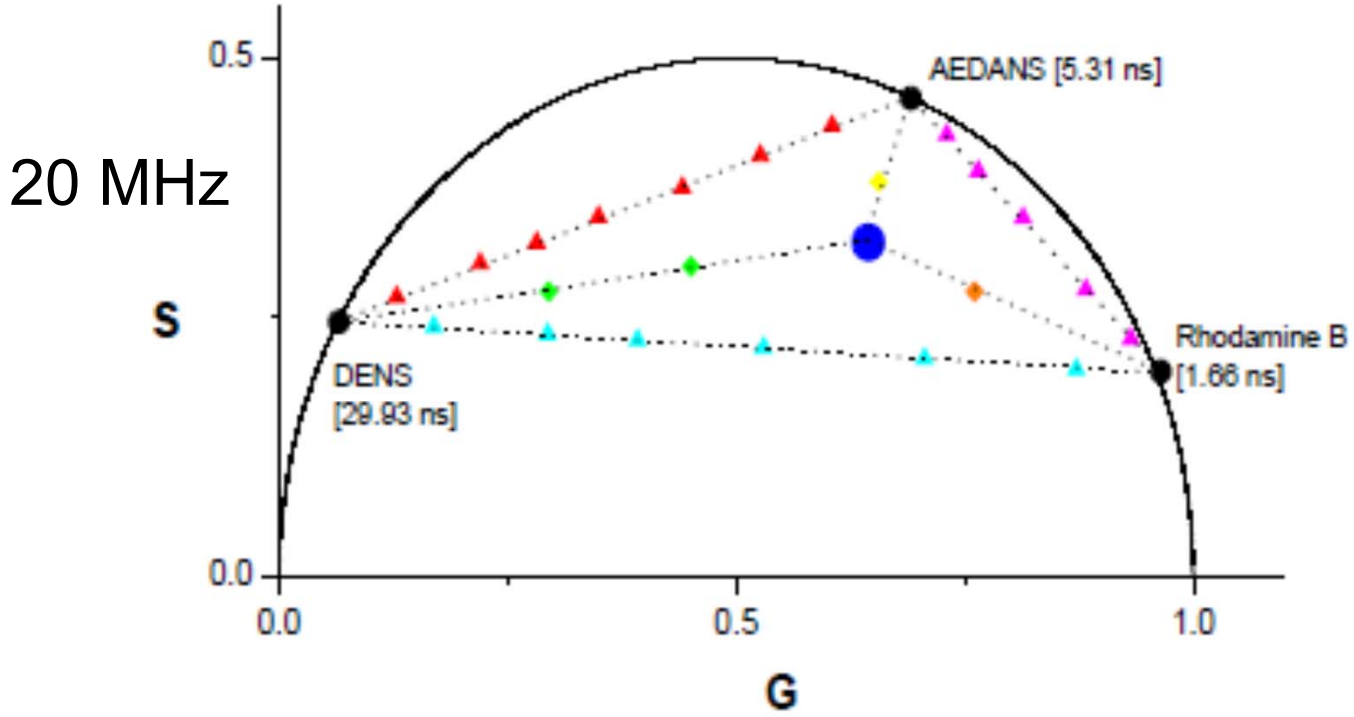

# Methodological measurements II

- When analyzed for different frequencies – position of the hypothetical triangle in universal circle is anticlockwisely shifted when modulation frequency is increased
- Middle points copy the curvature of the universal circle

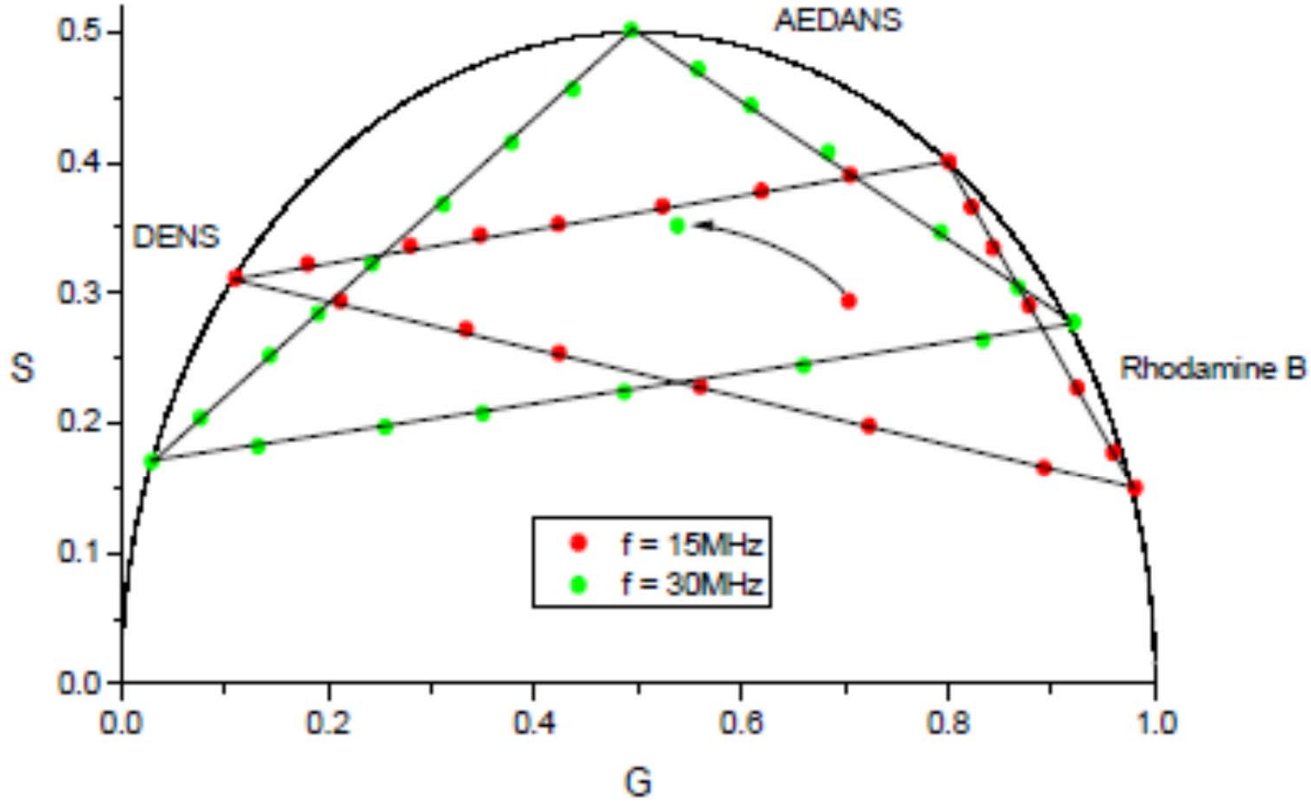

# Phasor Plots for the Analysis of Time-resolved Fluorescence

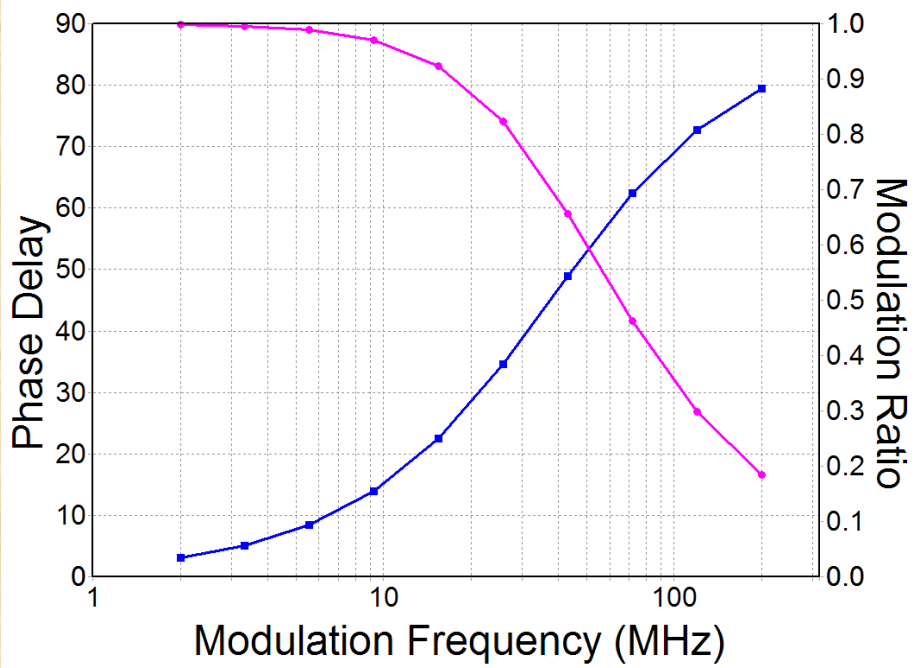


Figure 5.1 Phase and modulation data for a solution of Anthracene in ETOH; the excitation light source is a cw LED emitting at 370 nm. The measured decay time is 4.25 ns.

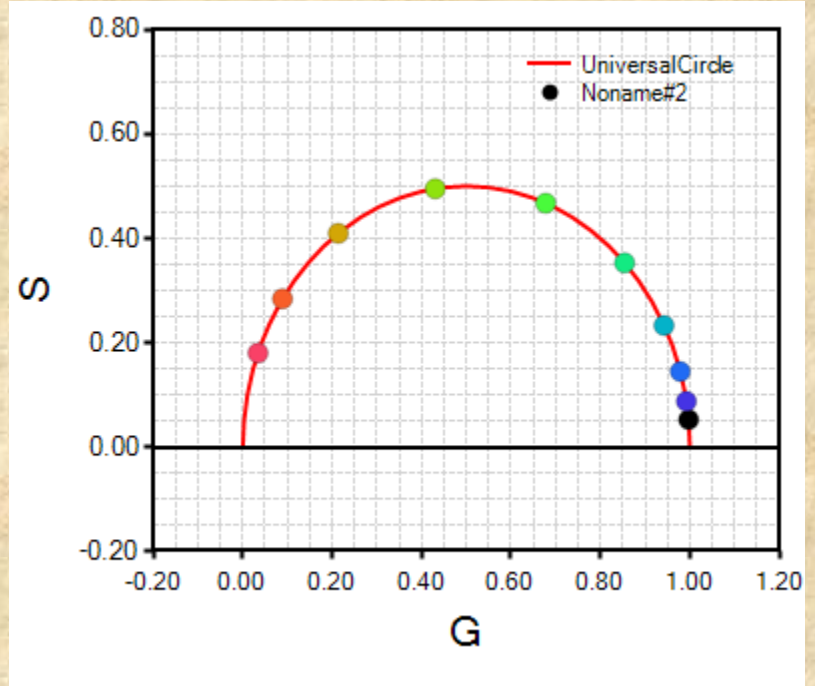


Figure 5.2 Polar plot representing the data.

Technical note by Eugene Povrozin, Norin Redes and Beniamino Barbieri
ISS Inc

http://iss.com/resources/pdf/technotes/Time-resolved_Fluorescence_Phasor_Plots.pdf

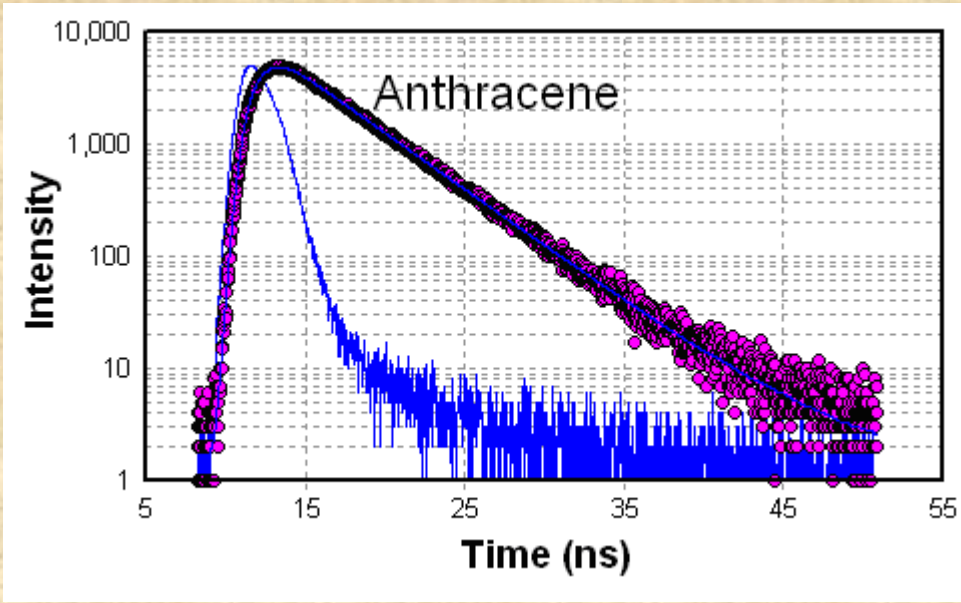


Figure 5.3 Decay time of a solution of Anthracene in ETOH; the excitation source is a pulsed LED emitting at 335 nm. The measured decay time is 4.24 ns.

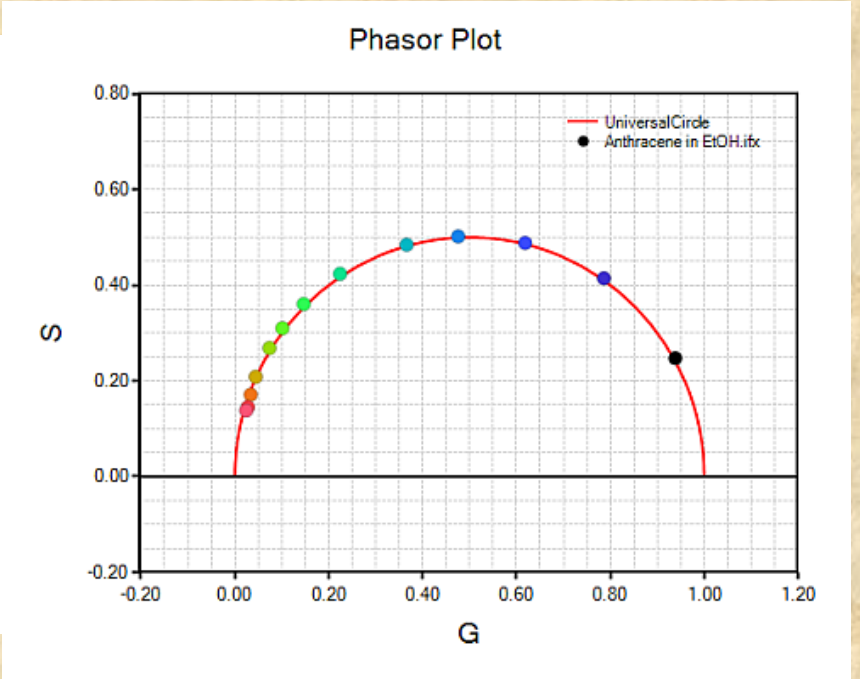


Figure 5.4 – Polar plot representing the data. The main frequency is 20 MHz; the other points are the harmonics, 40, 60, … MHz.

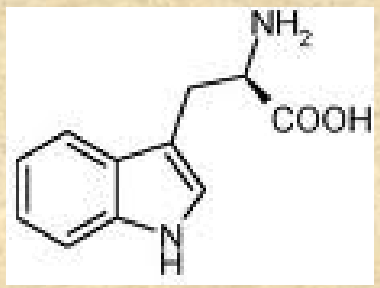


The pH dependent forms of tryptophan in solution are the zwitterionic and anionic forms due to the protonation of the amine and carboxyl groups – the pKa of the amine group is 9.39

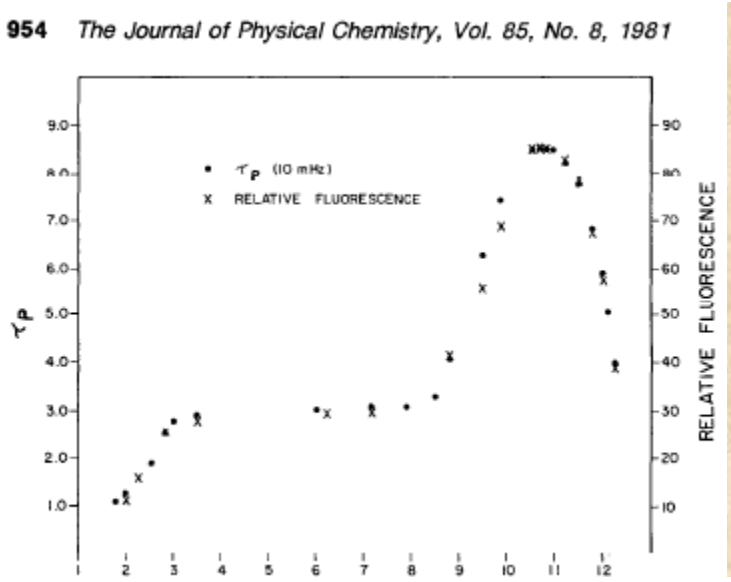



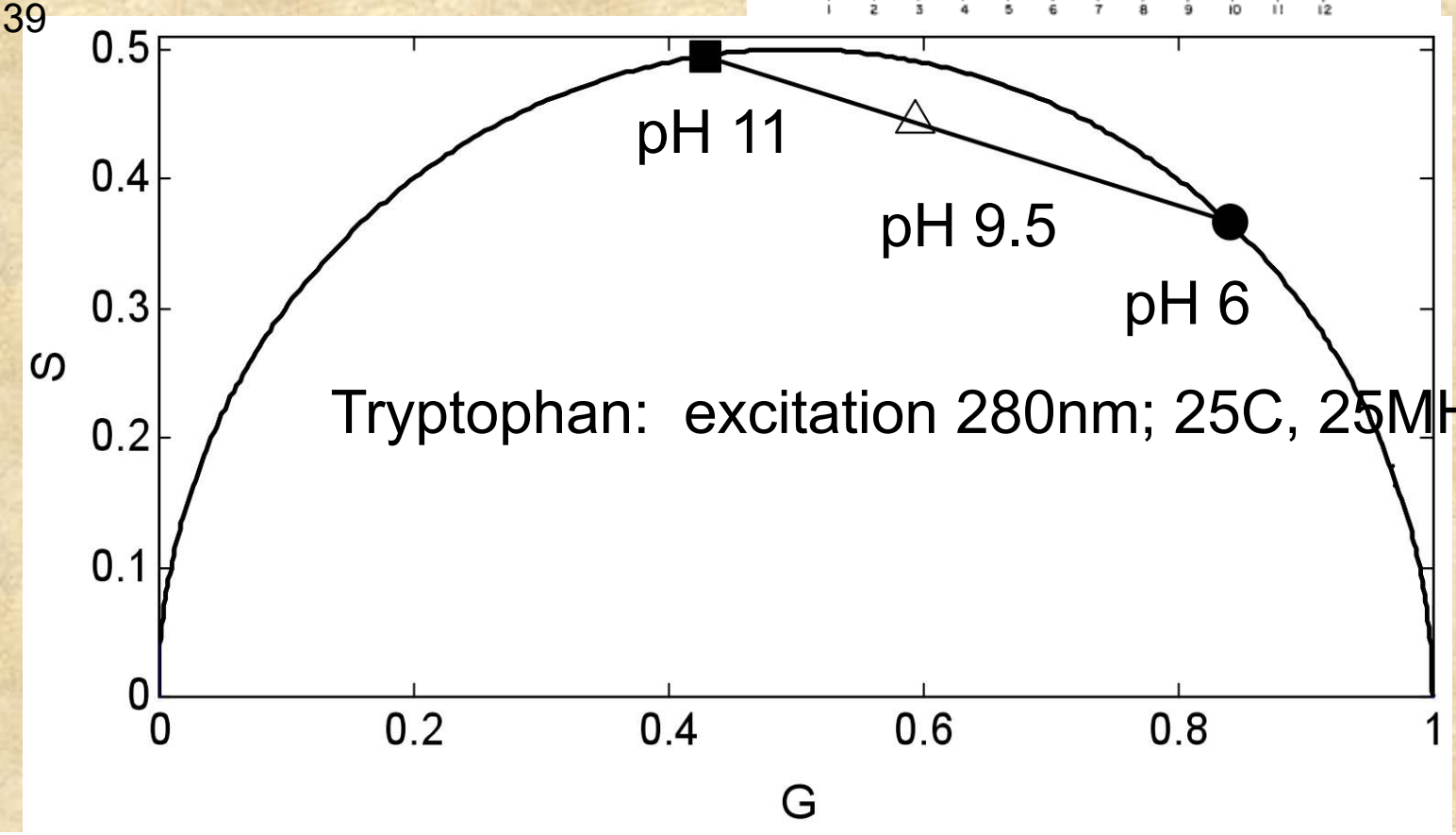

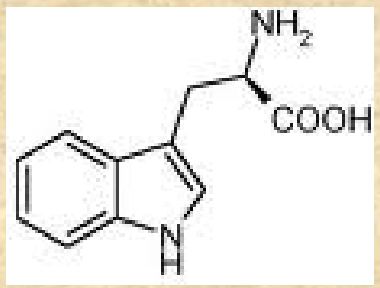


The pH dependent forms of tryptophan in solution are the zwitterionic and anionic forms due to the protonation of the amine and carboxyl groups – the pKa of the amine group is 9.39

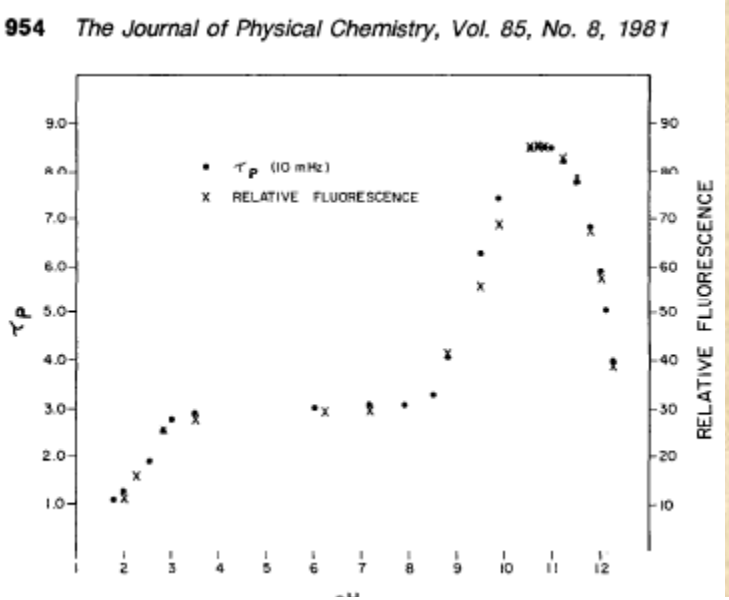


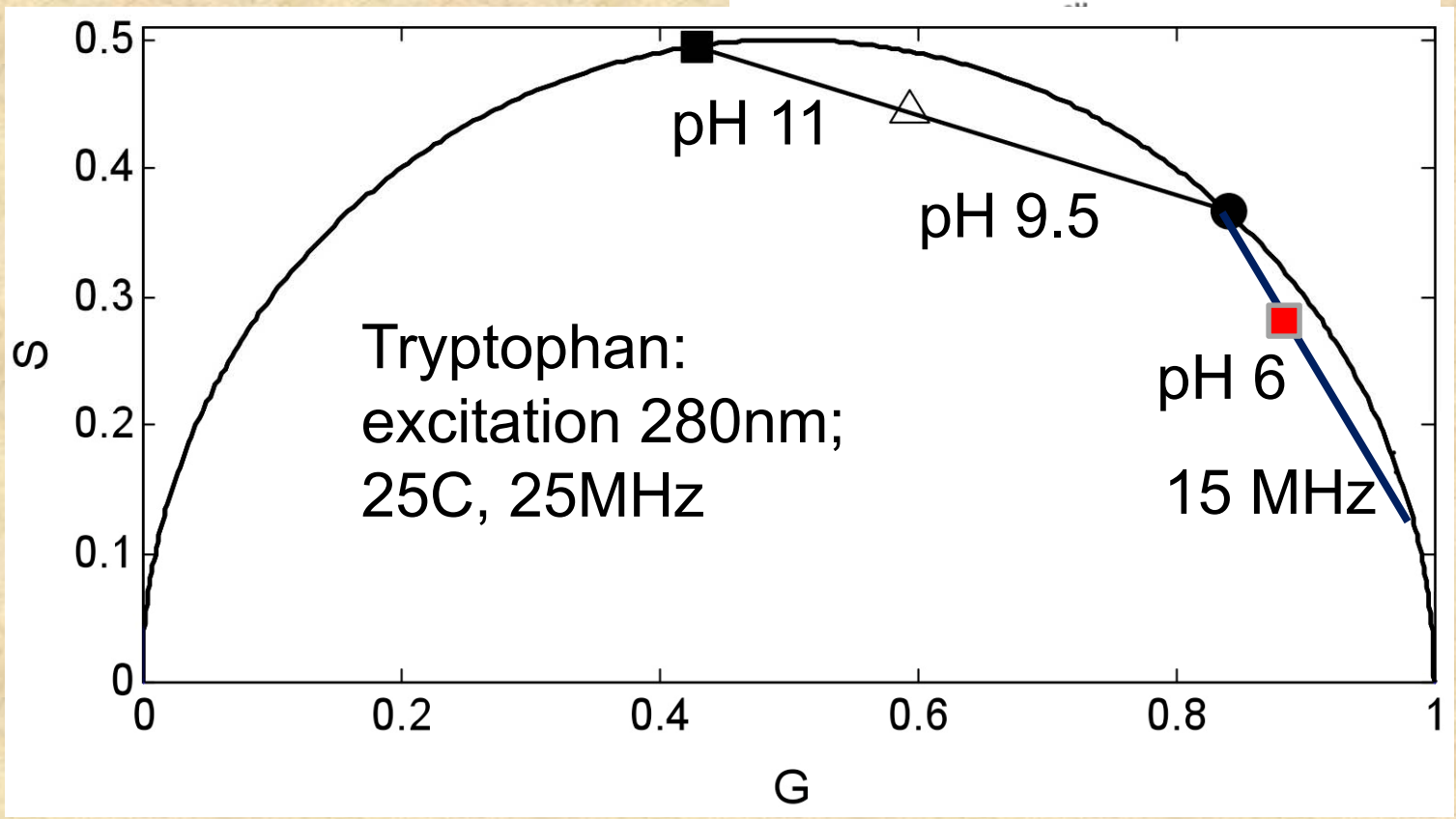

# NATA

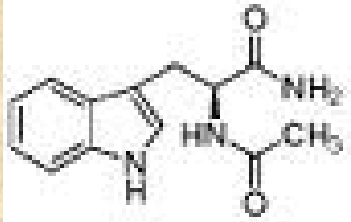


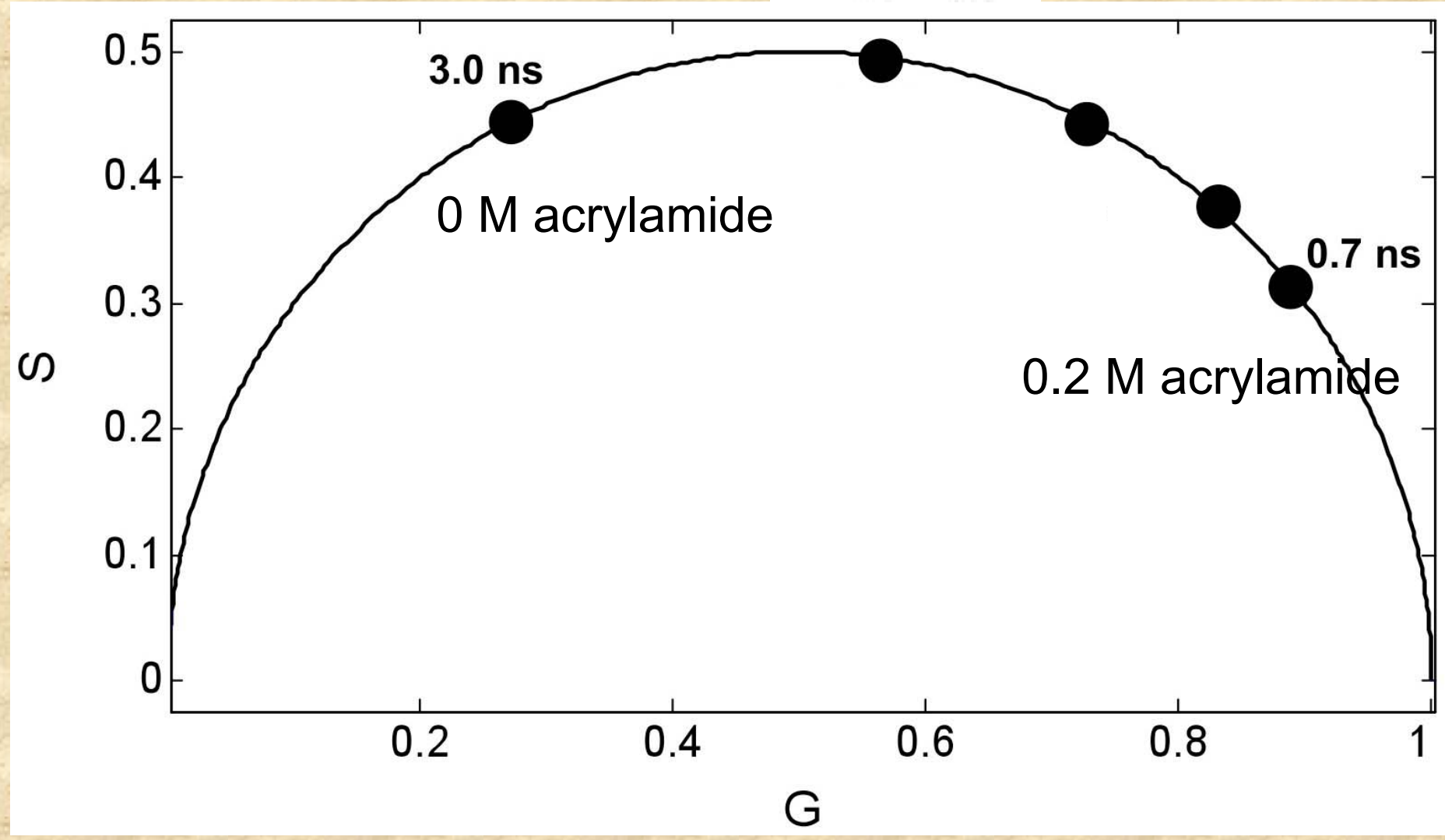


89 MHz; 20C

# lysozyme

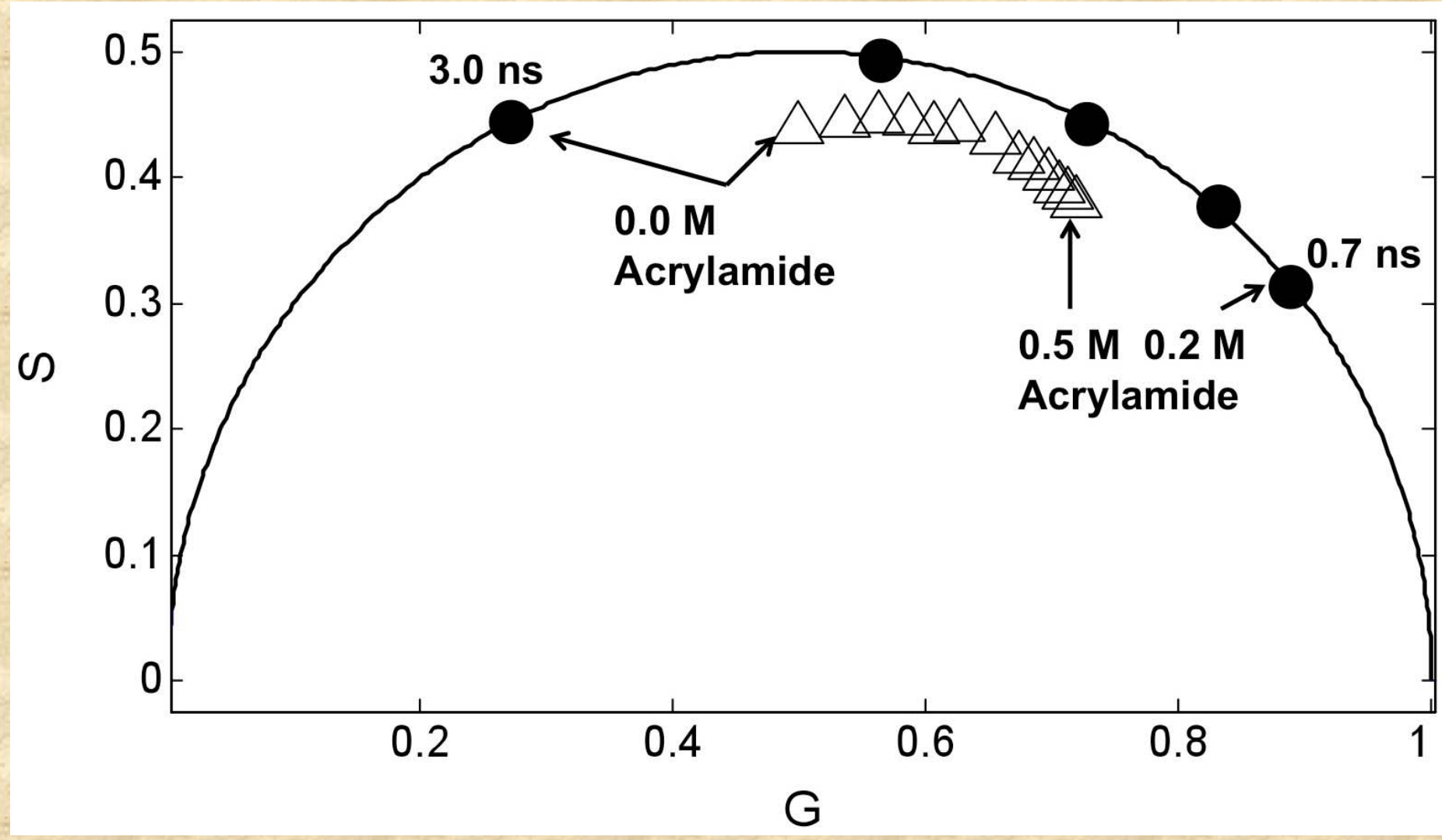


89 MHz; 20C

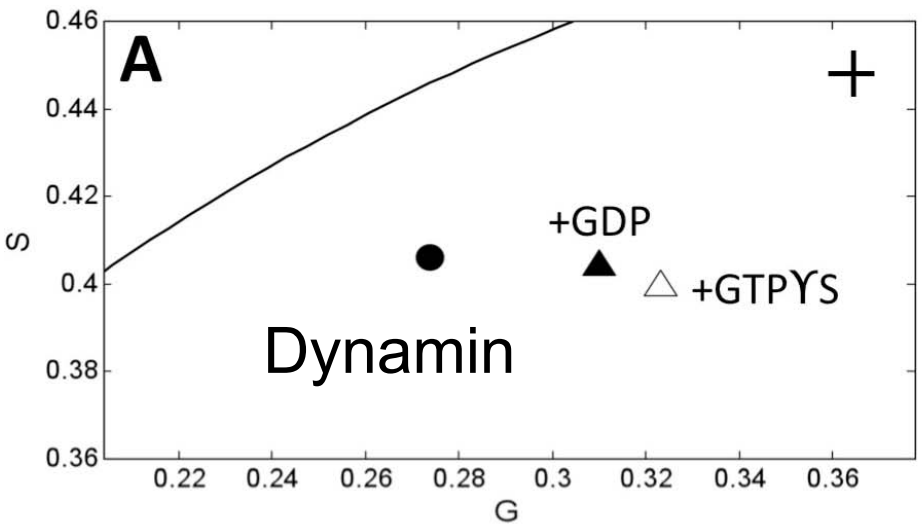
A
0.46
0.44
0.42
0.4
0.38
0.36
S
0.22
0.24
0.26
0.28
0.3
0.32
0.34
0.36
G
+GDP
+GTPγS
Dynamin

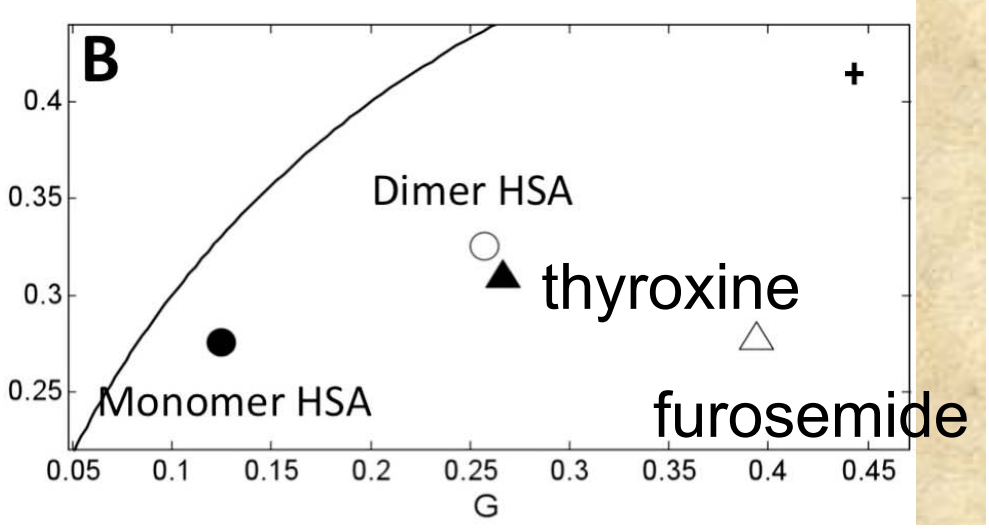
B
0.4
0.35
0.3
0.25
0.05
0.1
0.15
0.2
0.25
0.3
0.35
0.4
0.45
G
Dimer HSA
thyroxine
Monomer HSA
furosemide

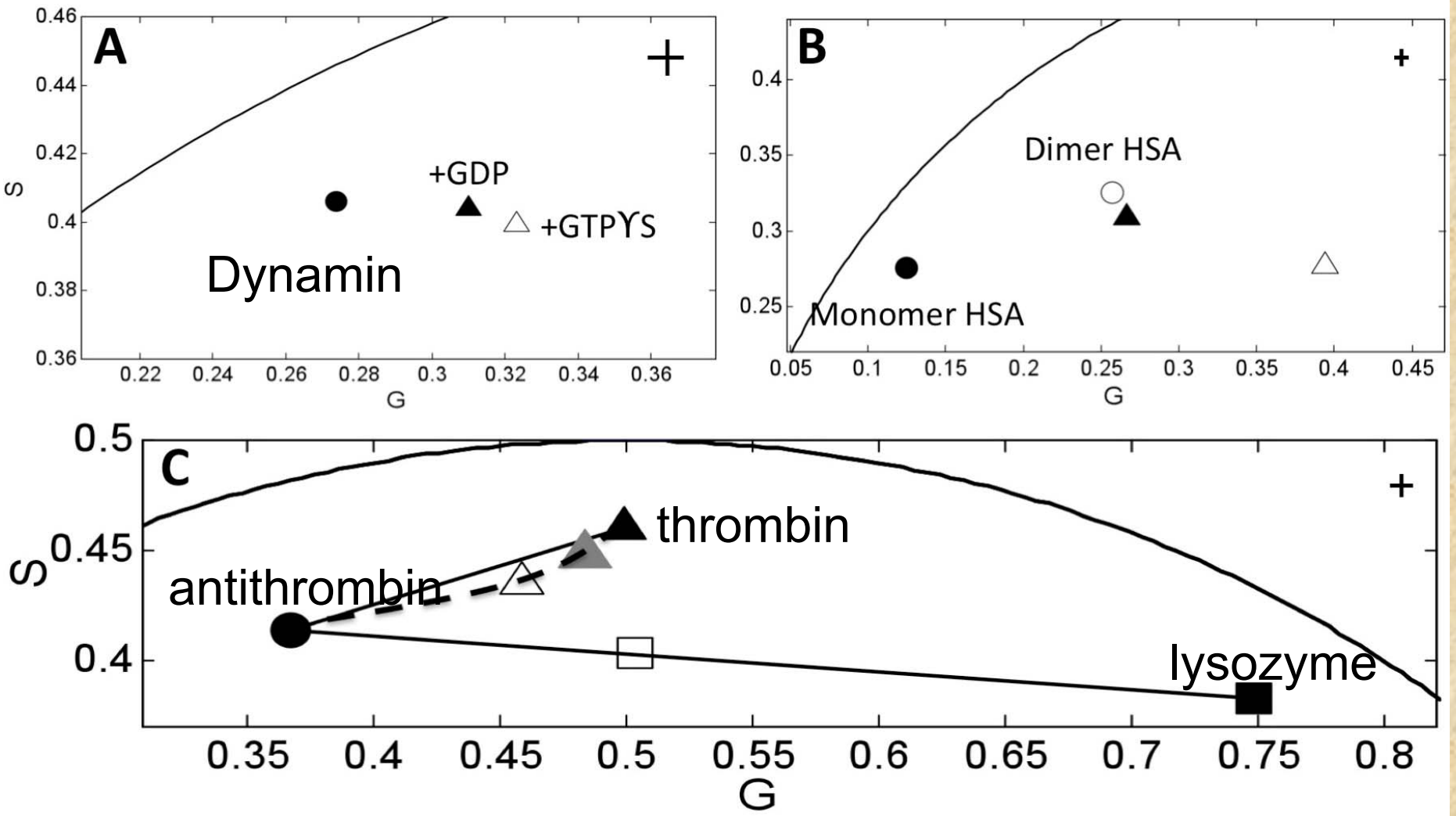
A
+GDP
+GTPγS
Dynamin
S
G
B
Dimer HSA
Monomer HSA
G
C
thrombin
antithrombin
lysozyme
S
G

# lysozyme

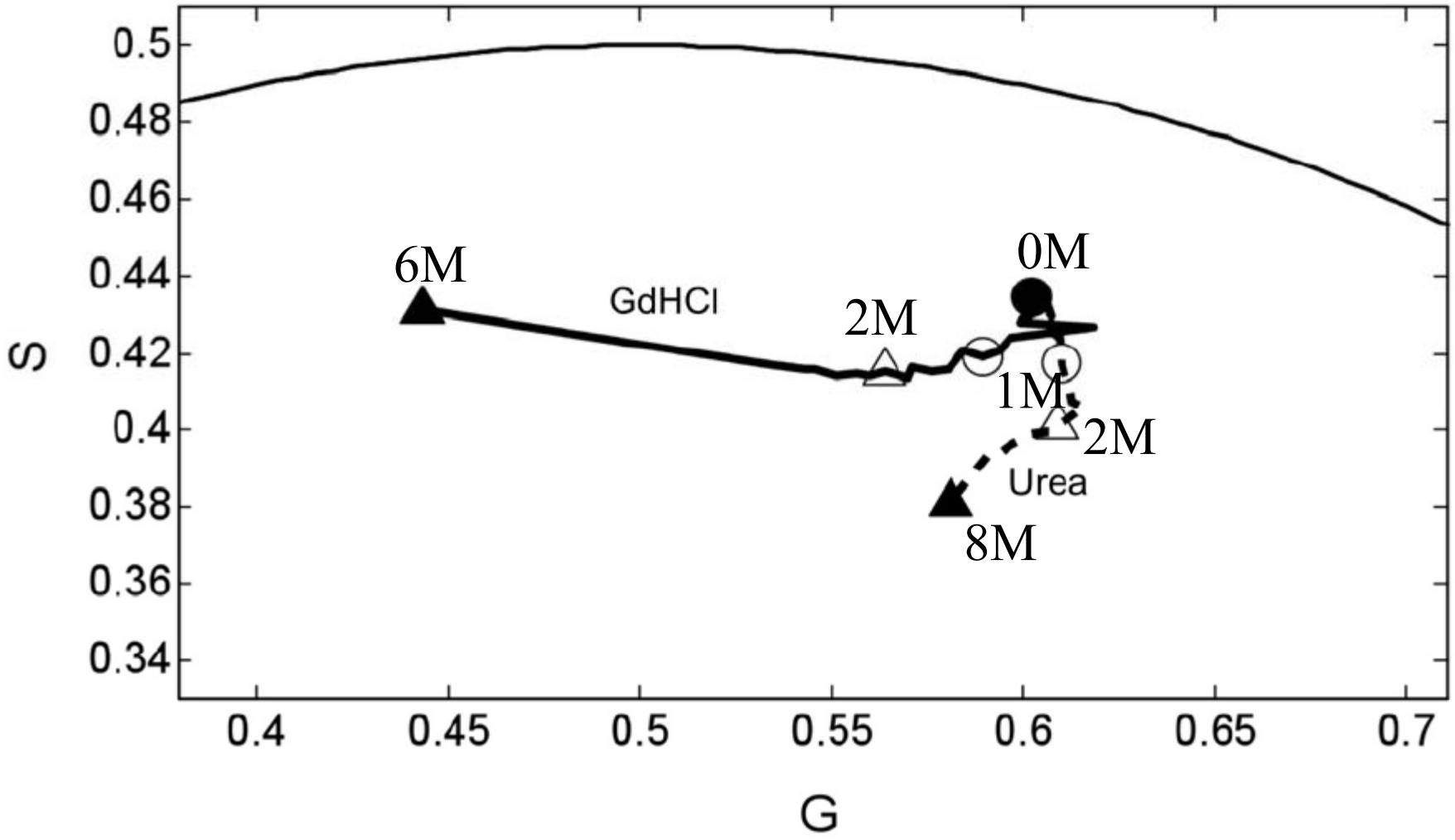
0.5
0.48
0.46
0.44
0.42
0.4
0.38
0.36
0.34
S
0.4
0.45
0.5
0.55
0.6
0.65
0.7
G
6M
GdHCl
2M
0M
1M
2M
Urea
8M

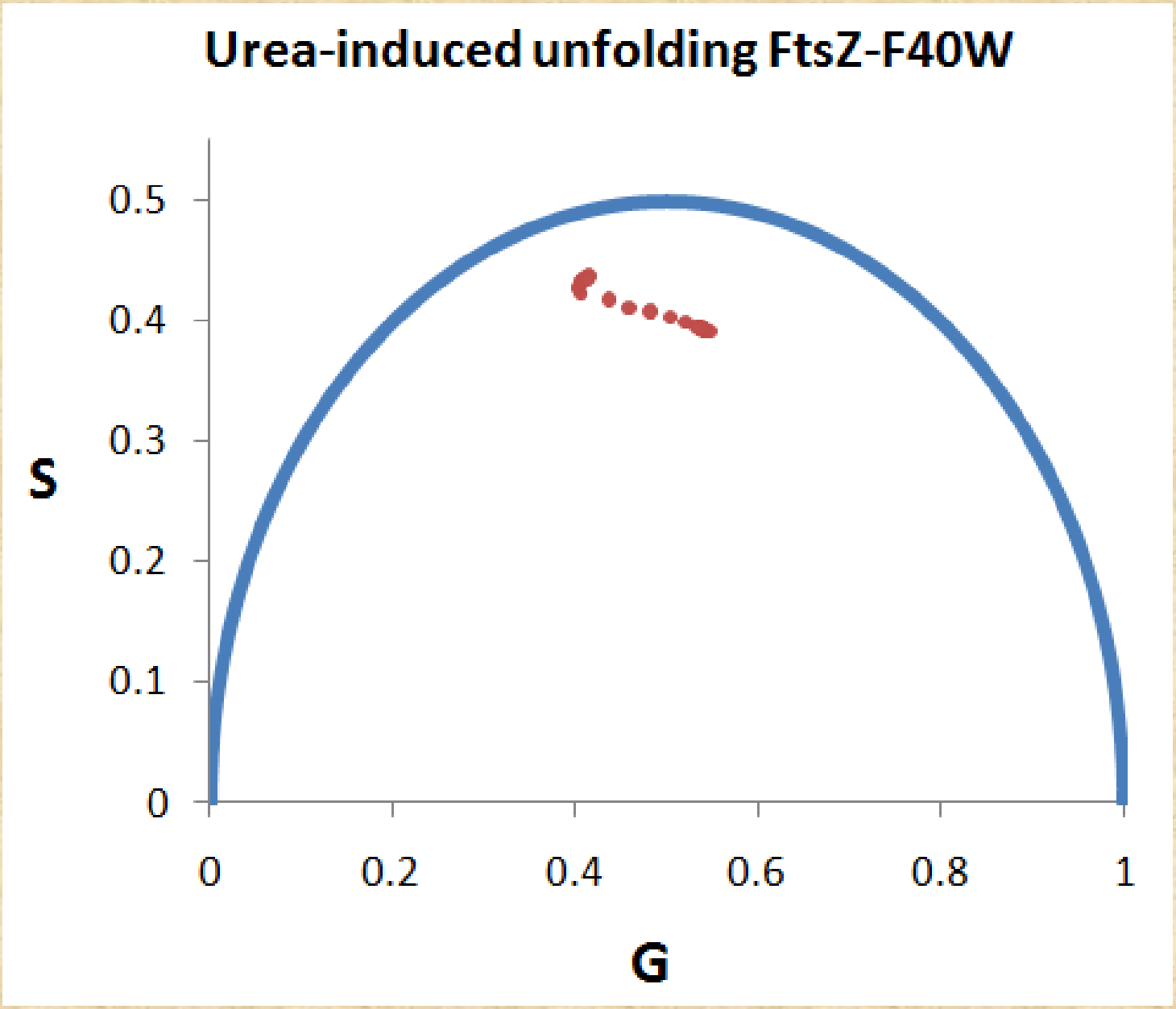


Data of Felipe Montecinos

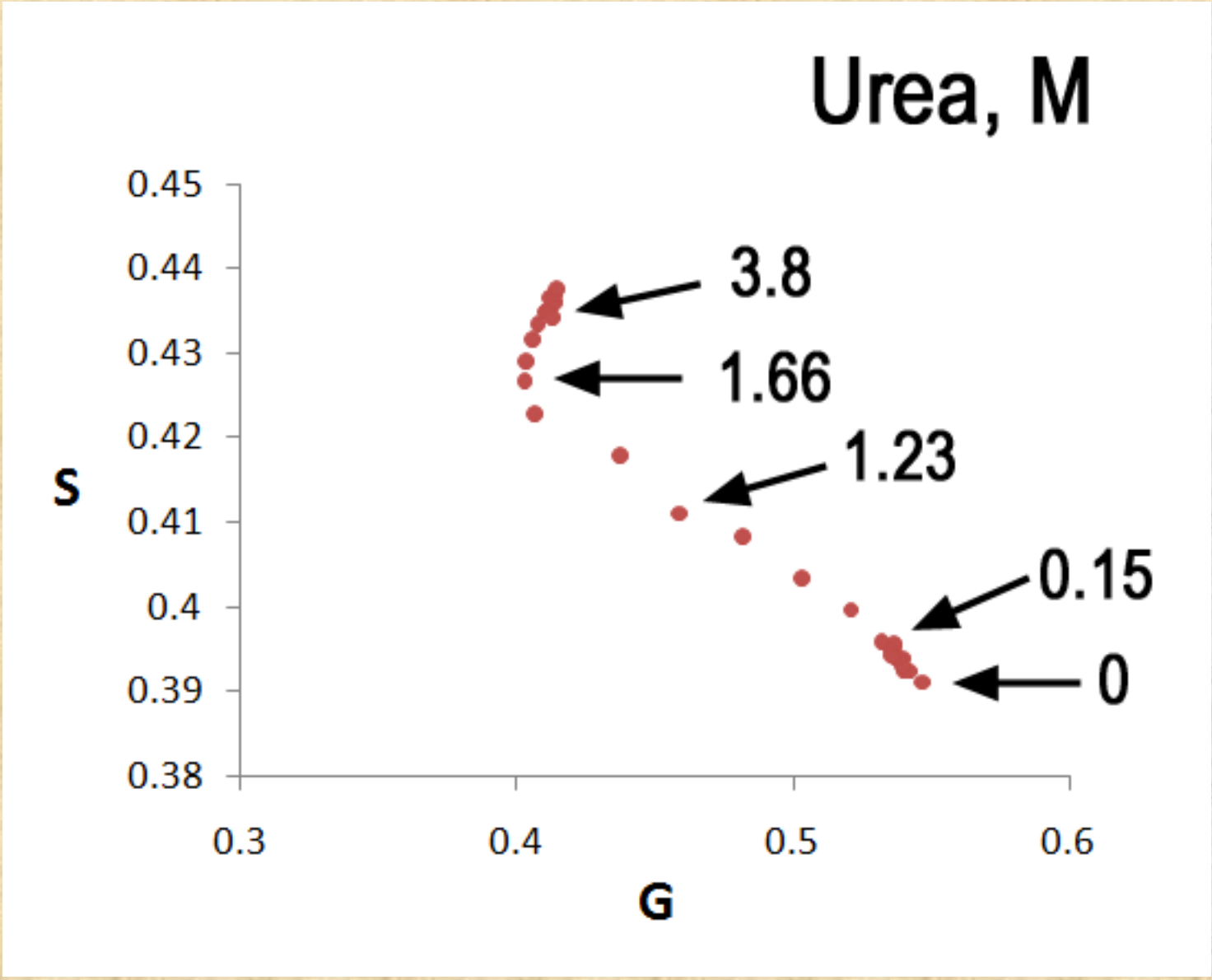


Data of Felipe Montecinos

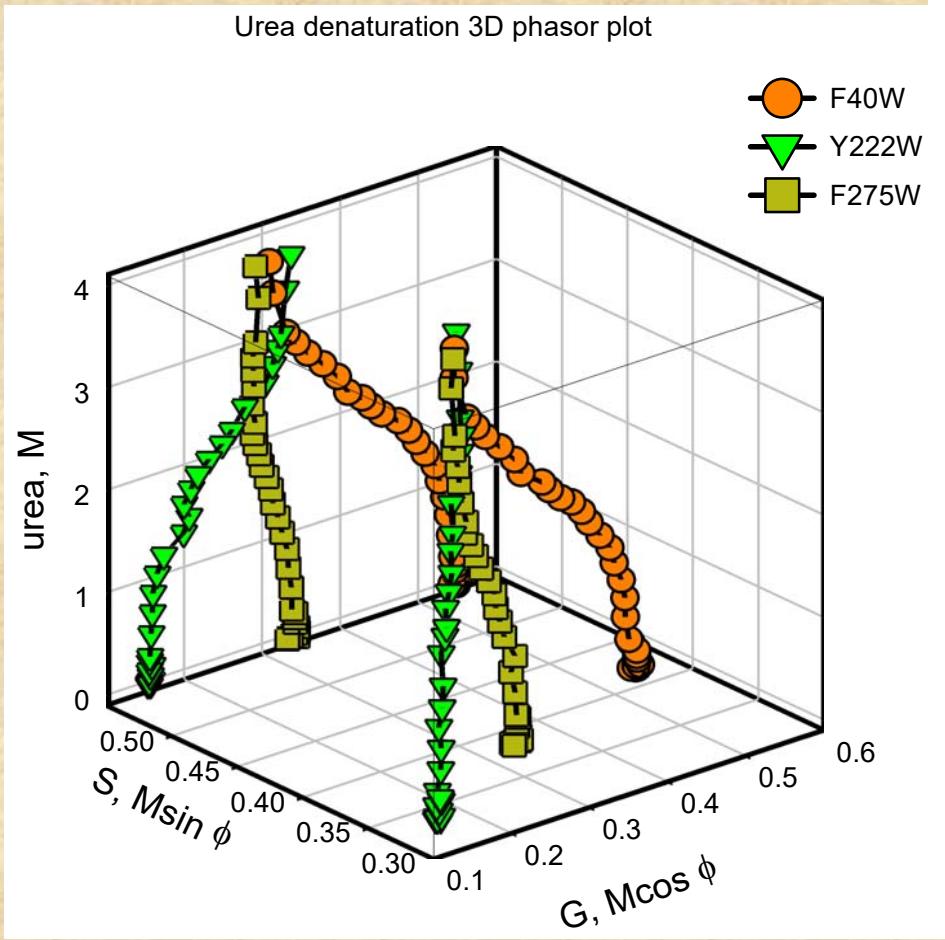


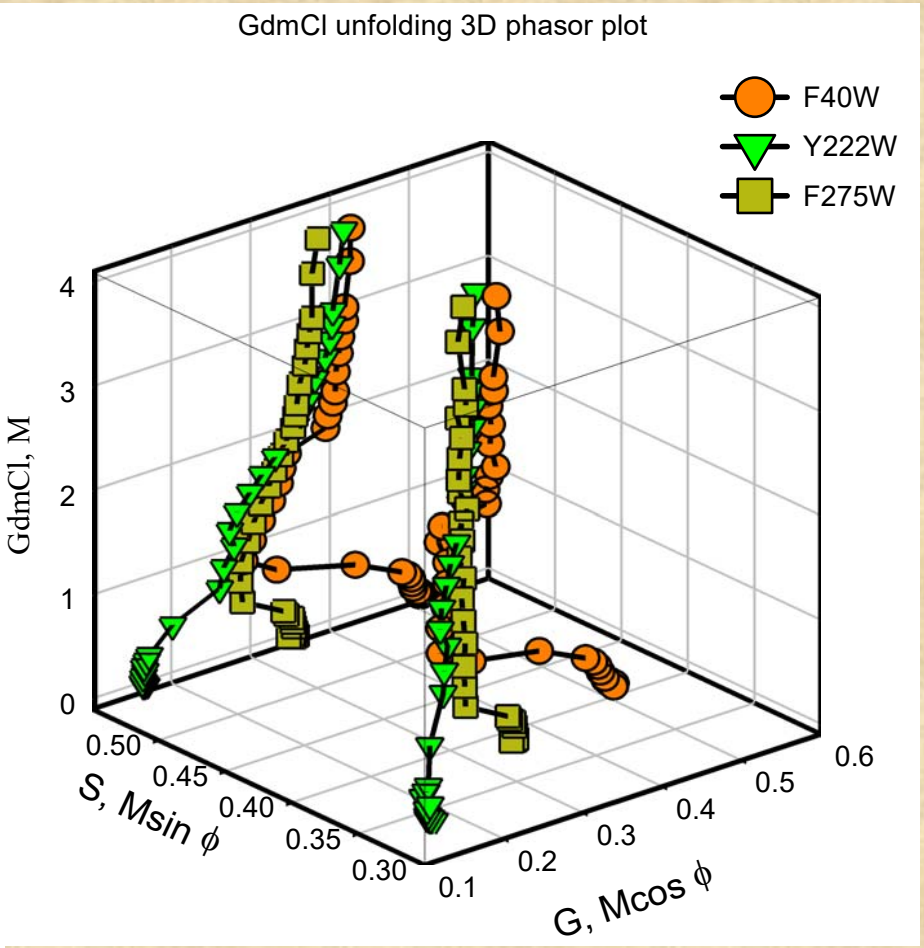


Montecinos-Franjola, F., James, N.G., Concha-Marambio, L., Brunet, J.E., Lagos, R., Monasterio, O., Jameson, D.M. (2014) Biochim Biophys Acta. 1844(7):1193-200. Single tyrptophan mutants of FtsZ: Nucleotide binding/exchange and conformational transitions.

*Journal of Microscopy*, 2011
*Received 27 May 2010; accepted 6 January 2011*
doi: 10.1111/j.1365-2818.2011.03488.x

# Spectral resolution in conjunction with polar plots improves the accuracy and reliability of FLIM measurements and estimates of FRET efficiency

Y.-C. CHEN* & R.M. CLEGG*,†
*Bioengineering Department, University of Illinois at Urbana-Champaign, Urbana, IL, U.S.A.
†Department of Physics, Center for Biophysics and Computational Biology, University of Illinois at Urbana-Champaign, Urbana, IL, U.S.A.

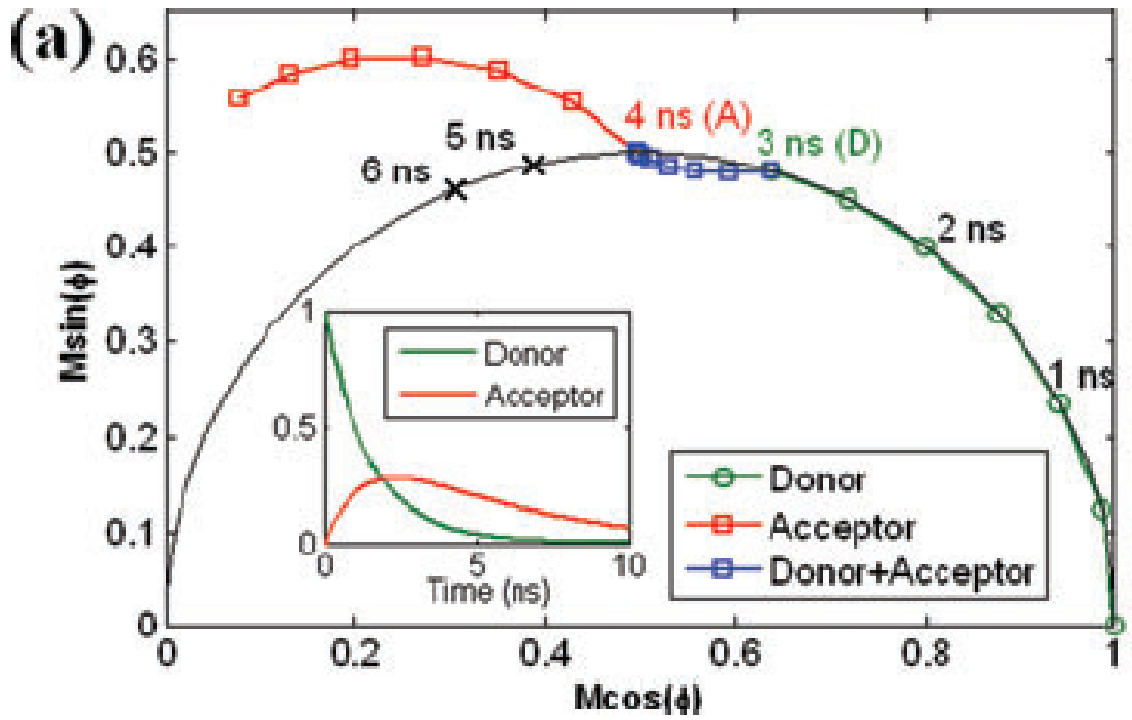

# FRET in GFP

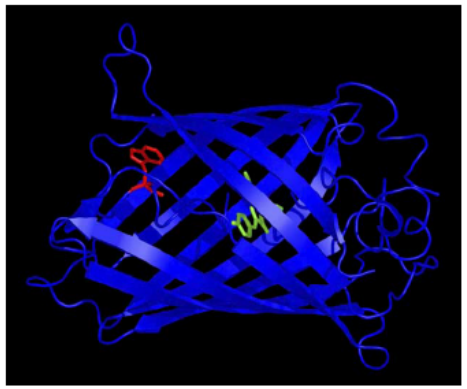

Fig. 1. 3D structure of GFP (blue) with the tryptophan in red and the fluorophore in green. (For interpretation of the references to colour in this figure legend, the reader is referred to the web version of this article.)

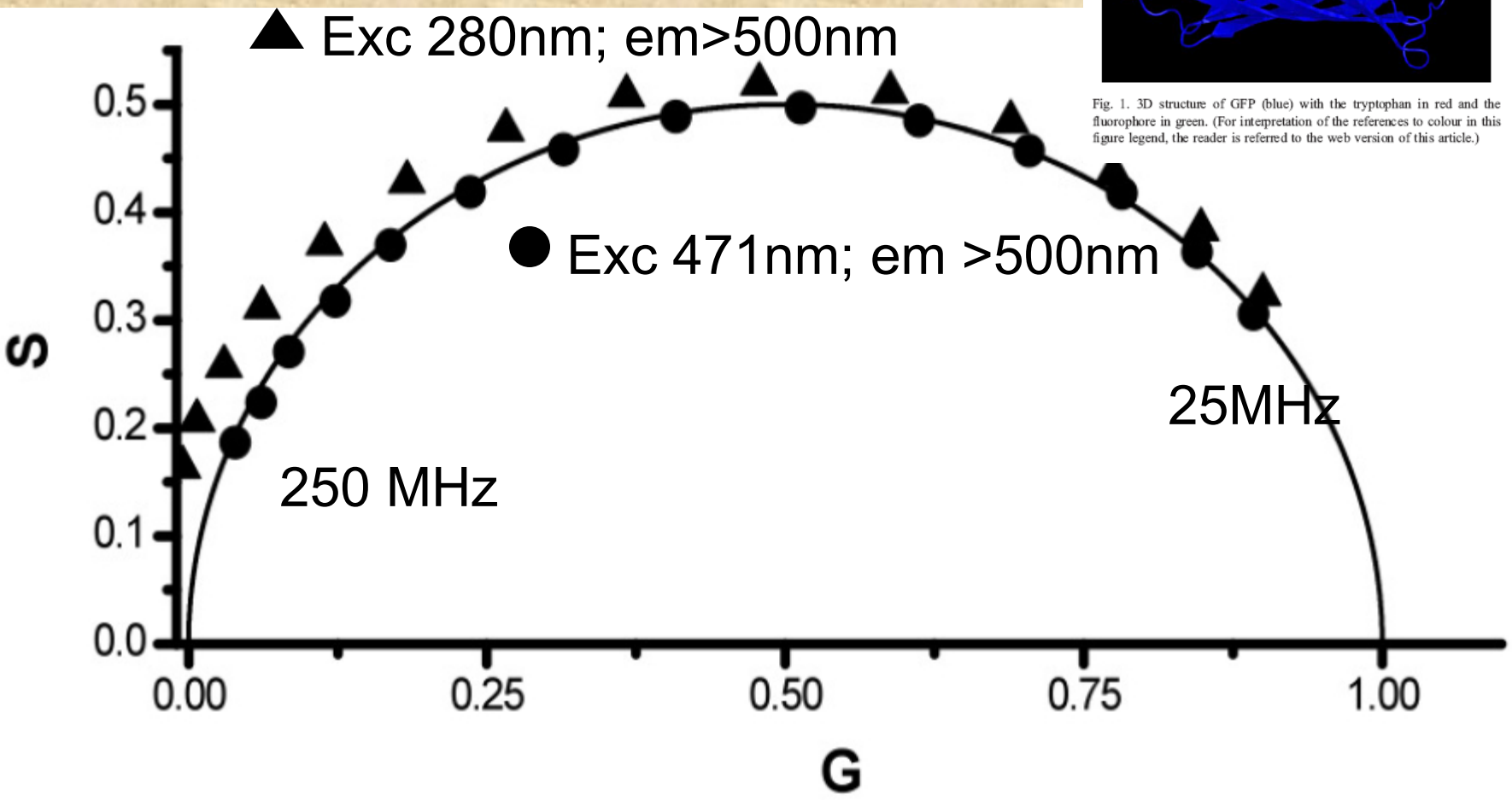

Methods and Applications in Fluorescence

PAPER

# Investigation of the conformational flexibility of DGAT1 peptides using tryptophan fluorescence

Jose L S Lopes[1,2], Ana P U Araujo[1] and David M Jameson[2]

[1] Institute of Physics of Sao Carlos, University of Sao Paulo, Sao Carlos, SP, Brazil
[2] Department of Cell and Molecular Biology, University of Hawaii at Manoa, Honolulu, HI, USA

## DGAT1 peptides

diacylglycerol acyltransferase 1 enzyme

Sit1 (FGDREFYRDWWNSES)

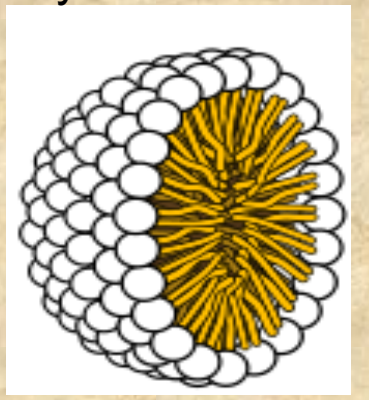

N-hexadecyl-N,N-dimethyl-3-ammonio-1-propanesulfonate (HPS)


JAKNAPP 26

s

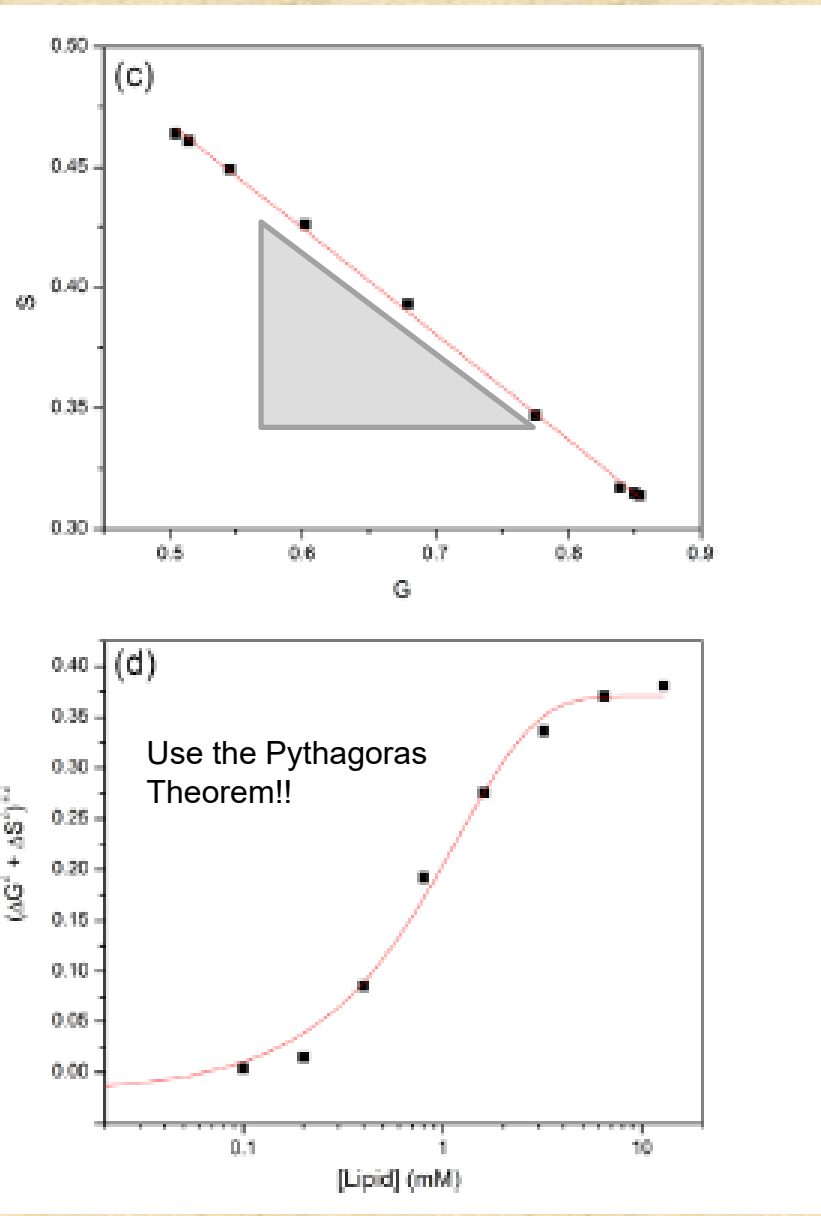
(c)
S
G
0.50
0.45
0.40
0.35
0.30
0.5
0.6
0.7
0.8
0.9
(d)
Use the Pythagoras Theorem!!
[Lipid] (mM)
0.40
0.35
0.30
0.25
0.20
0.15
0.10
0.05
0.00
0.1
1
10

# The protein Prdx 1 (a peroxiredoxin) decamer at high concentrations whi dissociates into dimers upon dilutio

Decamer

Dime

(done in collaboration with Matias Möller, Joaquin Dallarizza, Sebastian Villar and Ana Denicola – in Uruguay)

In fact we don't care how complex the lifetime is since we will only get one phasor point at any given concentration. We only hoped that the lifetime of the protein changes upon the decamer to dimer transition.

I have recently been told that when cleaner buffers were prepared the main line continued without the downward curvature

Which it does!

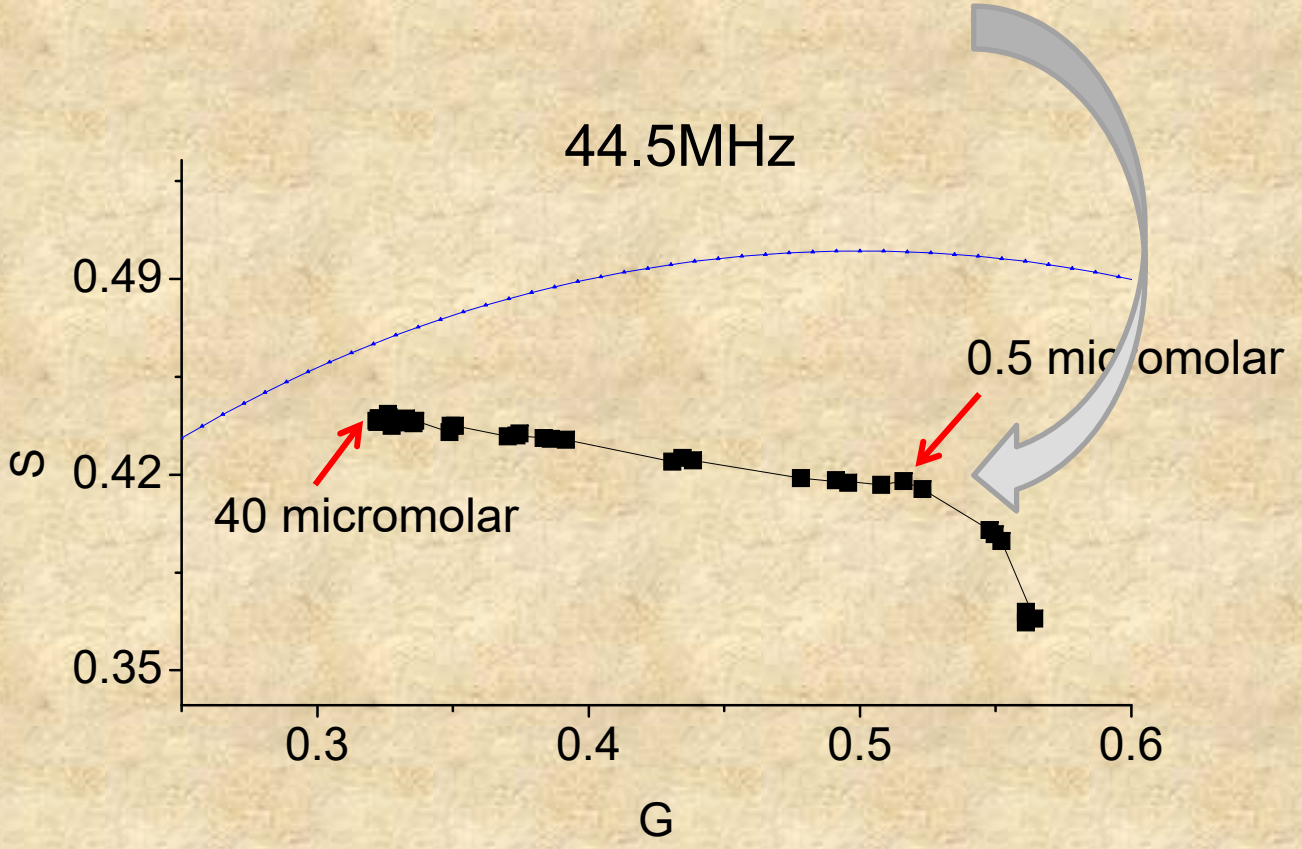

# The degree of dissociation can then be mapped along the hypotenuse

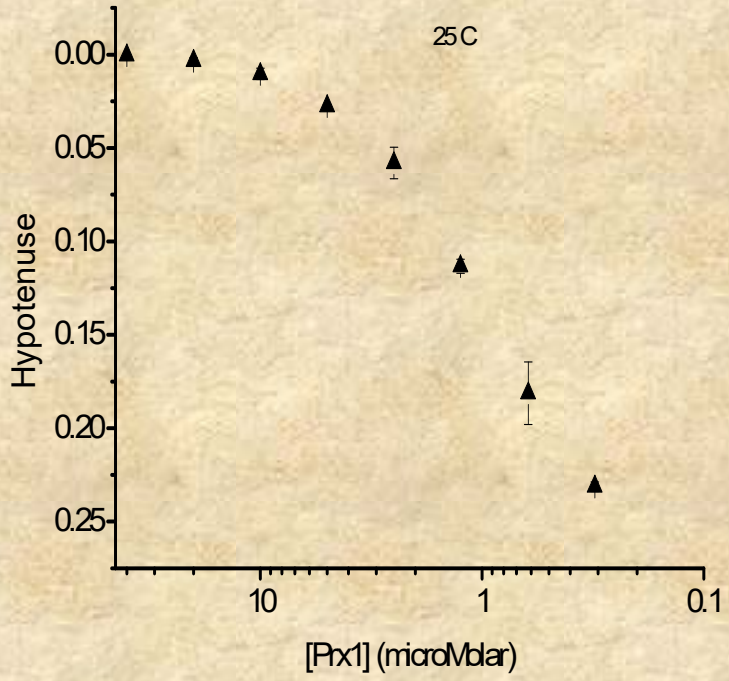


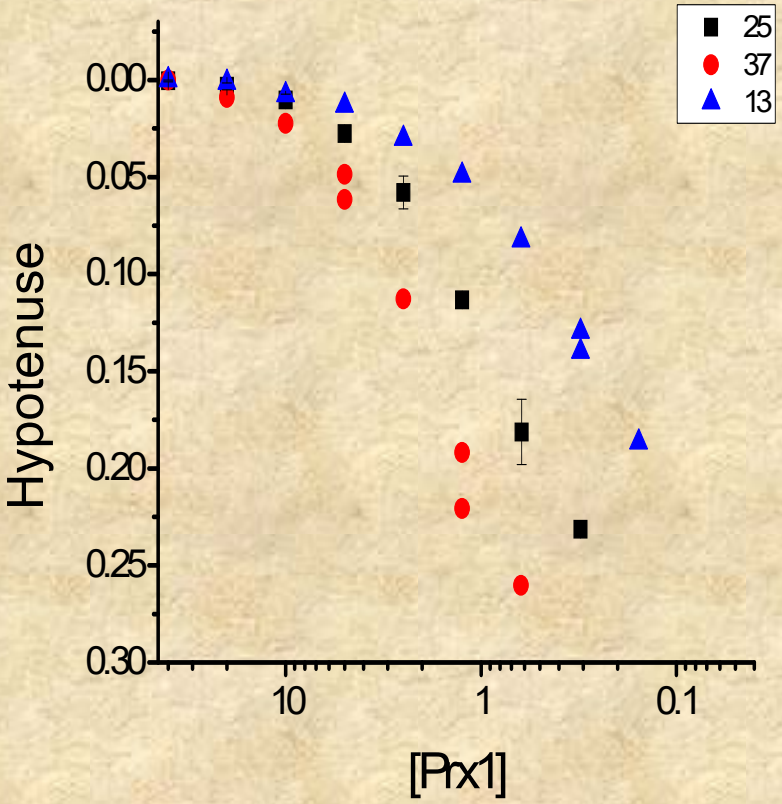

# Utilization in lipid vesicles

- Vesicle – small membrane enclosed sac
- Laurdan in DMPC vesicles (transition temperature 23 °C)
- Measured for temperature range from 5 to 55°C
- Similar behaviour to glycerol solution

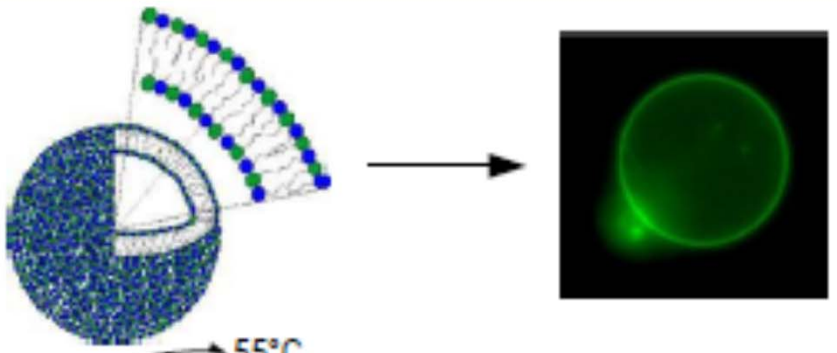

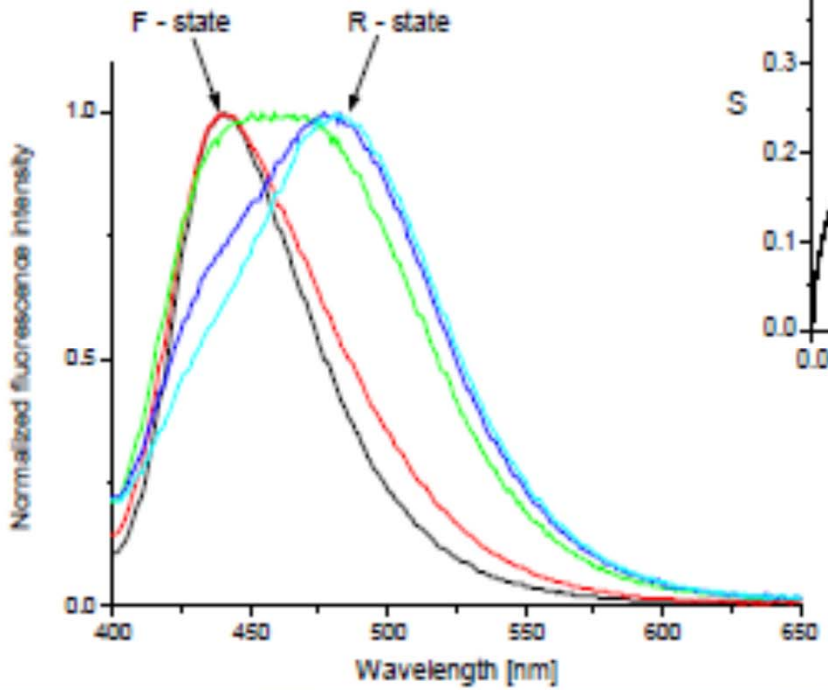


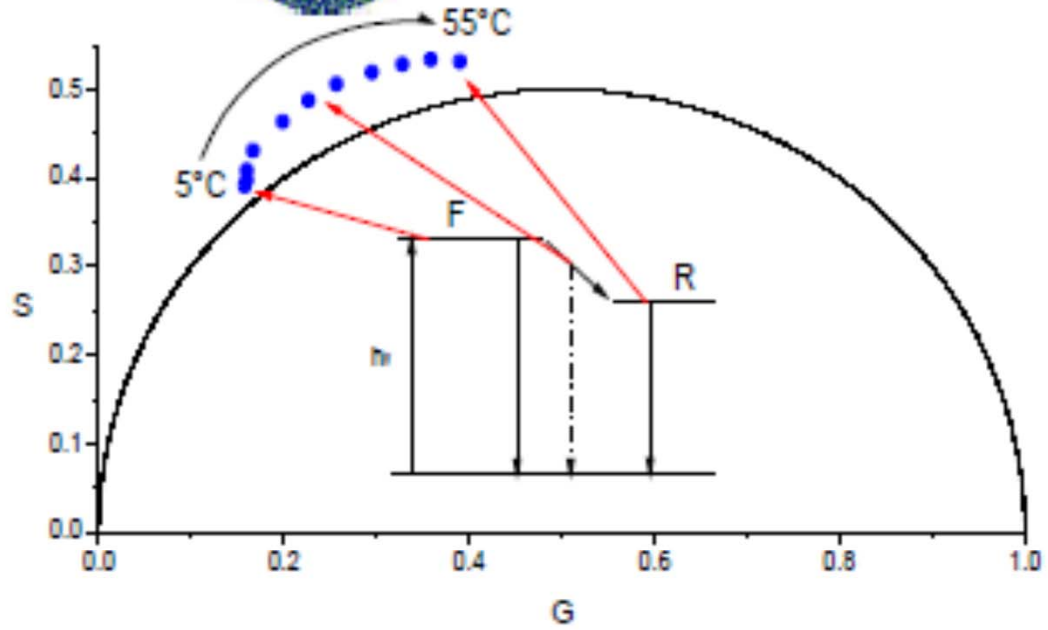


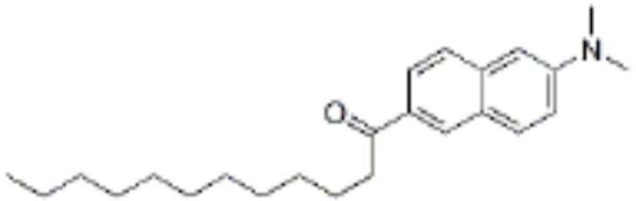

# Phase transitions of complex lipid systems

Data of Leonel Malacrida

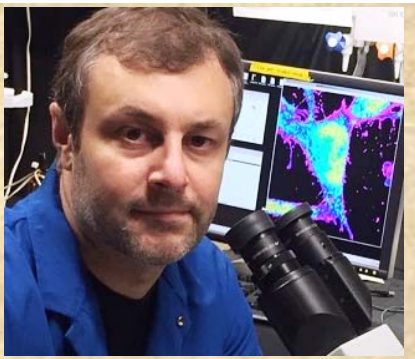

- DPPC
- DPPC:PC:Chol (1:1)+20% mol Chol
- DPPC:DOPC:Chol (1:1)+20% mol Chol

Good models for Pulmonary Surfactant

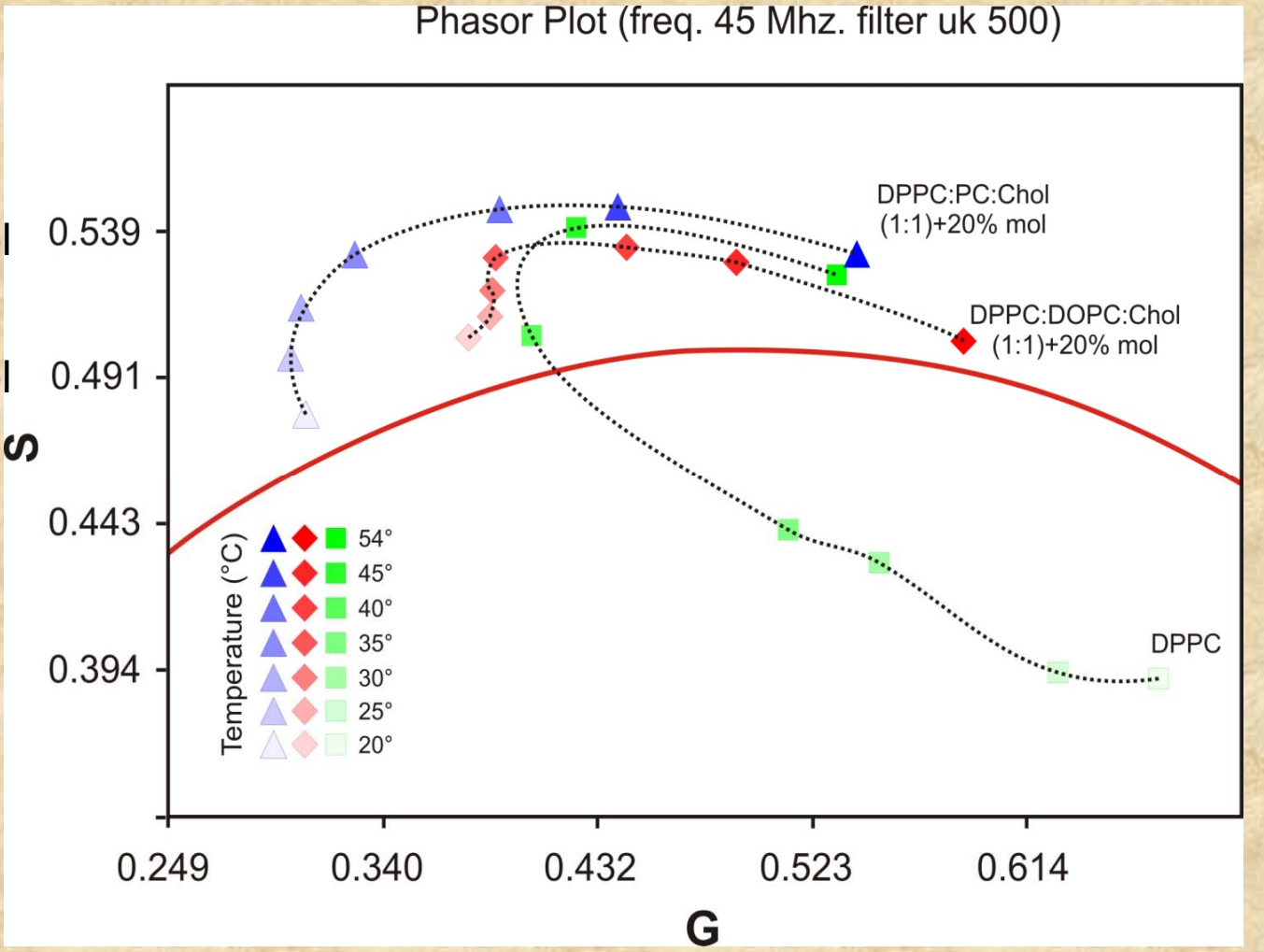

G-Quadruplex DNA are four stranded structures containing two or more stacked square-planar G-tetrads, composed of four Hoogstein hydrogen bonded guanines.

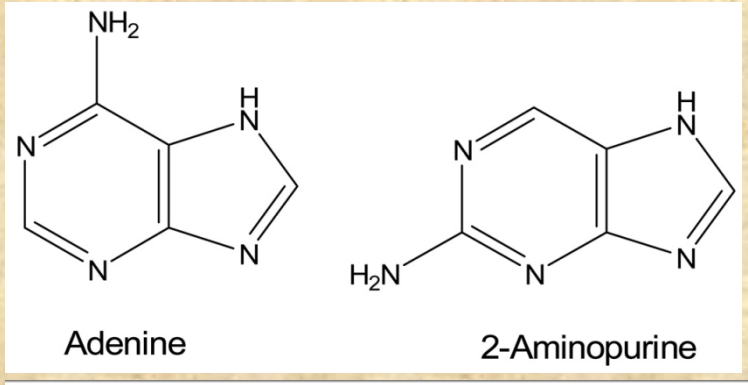


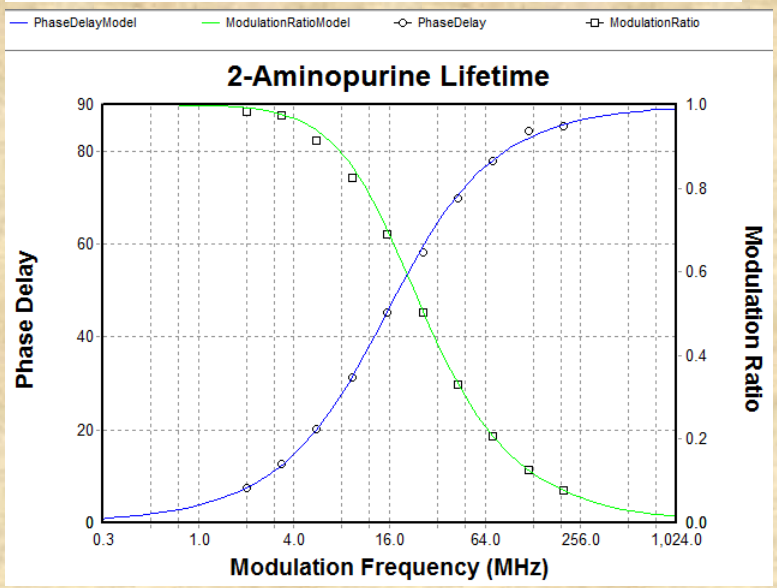


2-Aminopurine free in aqueous solution gives a single exponential lifetime of ~10 ns.

G-Quadruplex structure and stability illuminated by phasor plots
*Robert Buscaglia, David M. Jameson and Jonathan B. Chaires*
*Nucleic Acid Research In Press*

# 2-aminopurine Bases in Human Telomere Quadruplex Structures – Unique Environments for Each Position

| | |
|---|---|
| 1AP - | 5`-**X**GGGTTAGGGTTAGGGTTAGGG |
| 7AP - | 5`-AGGGTT**X**GGGTTAGGGTTAGGG |
| 13AP - | 5`-AGGGTTAGGGTT**X**GGGTTAGGG |
| 19AP - | 5`-AGGGTTAGGGTTAGGGTT**X**GGG |

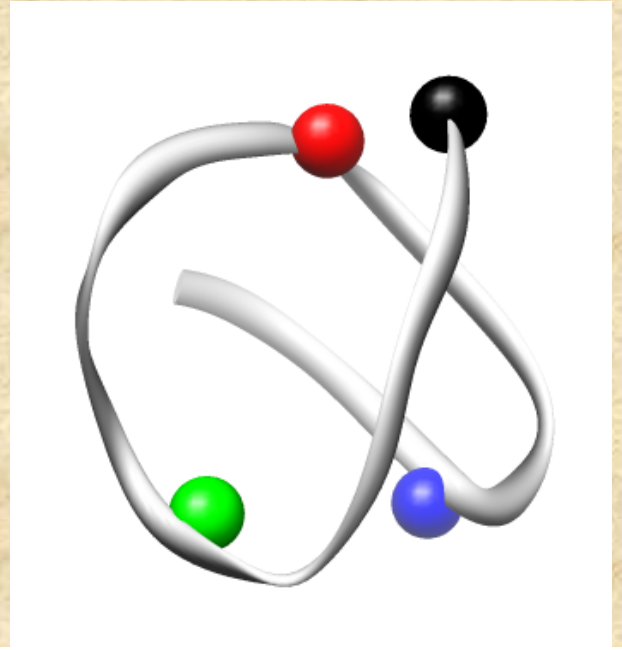

# Potassium and Sodium Phasors

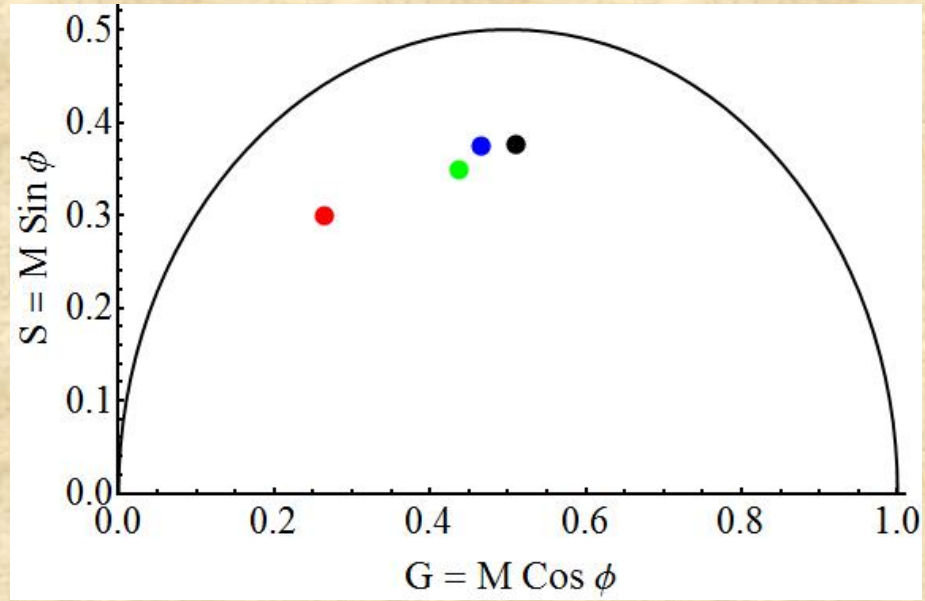


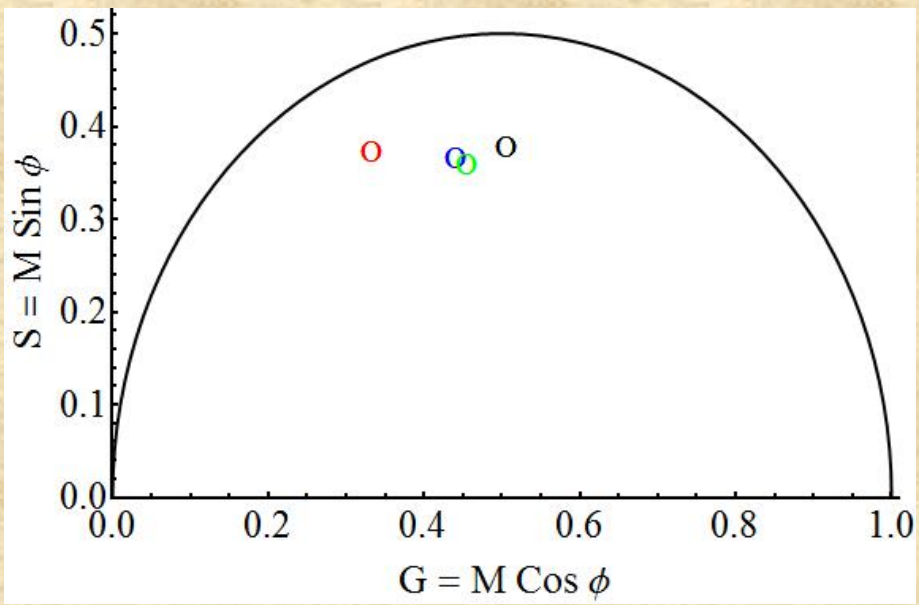


**$K^+$** **$Na^+$**

5’- **A**GGGTTAGGGTTAGGGTTAGGG
5’- AGGGTT**A**GGGTTAGGGTTAGGG
5’- AGGGTTAGGGTT**A**GGGTTAGGG
5’- AGGGTTAGGGTTAGGGTT**A**GGG

# Substitution of potassium for sodium changes the structure and hence the lifetime of the 2-aminopurine Bases in Human Telomere Quadruplexex

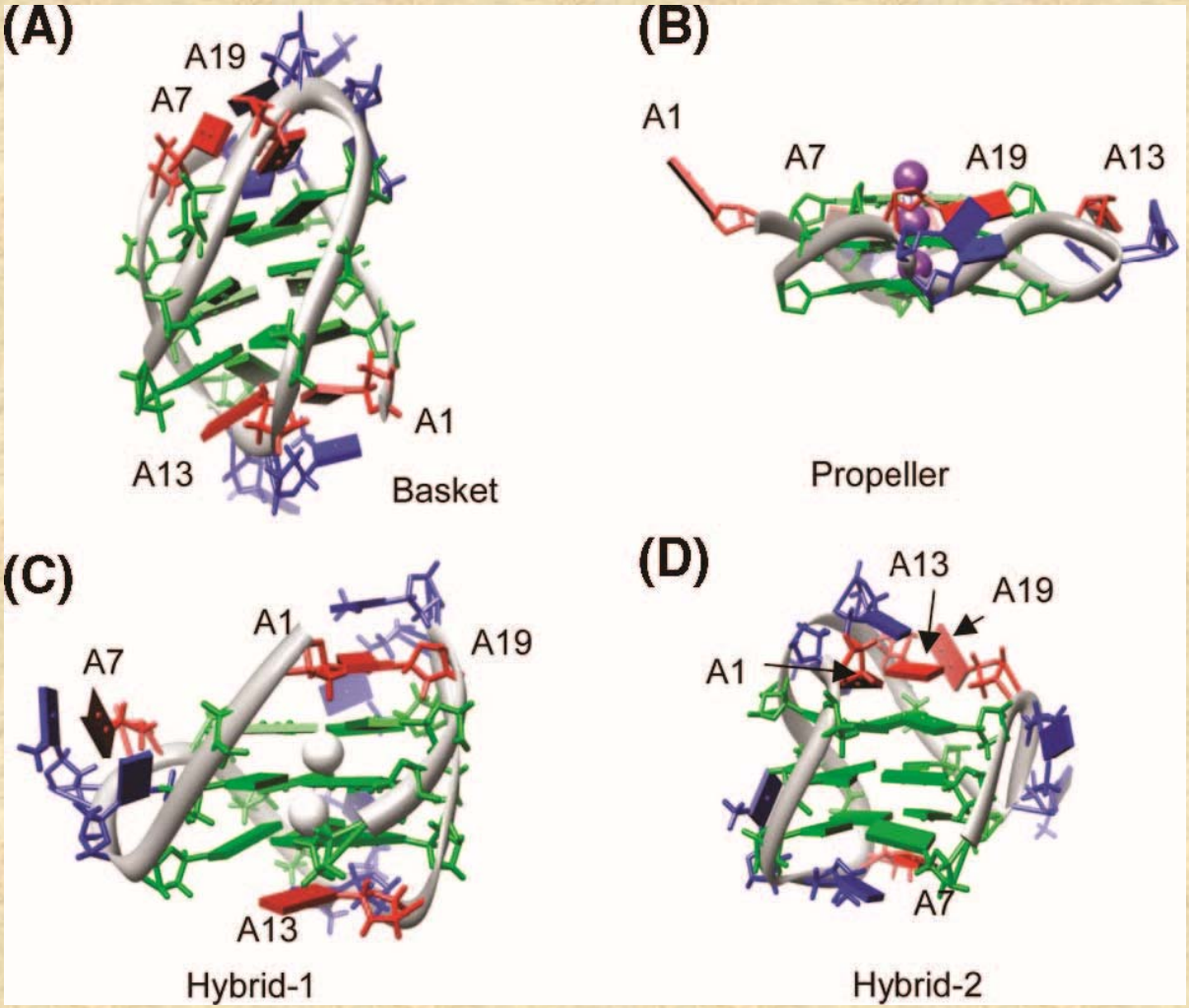

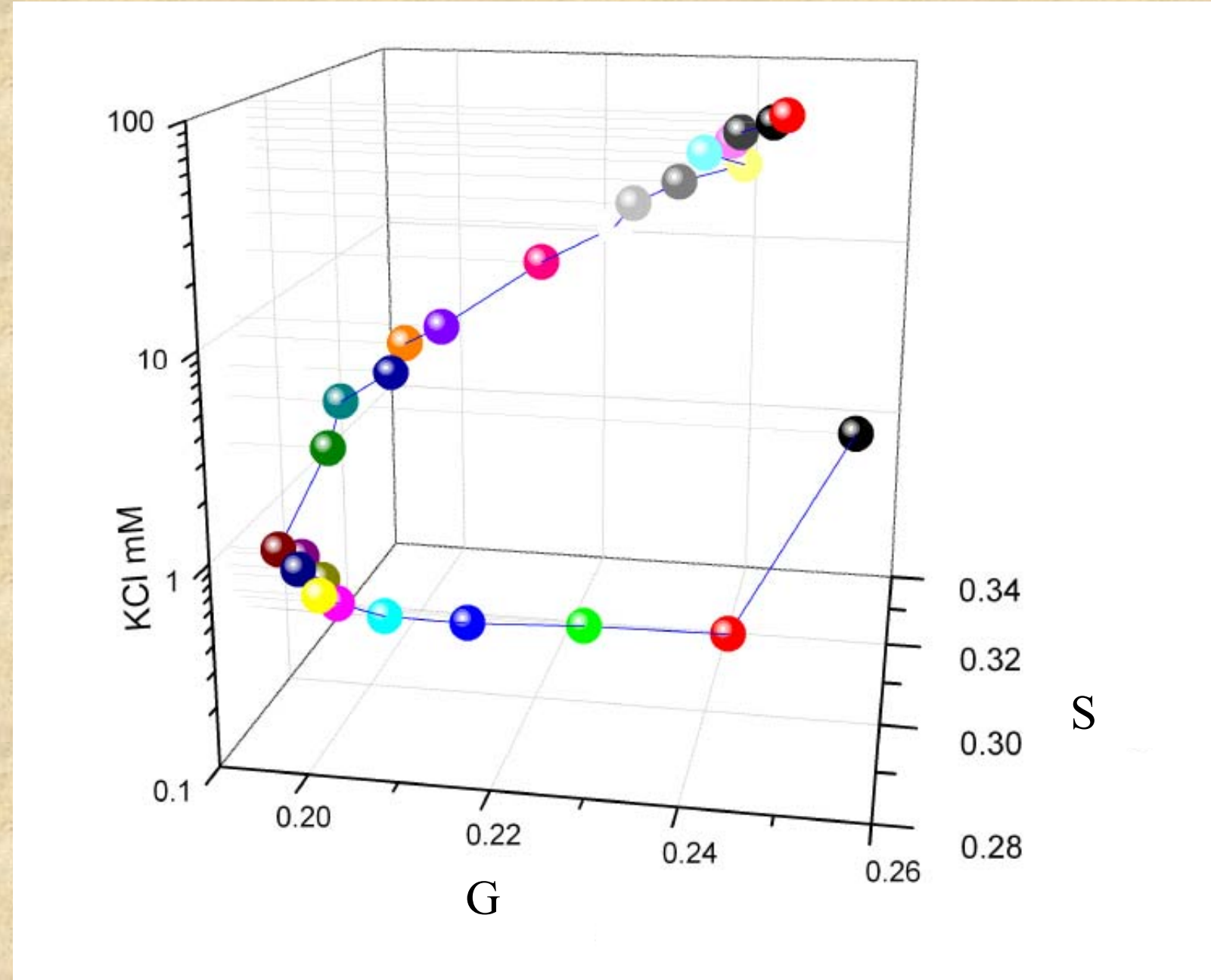


Buscaglia, R., Jameson, D.M. and Chaires, J.B. (2012) Nucleic Acids Res. 40:4203-4215. G-Quadruplex structure and stability illuminated by 2-aminopurine phasor plots.

# Phasor approach to fluorescence lifetime microscopy distinguishes different metabolic states of germ cells in a live tissue

13582–13587 | PNAS | August 16, 2011 | vol. 108 | no. 33

Chiara Stringari[a], Amanda Cinquin[b,c], Olivier Cinquin[b,c], Michelle A. Digman[a], Peter J. Donovan[b,d], and Enrico Gratton[a,1]

[a]Laboratory of Fluorescence Dynamics, Biomedical Engineering Department, [b]Department of Developmental and Cell Biology, [c]Center for Complex Biological Systems, and [d]Department of Biological Chemistry and the Sue and Bill Gross Stem Cell Research Center, University of California, Irvine, CA 92697

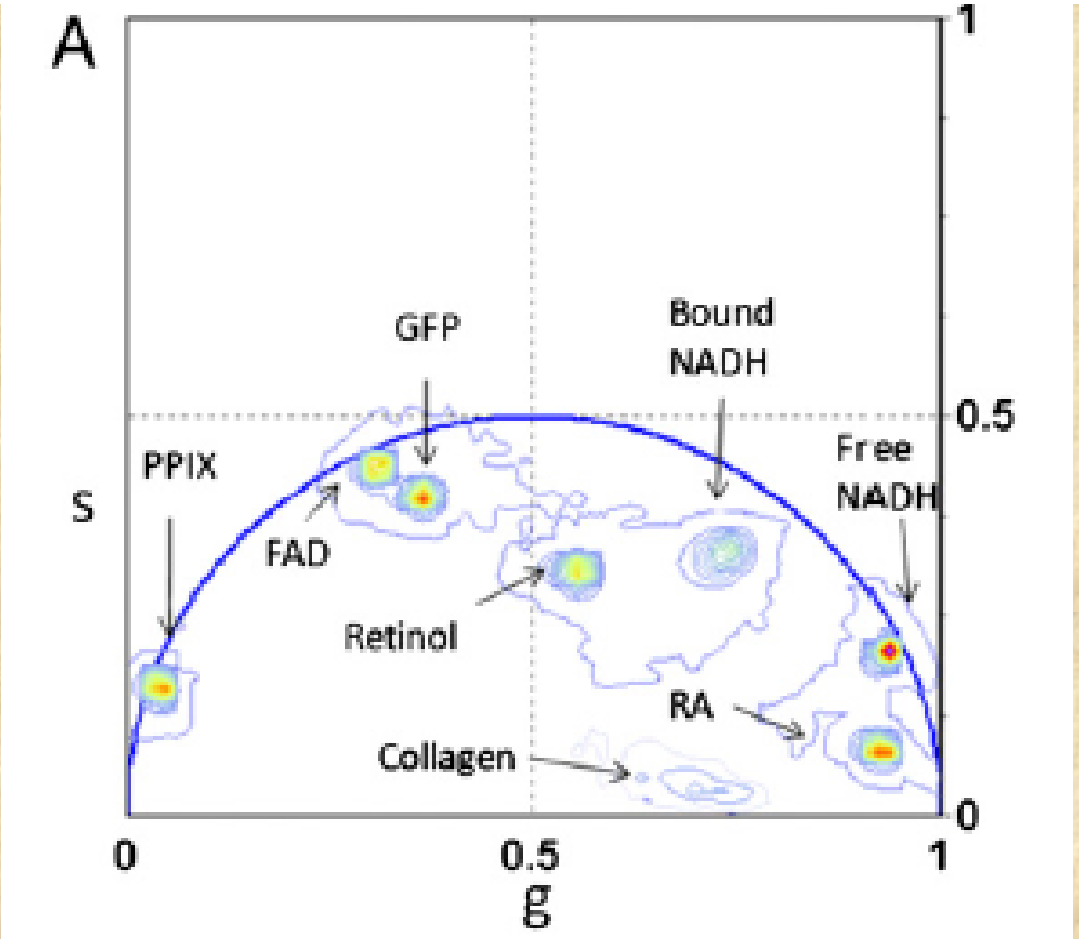

**I should note that PhasorPy is an open-source Python library for the analysis of fluorescence lifetime and hyperspectral images available on the website: https://www.phasorpy.org.**

# *Time-Resolved Anisotropy and Excited State Reactions*

**Many of these slides were prepared by Theodore Hazlett**

Time-resolved methodologies provide information on the changes of orientation as a function of time of a system. The time-domain approach is usually termed the **anisotropy decay** method while the frequency-domain approach is known as **dynamic polarization**. In principle both methods yield the same information.

In the time-domain anisotropy method the sample is illuminated by a pulse of vertically polarized light and the decay over time of both the vertical and horizontal components of the emission are recorded. The anisotropy function is then plotted versus time as illustrated here:

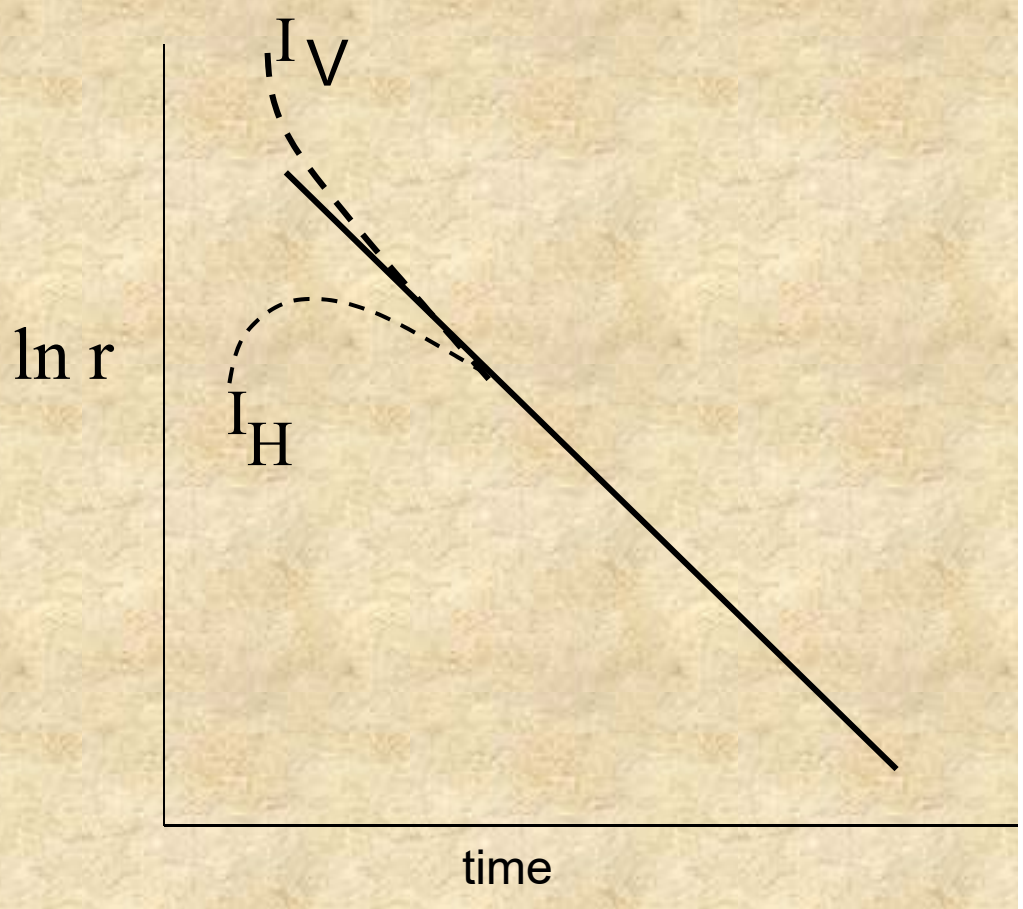


Note that the horizontal component actually increases during short times, since initially the fluorophores have not rotated significantly. As time passes though the number of horizontally oriented molecules increases

## Simplest Case: Spherical Body

### Fully Symmetrical

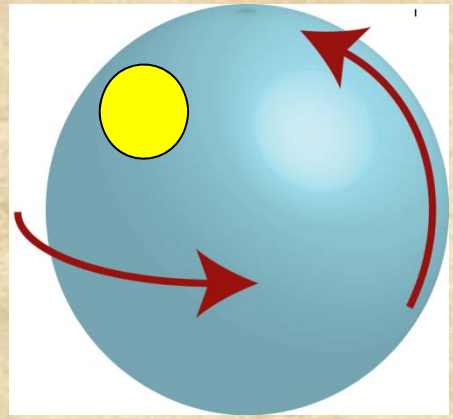

(in this case we assume that the fluorophore has no local mobility – such is the case for non-covalent interactions)

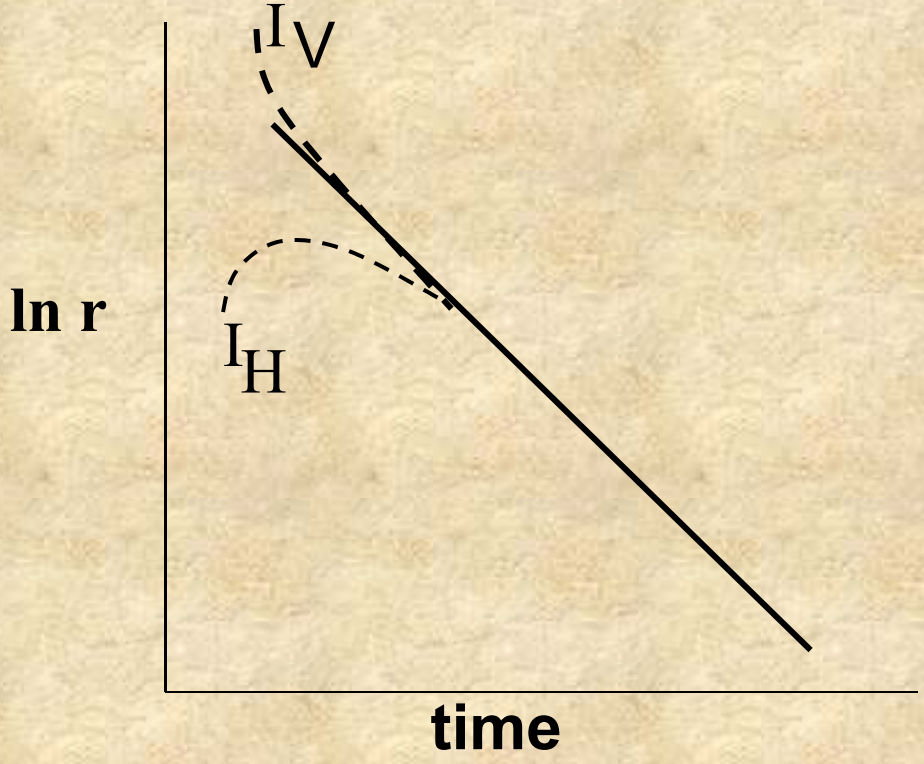


The decay of the anisotropy with time, r(t), for a sphere is given by:

$$r = \frac{Iv - Ih}{Iv + 2Ih} = r_o e^{-\left(t/\tau_c\right)}$$

$\tau_c$ is the rotational correlation time

$$\tau_c = \frac{1}{6 \cdot D_{rotation}}$$

In the case of non-spherical particles the time-decay of anisotropy function is more complicated. Mathematically simple symmetrical ellipsoids give us a sense of how changes in Shape affect the rotational diffusion rates.

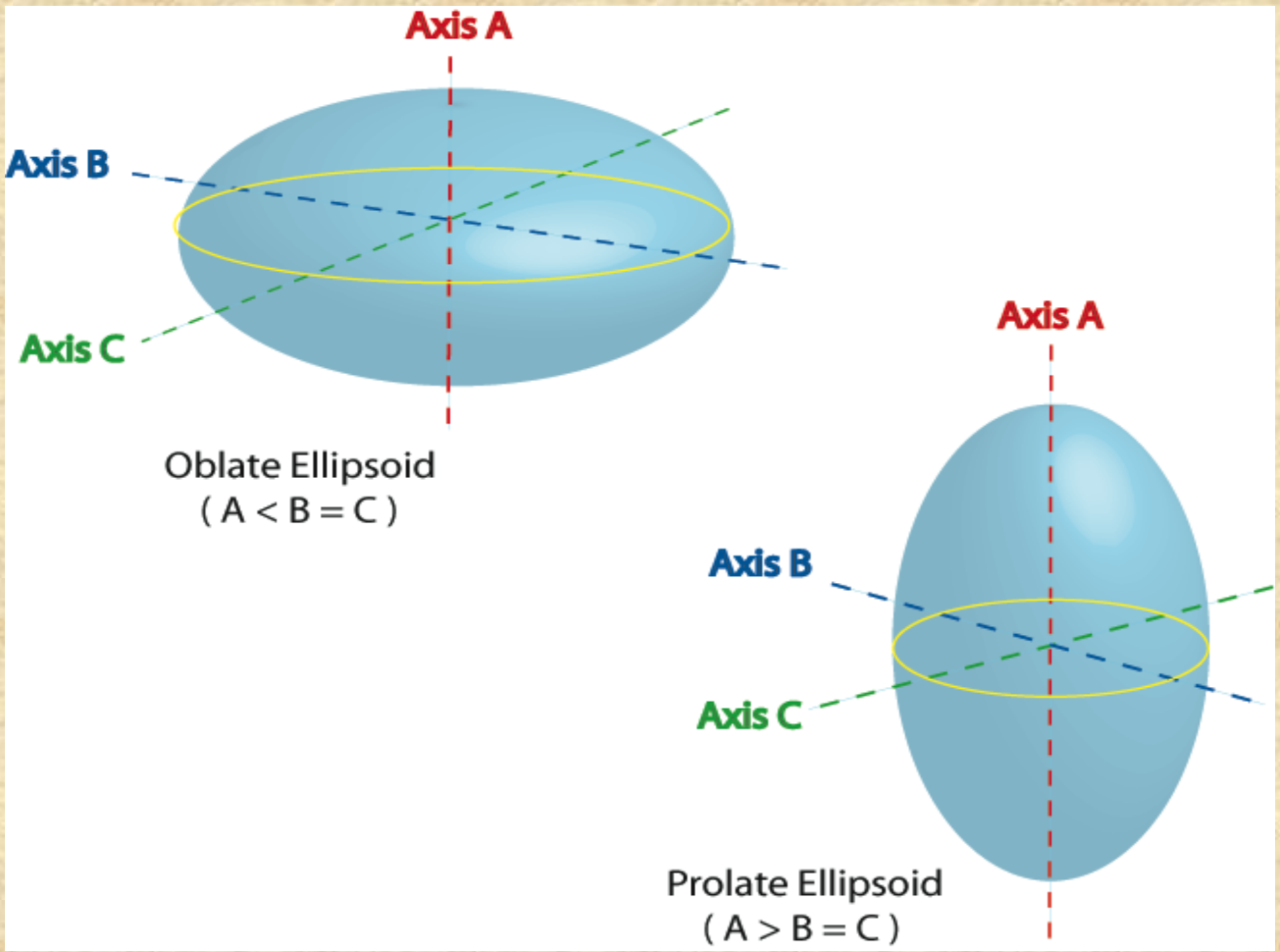

# Effect of Shape on Diffusion

## Translational Diffusion

20:1 Prolate

20:1 Oblate

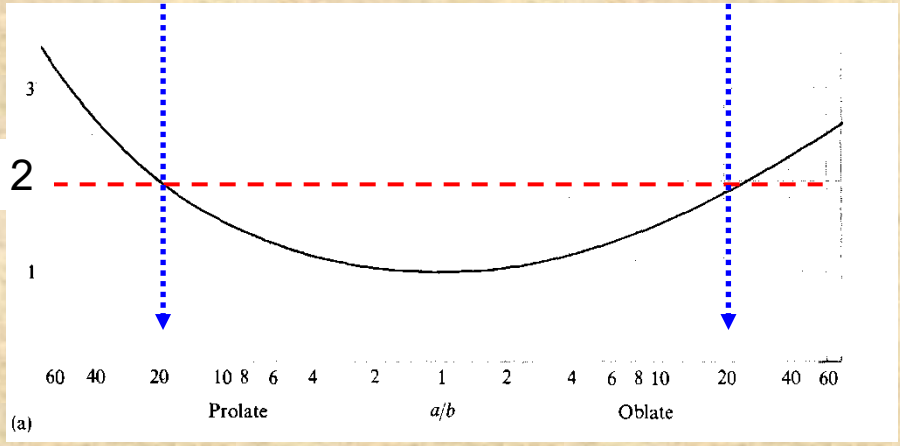


## Rotational Diffusion

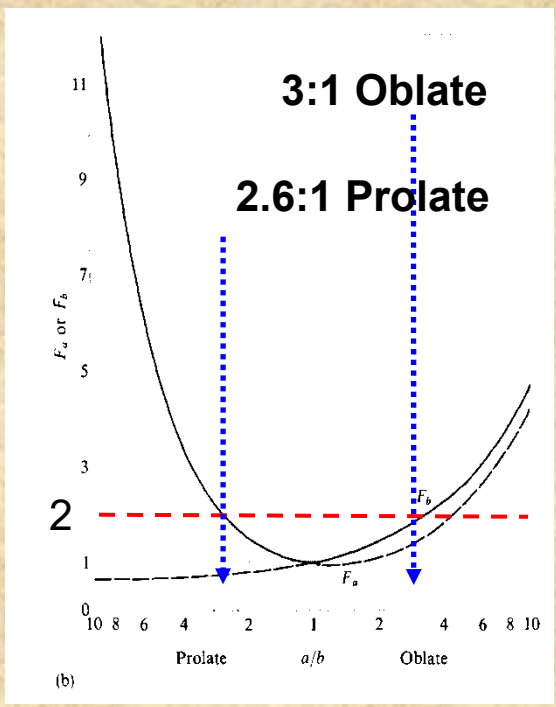


**Rotational Diffusion is much more influenced by macromolecular shape than is Translational diffusion**

# How are these Shapes Modeled?

In the case of symmetrical ellipsoids of revolution the relevant expression is:

$$r(t) = r_1 e^{\left(\frac{-t}{\tau_{c1}}\right)} + r_2 e^{\left(\frac{-t}{\tau_{c2}}\right)} + r_3 e^{\left(\frac{-t}{\tau_{c3}}\right)}$$

where: $\tau_{c1} = 1/6D_2$

$\tau_{c2} = 1/(5D_2 + D_1)$

$\tau_{c3} = 1/(2D_2 + 4D_1)$

$D_1$ and $D_2$ are the rotational diffusion coefficients about the axes of symmetry and about either equatorial axis, respectively.

Resolution of the rotational rates is limited in practice to two rotational correlation times which differ by at least a factor of two.

# What do the Anisotropy Amplitudes (r1, r2, & r3) Represent?

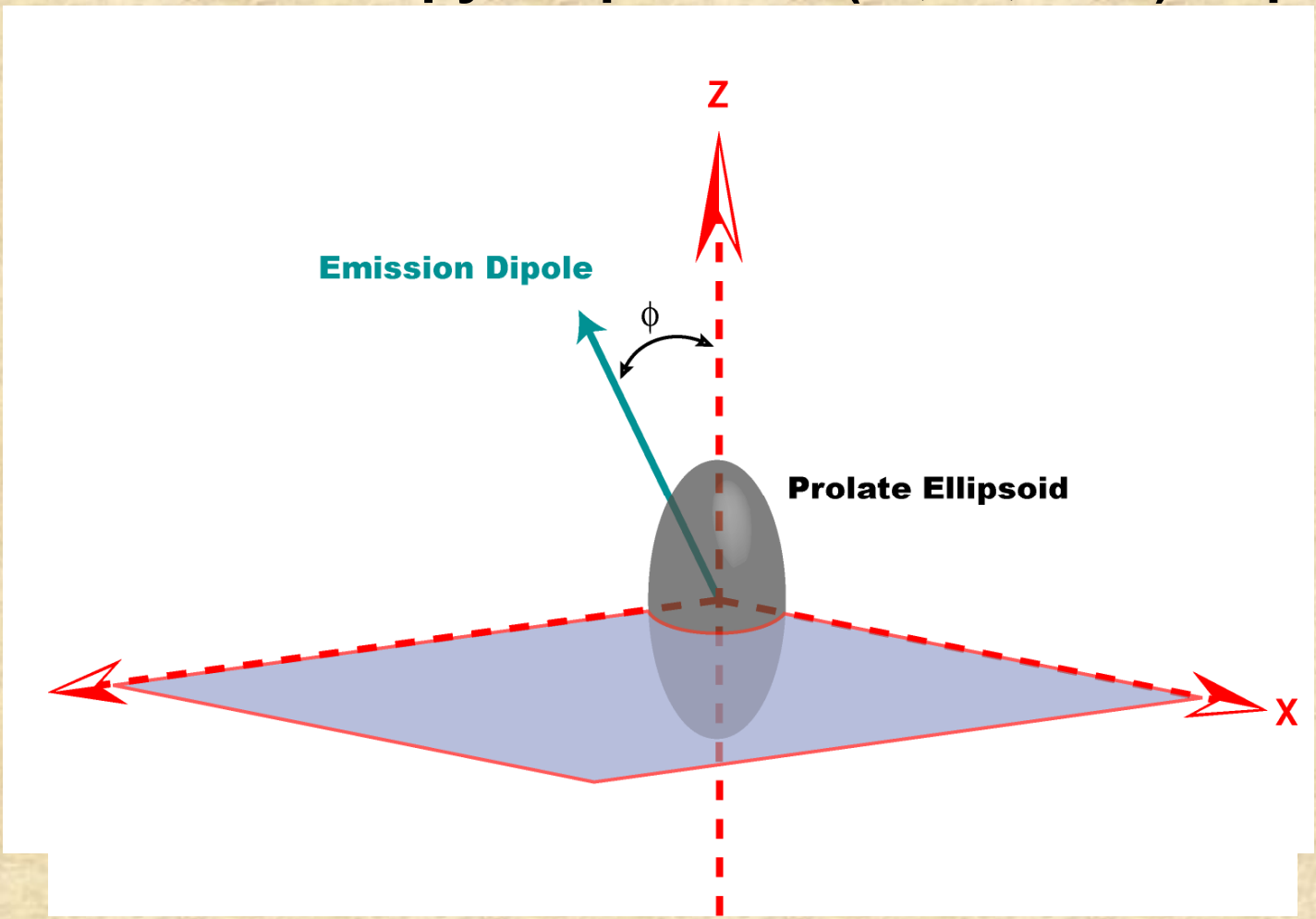


**The amplitudes relate to orientation of the probe with respect to the axis of symmetry for the ellipsoid *(we are assuming colinear excitation and emission dipoles)*.**

$$r_1 = 0.1(3\cos^2\phi - 1)^2$$
$$r_2 = 0.3\sin^2(2\phi)$$
$$r_3 = 0.3\sin^4(\phi)$$

# Multiple Rotating Species (mixtures)

$$r(t) = r_1 e^{\left(\frac{-t}{\tau_{c1}}\right)} + r_2 e^{\left(\frac{-t}{\tau_{c2}}\right)}$$

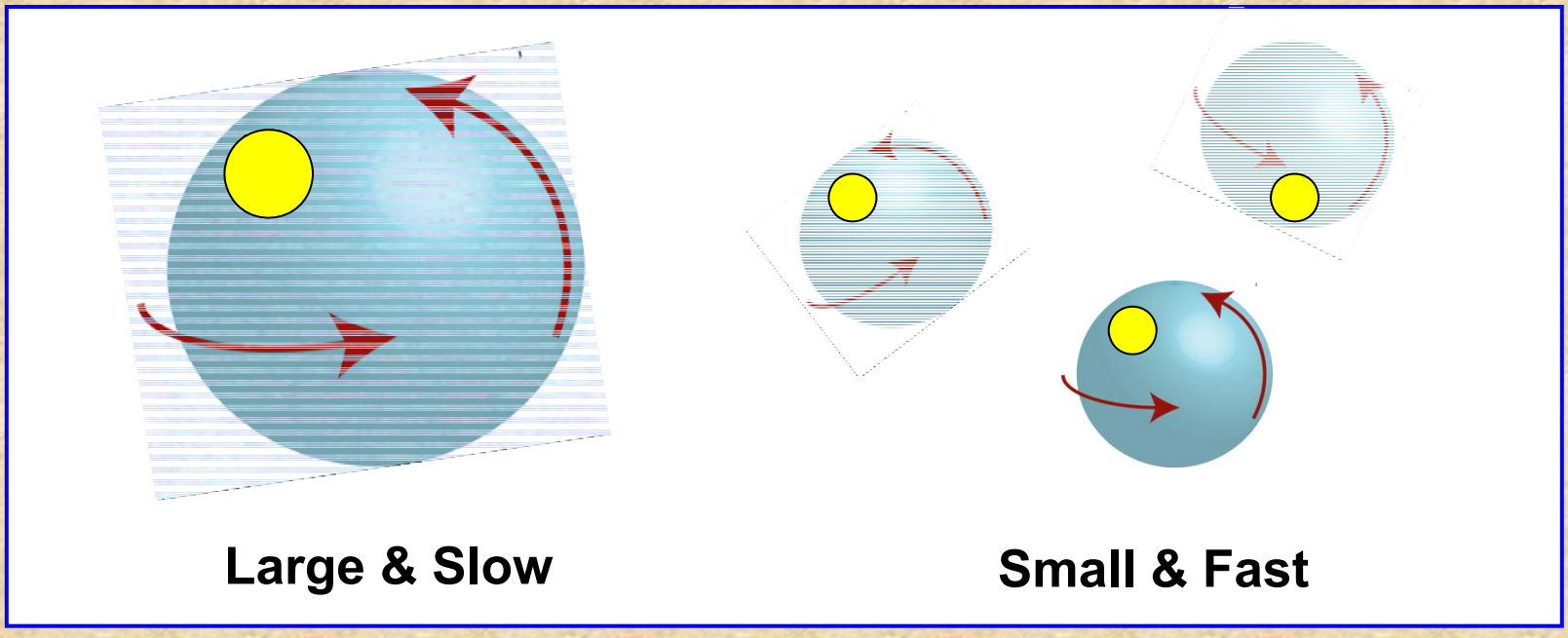

Large & Slow

Small & Fast

# Mixed systems Show
# Simple, Multi-Exponential Behavior

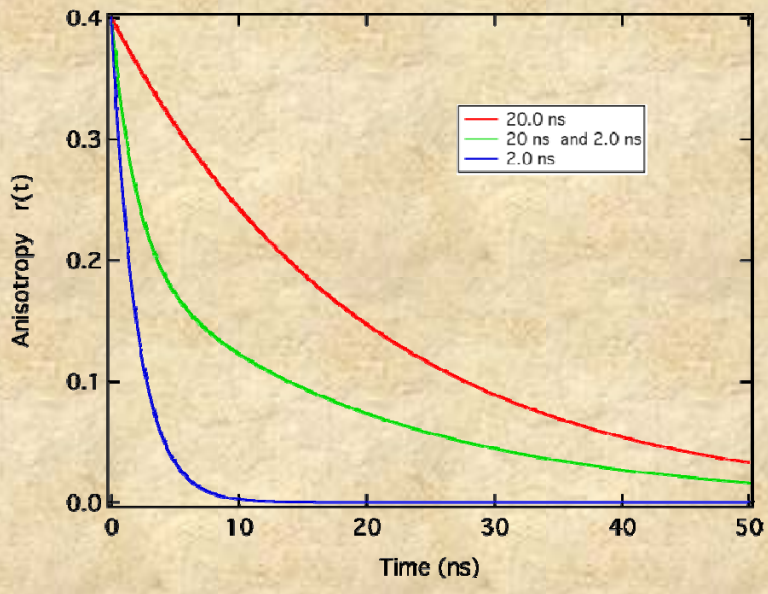


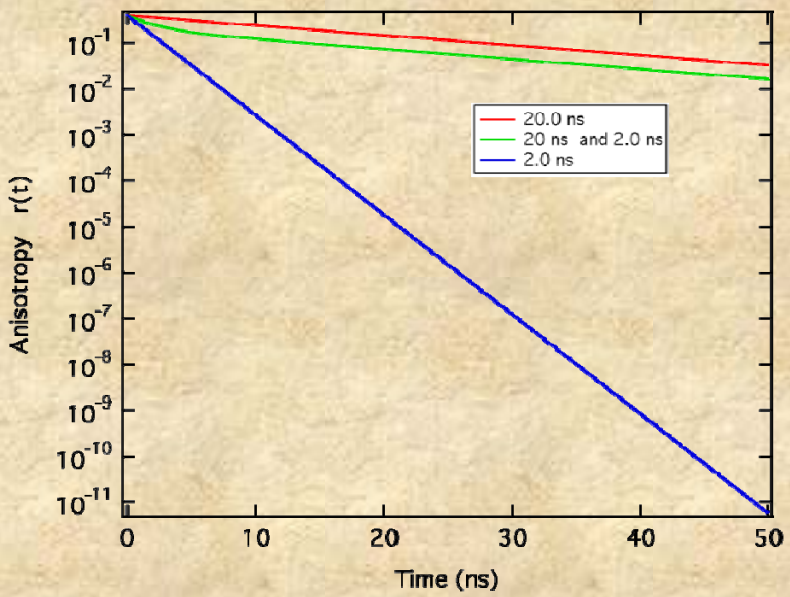


**With separate species the decays reflect the sum of the exponential components present.**

# Multiple Rotational Modes:
# Local relaxation + Global rotation

Is the case of a **"local"** rotation of a probe attached to a spherical particle any different than multiple species?

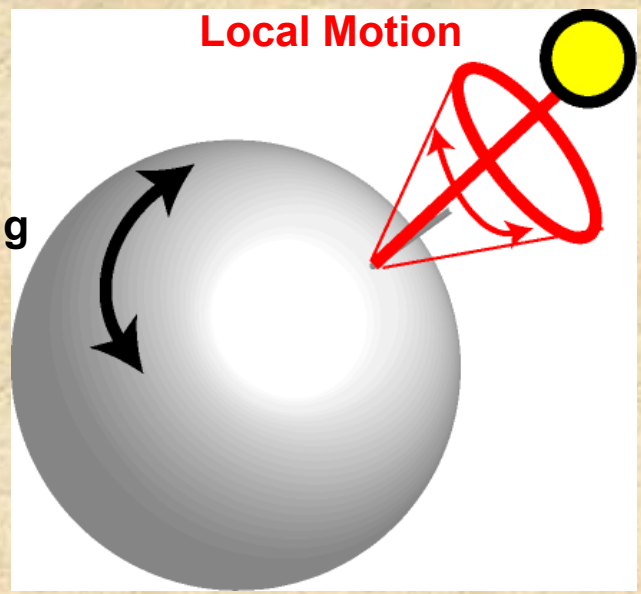


**This common system represents a condition containing a hindered motion.**

**The expression for this case is:**

$$r(t) = r_1 \cdot e^{-(t/\tau_{c1})} + r_2 \cdot e^{-(t/\tau_{c1} + t/\tau_{c2})}$$

Where $\tau_{c1}$ represents the "Global" probe motion, $\tau_{c2}$ represents the "Local" rotation of the macromolecule.

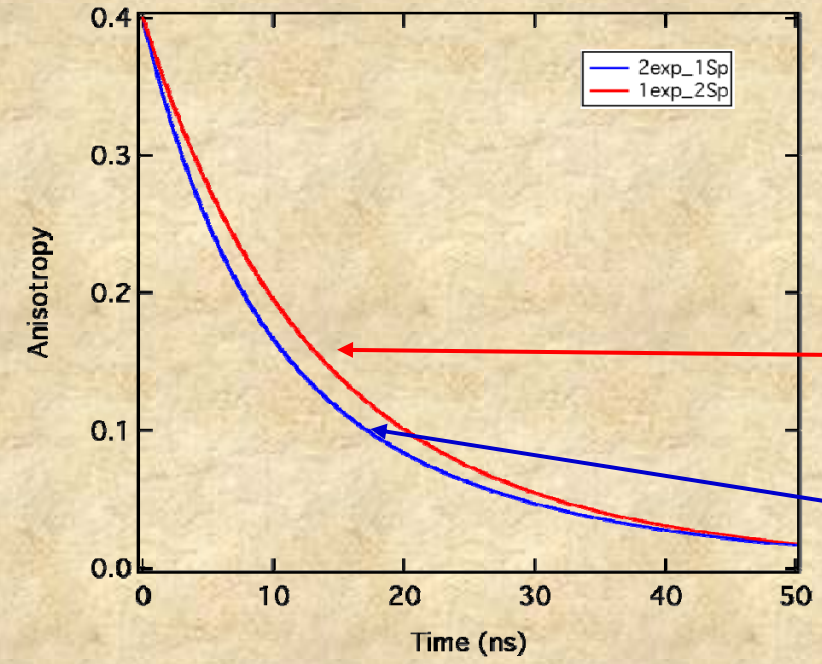


**Equal pre-exponentials terms containing two rotational components of 20 ns and 10 ns**

**The "Mixed" case**

**The "Local & Global" case**

# Hindered Rotational Systems
# Membrane Bilayers

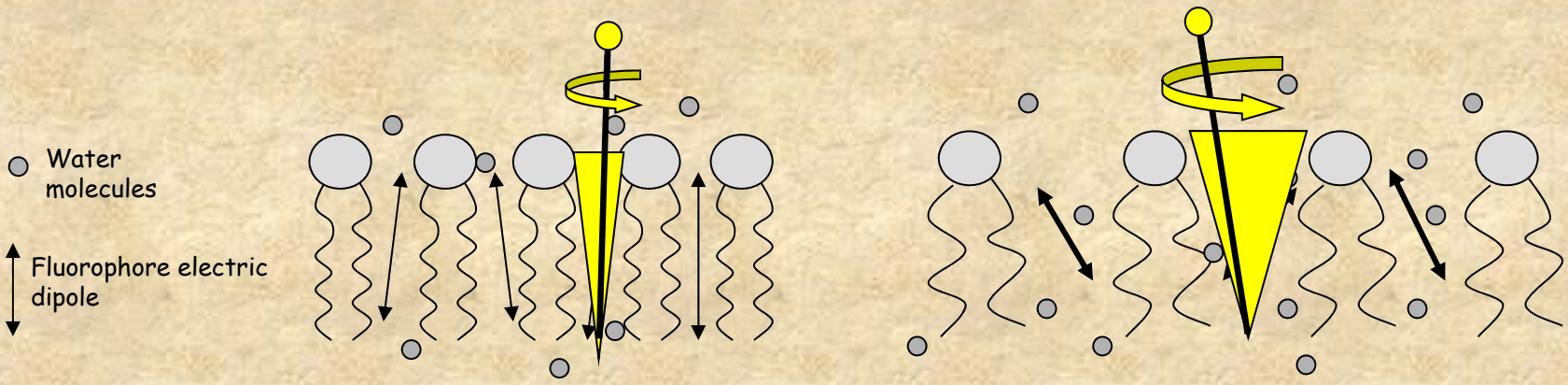


**Wobble-in-a-Cone Concept**

1) **Freedom of motion**
2) **The rate of motion**

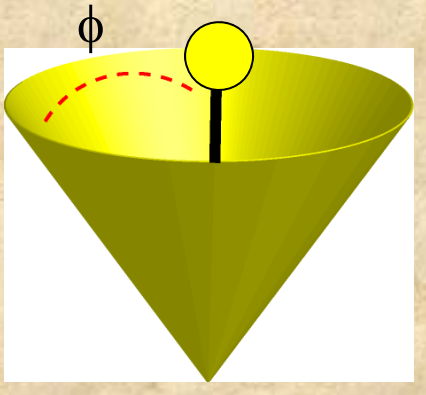

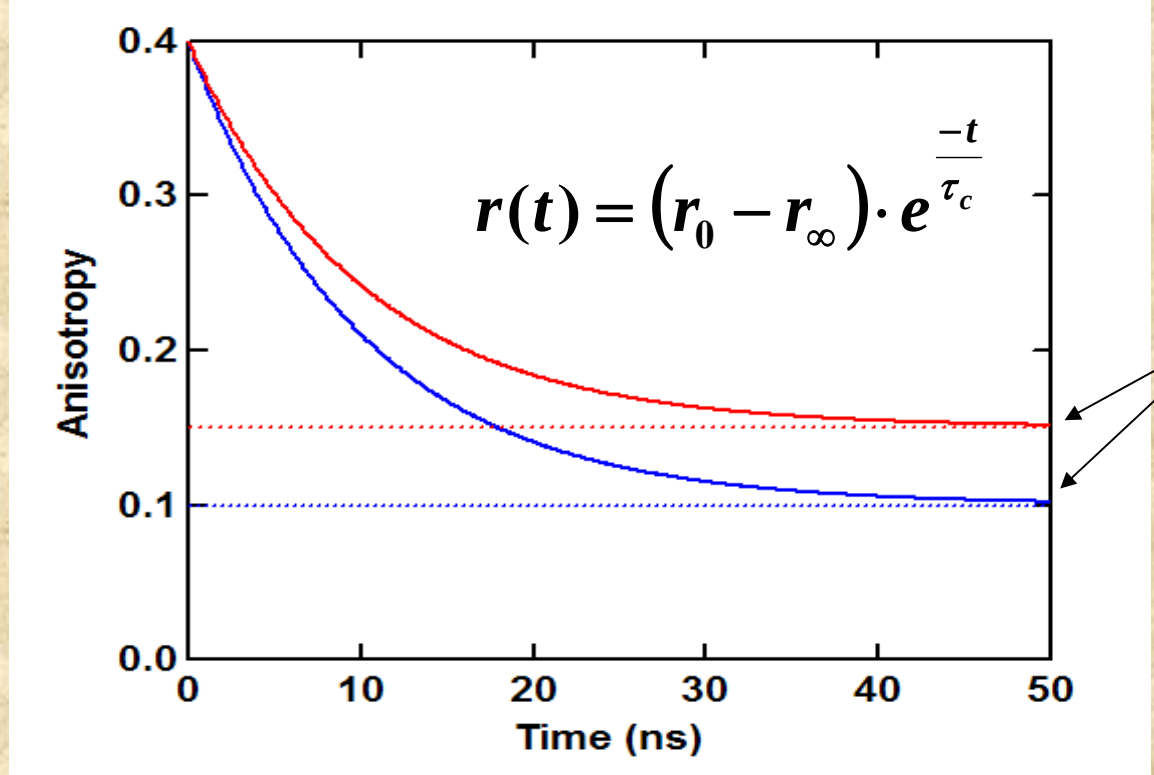


$$\frac{r_0}{r_\infty} = \left\langle \frac{3 \cdot \cos^2(\phi) - 1}{2} \right\rangle^2$$

**Motion**

$\tau_c$ = 20 ns

**Angular Freedom**

$\phi$= 52 degrees

$\phi$= 44 degrees

# Analysis of Fluorophore Rotation in an Artificial Bilayer

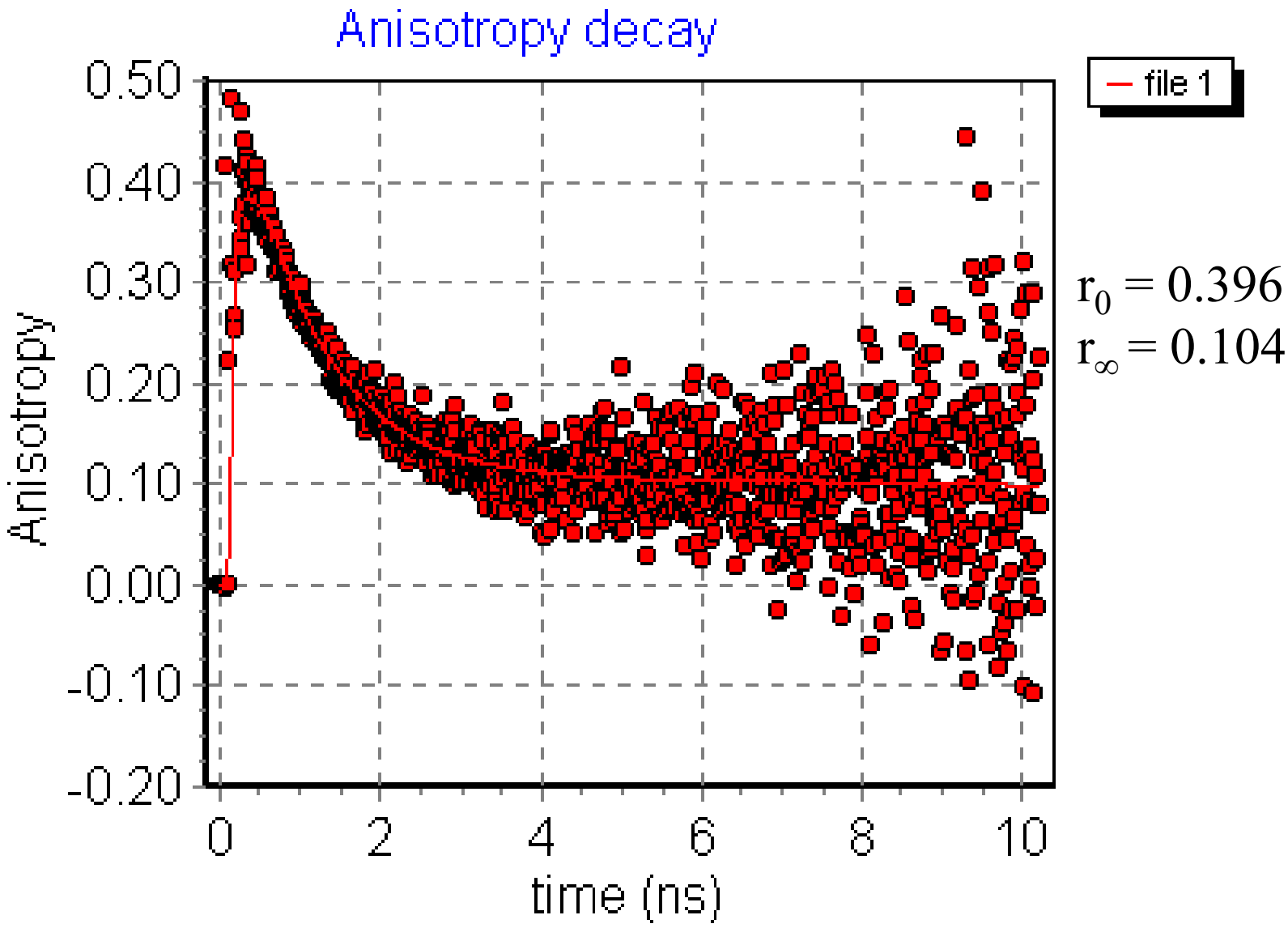

# *Phase & Modulation Measurements*

**In dynamic polarization measurements**, the sample is illuminated with vertically polarized, modulated light. The phase delay (dephasing) between the parallel and perpendicular components of the emission is measured as well as the modulation ratio of the AC contributions of these components. The expressions a spherical particle are:

$$\Delta\phi = \tan^{-1}\left[\frac{18\omega r_o R}{\left(k^2+\omega^2\right)\left(1+r_o-2r_o^2\right)+6R\left(6R+2k+kr_o\right)}\right]$$

$$Y^2 = \frac{\left(\left(1-r_o\right)k+6R\right)^2+\left(1-r_o\right)^2\omega^2\right)}{\left[\left(1+2r_o\right)k+6R\right]^2+\left(1+2r_o\right)^2\omega^2}$$

Where $\Delta\phi$ is the phase difference, Y the modulation ratio of the AC components $\omega$ the angular modulation frequency, $r_o$ the limiting anisotropy, k the radiative rate constant ($1/\tau$) and R the rotational diffusion coefficient.

The illustration below depicts the $\Delta\phi$ function for the cases of spherical particles with different rotational relaxation times.

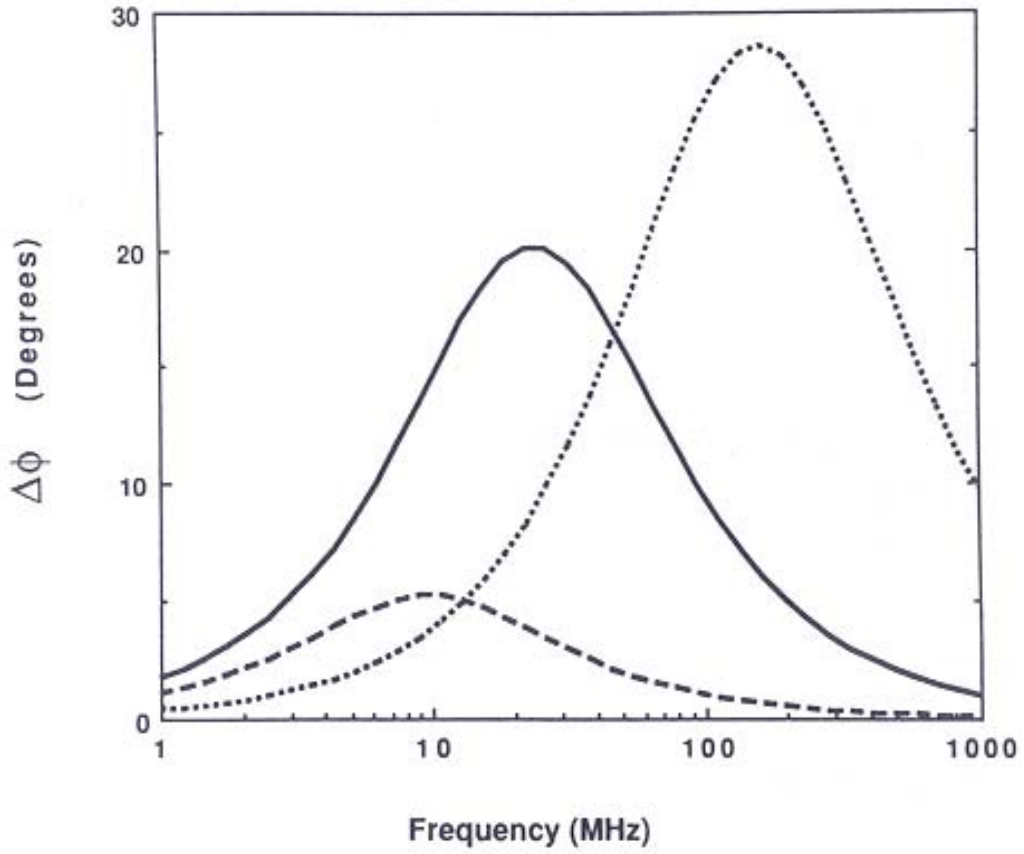


Differential phase data for an isotropic rotator with a 3-nsec (dotted line), 30-nsec (solid line), or 300-nsec (dashed line) rotational relaxation time. In each case a lifetime of 20 nsec was used and colinear excitation and emission dipoles were assumed.

The figures here show actual results for the case of ethidium bromide free and bound to tRNA - one notes that the fast rotational motion of the free ethidium results in a shift of the “bell-shaped” curve to higher frequencies relative to the bound case. The lifetimes of free and bound ethidium bromide were approximately 1.8 ns and 27 ns respectively.



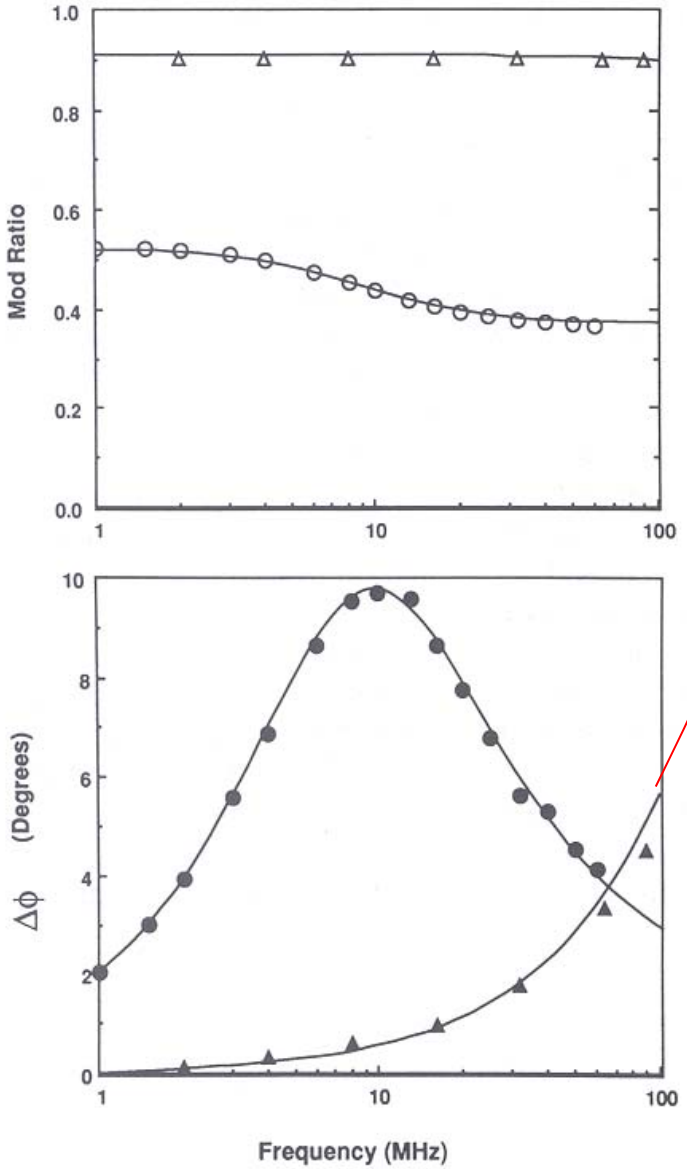


**FIGURE 9.** Differential phase (closed symbols) and modulation (open symbols) data for ethidium bromide in solution (triangles) and ethidium bromide bound to tRNA (circles). The resolved rotational relaxation times (5°C) were 144 and 0.5 nsec for free and bound ethidium bromide, respectively. The curves are the least-squares fit to the data.

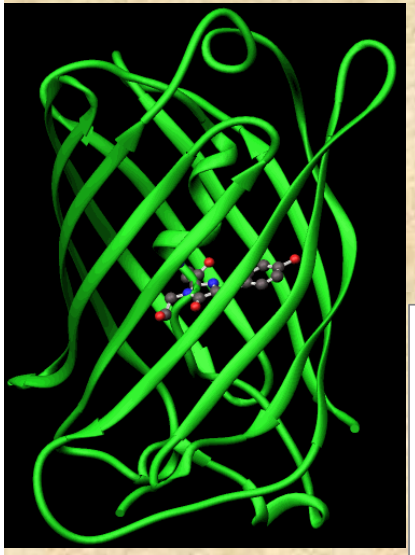

## In GFP the fluorophore is rigidly attached to the protein framework

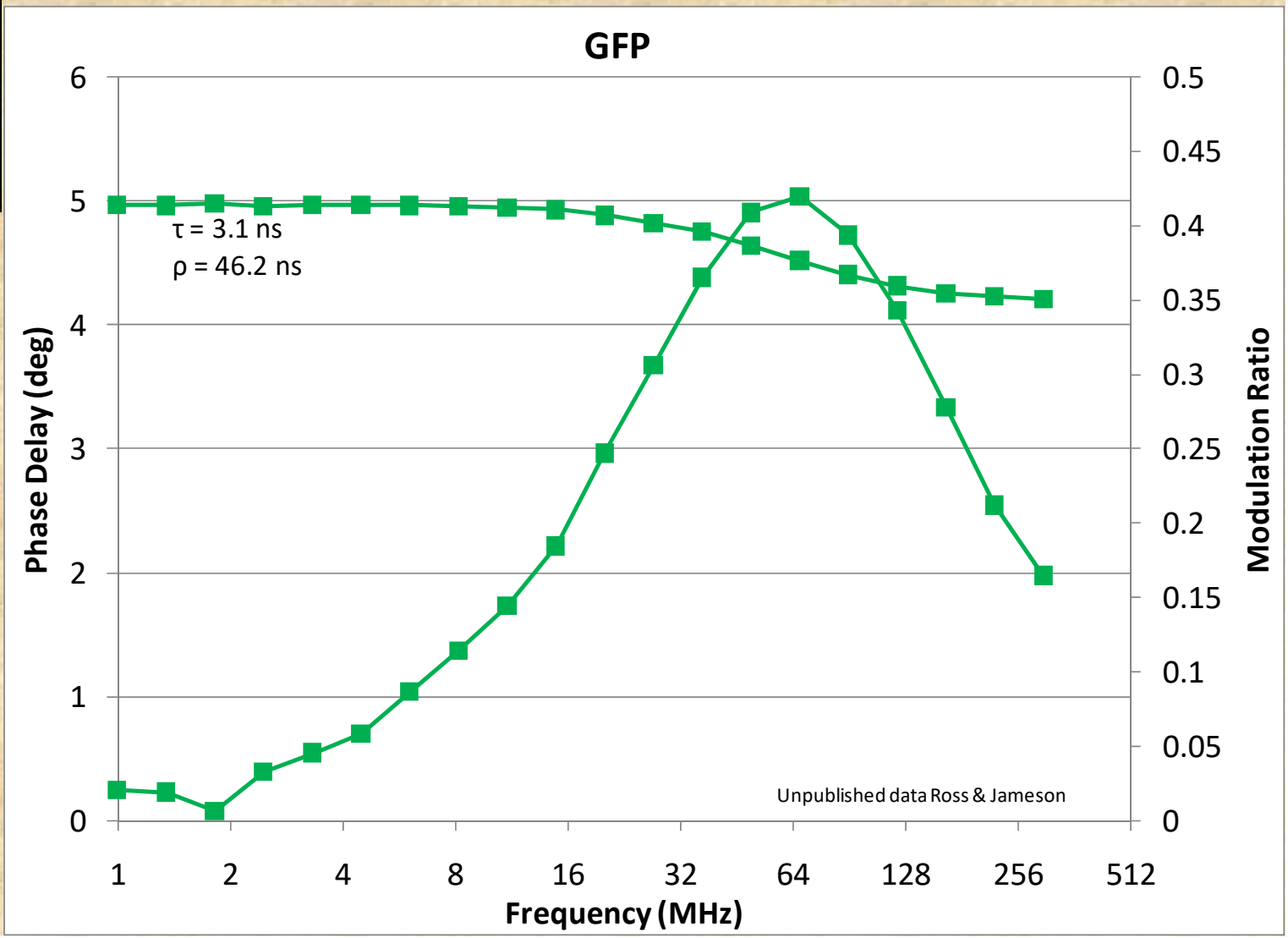

In the case of local plus global motion, the dynamic polarization curves are altered as illustrated below for the case of the single tryptophan residue in elongation factor Tu which shows a dramatic increase in its local mobility when EF-Tu is complexed with EF-Ts.

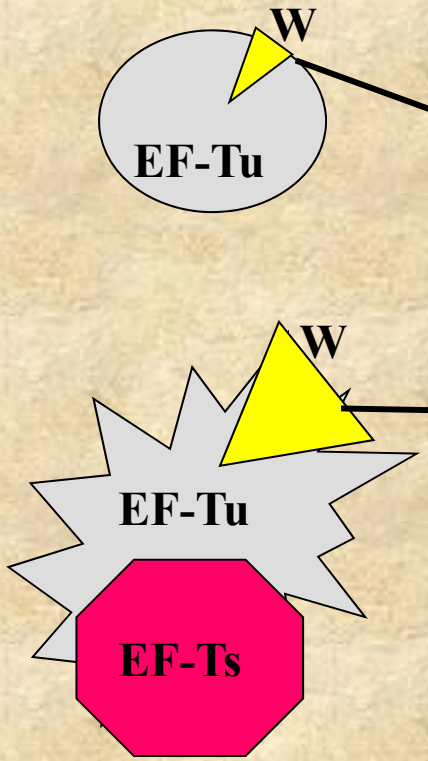


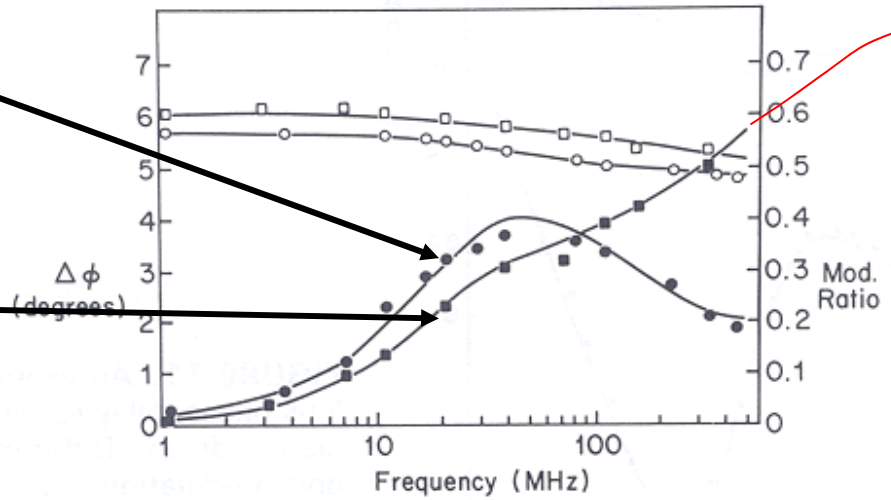


**FIGURE 10.** Multifrequency differential phase (closed symbols) and modulation (open symbols) data for elongation factor Tu complexed with GDP (circles) and elongation factor Ts (squares). Curves represent the least-squares fit to the data.

**From: Jameson, D.M., Gratton, E. and Eccleston, J.F. (1987) *Biochemistry 26*:3894-3901. Intrinsic Fluorescence of Elongation Factor Tu in its Complexes with GDP and Elongation Factor Ts.**

How about this case?

**Negative phase delay?!**

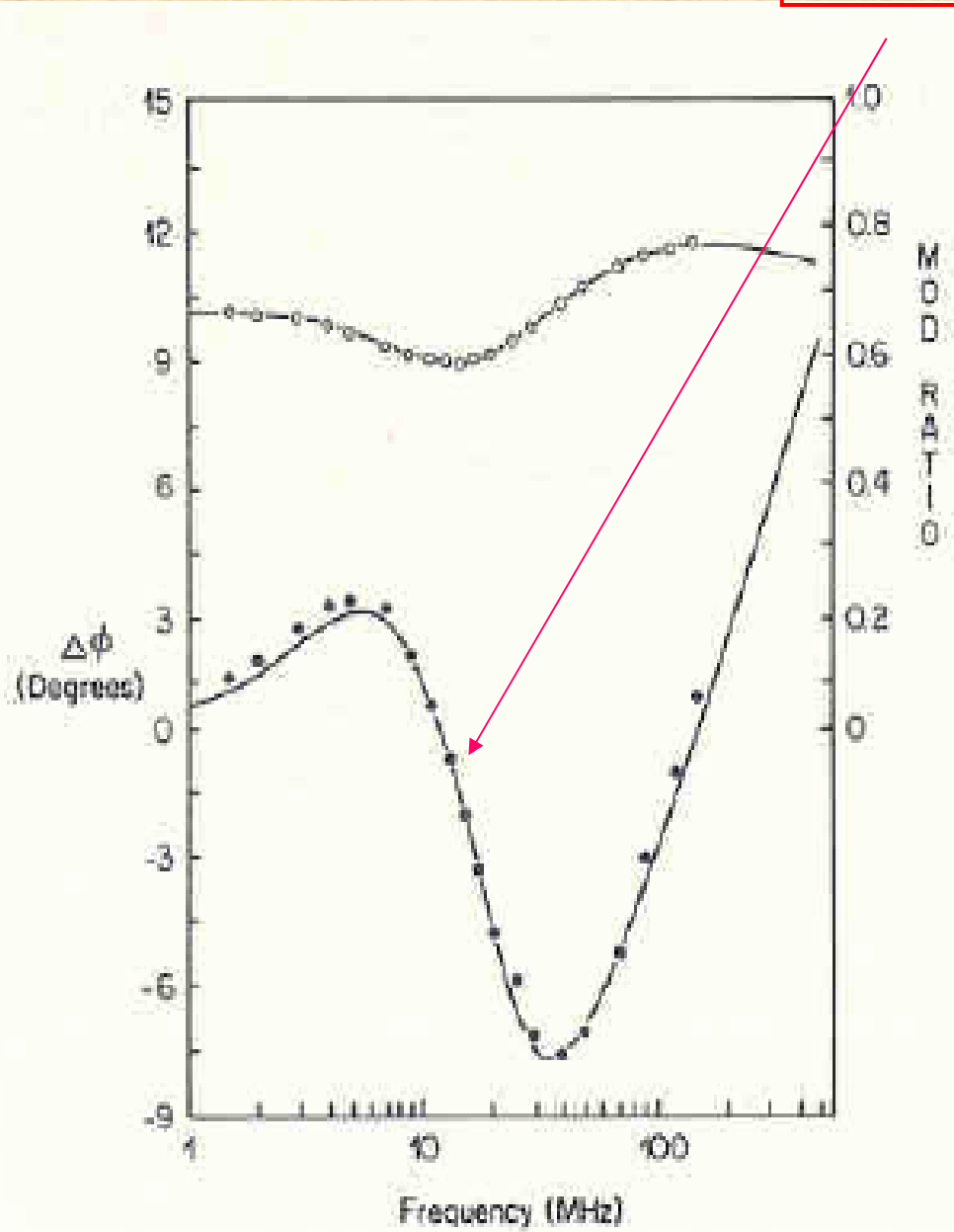


## Anomalous Phase Delay (Chip Dip)

**tRNA + Ethidium Bromide (equilibrium conditions)**

Compare to individual species

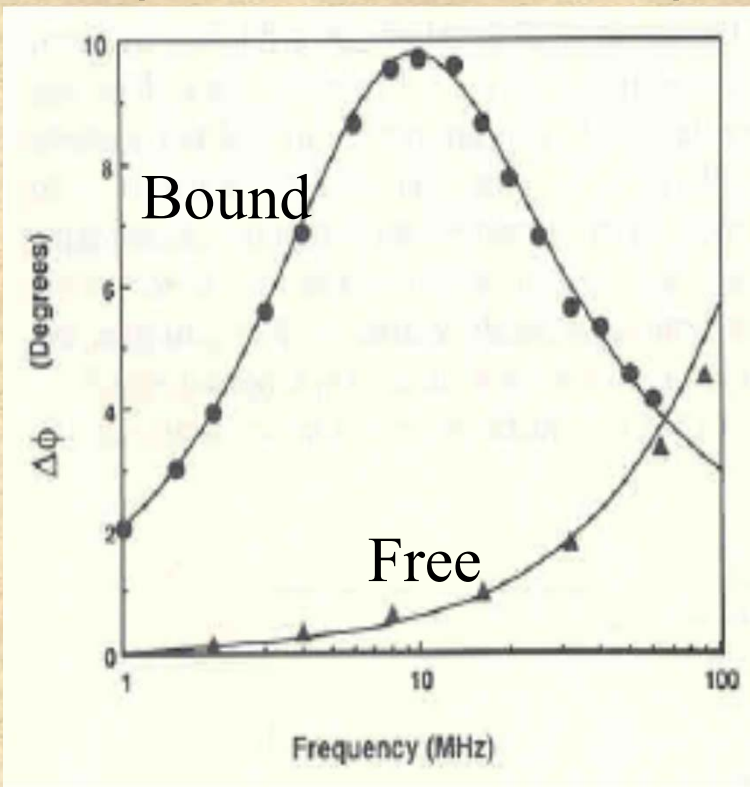

# What do We have in Our Mixture?

+

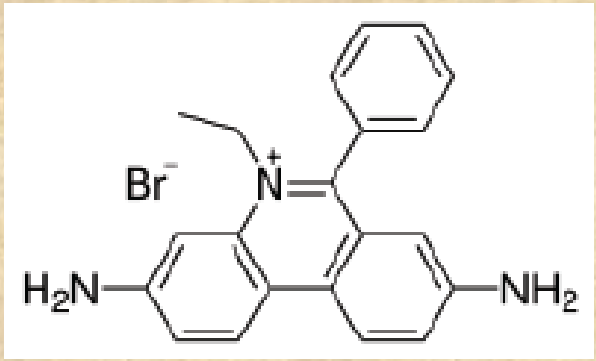


**Ethidium Bromide**

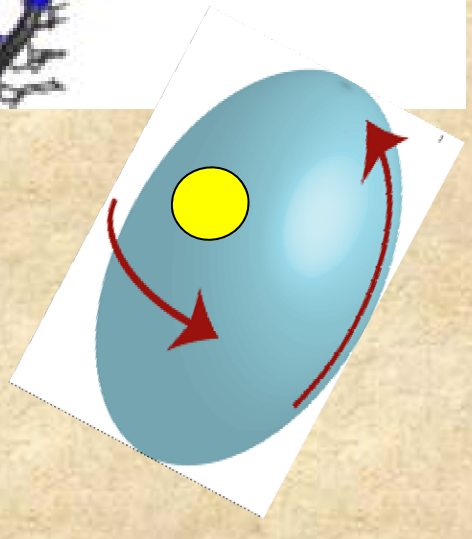

+

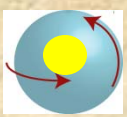

**Slow rotation + long lifetime**

**Fast rotation + short lifetime**

**Time Domain Equivalent of the Anomalous Phase Delay**

**Also known as the "Dip and Rise"**

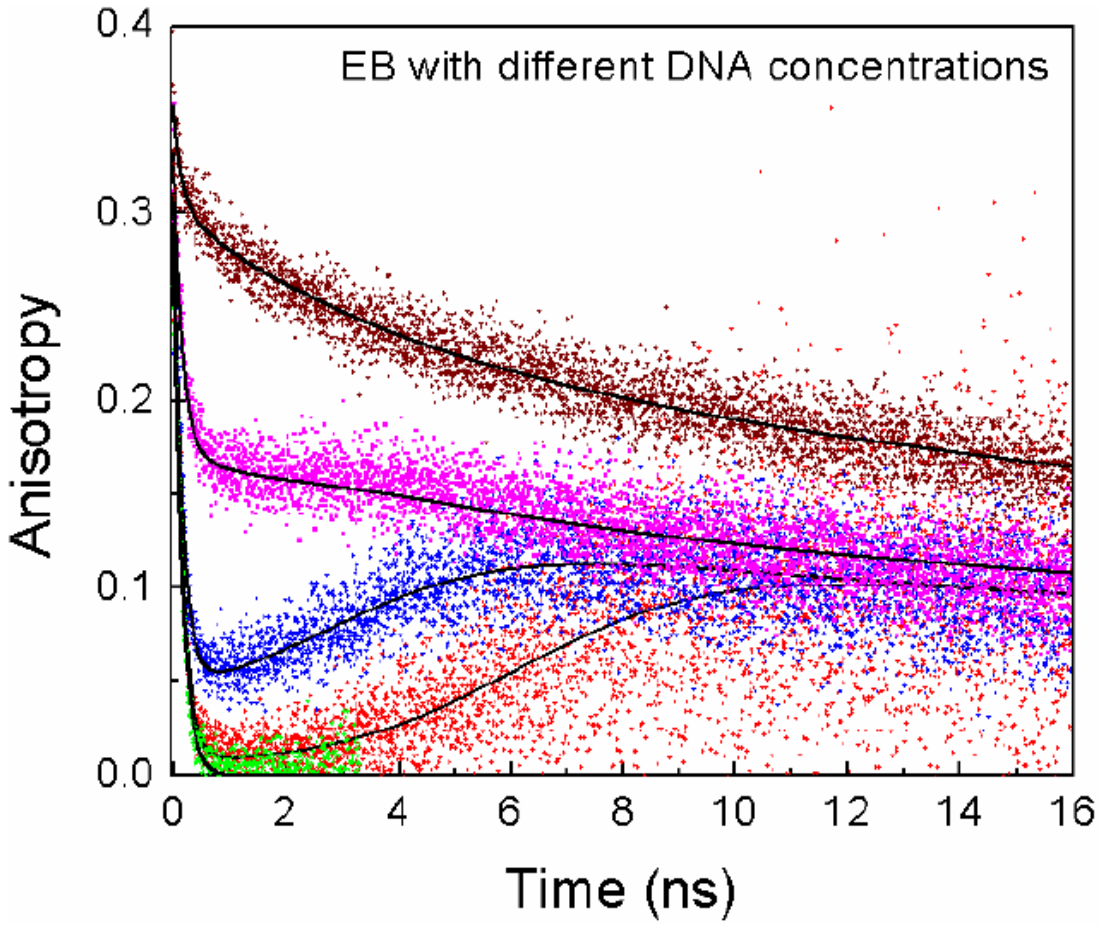


**Figure 6.** Associated anisotropy decays of free EB and EB–DNA mixtures; with EB-36.9 $\mu$M and DNA-0 $\mu$M (green), DNA-5.85 $\mu$M (red), DNA-33.16 $\mu$M (blue), DNA-97.53 $\mu$M (pink), DNA-585 $\mu$M (brown).

IOP Publishing Methods and Applications in Fluorescence
Methods Appl. Fluoresc. 2 (2014) 015003 (6pp) doi:10.1088/2050-6120/2/1/015003

**Associated anisotropy decays of ethidium bromide interacting with DNA**

Rahul Chib[1], Sangram Raut[1], Sarika Sabnis[1], Preeti Singhal[1], Zygmunt Gryczynski[1,2] and Ignacy Gryczynski[1]

Final comment: Although we have discussed analysis of rotational rates in terms of discrete components, in some cases a more realistic approach may be to use distribution functions

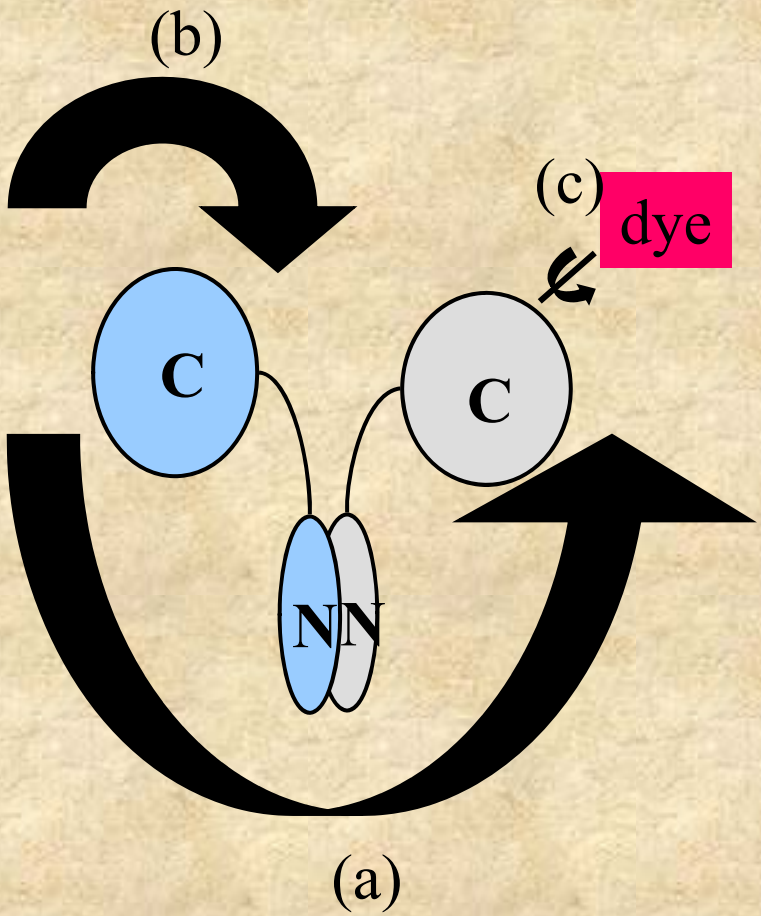


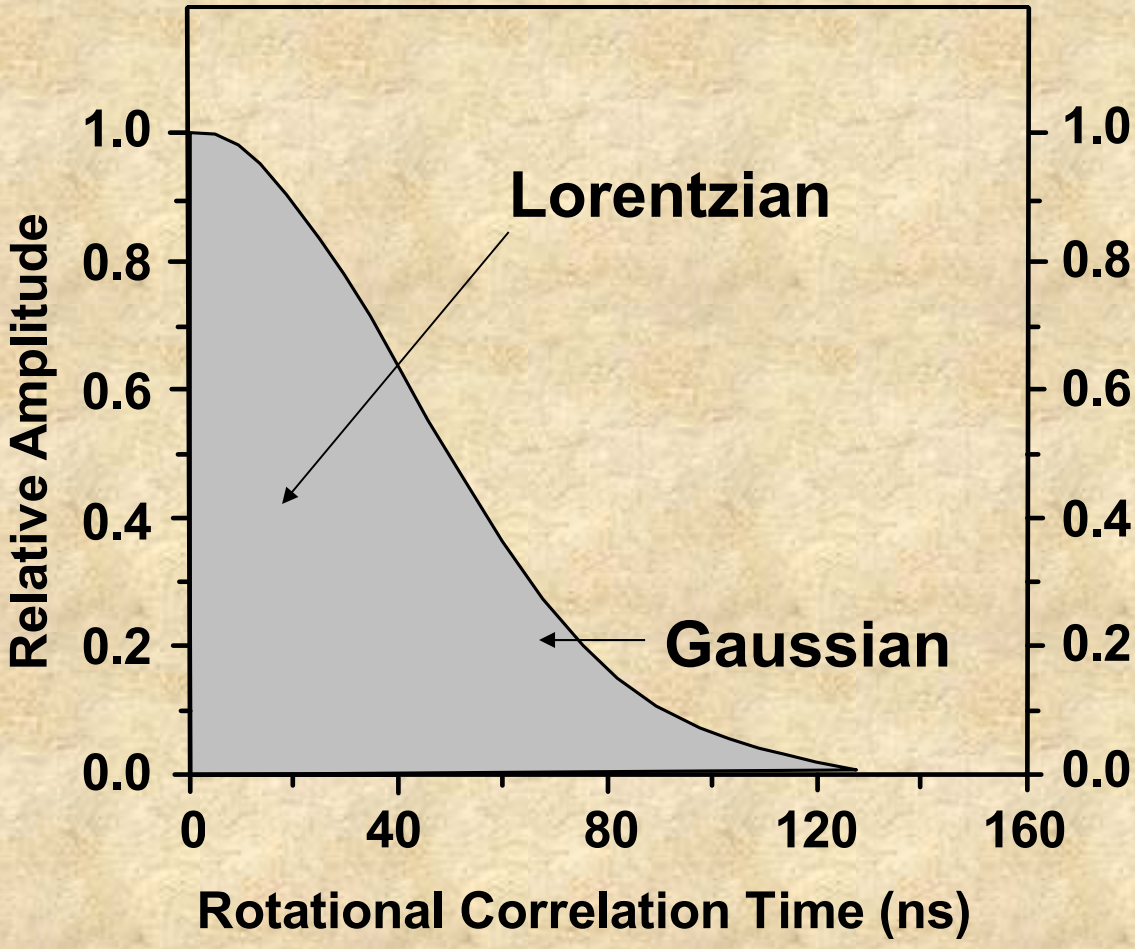


See: Analysis of anisotropy decays in terms of correlation time distributions, measured by frequency-domain fluorometry. Biophys Chem. 1994 Sep;52(1):1-13. Gryczynski I, Johnson ML, Lakowicz JR.

# Quenching

A number of processes can lead to a reduction in fluorescence intensity, i.e., quenching

These processes can occur during the excited state lifetime – for example collisional quenching, energy transfer, charge transfer reactions or photochemistry – or they may occur due to formation of complexes in the ground state

We shall focus our attention on the two quenching processes usually encountered – namely collisional (dynamic) quenching and static (complex formation) quenching

## Collisional Quenching

Collisional quenching occurs when the excited fluorophore experiences contact with an atom or molecule that can facilitate non-radiative transitions to the ground state. Common quenchers include $O_2$, $I^-$, $Cs^+$ and acrylamide.

In the simplest case of collisional quenching, the following relation, called the **Stern-Volmer equation**, holds:

$$F_0/F = 1 + K_{SV}[Q]$$

where $F_0$ and F are the fluorescence intensities observed in the absence and presence, respectively, of quencher, [Q] is the quencher concentration and $K_{SV}$ is the **Stern-Volmer quenching constant**

In the simplest case, then, a plot of F0/F versus [Q] should yield a straight line with a slope equal to $K_{SV}$.

Consider the case of fluorescein quenched by iodide ion ($I^-$).

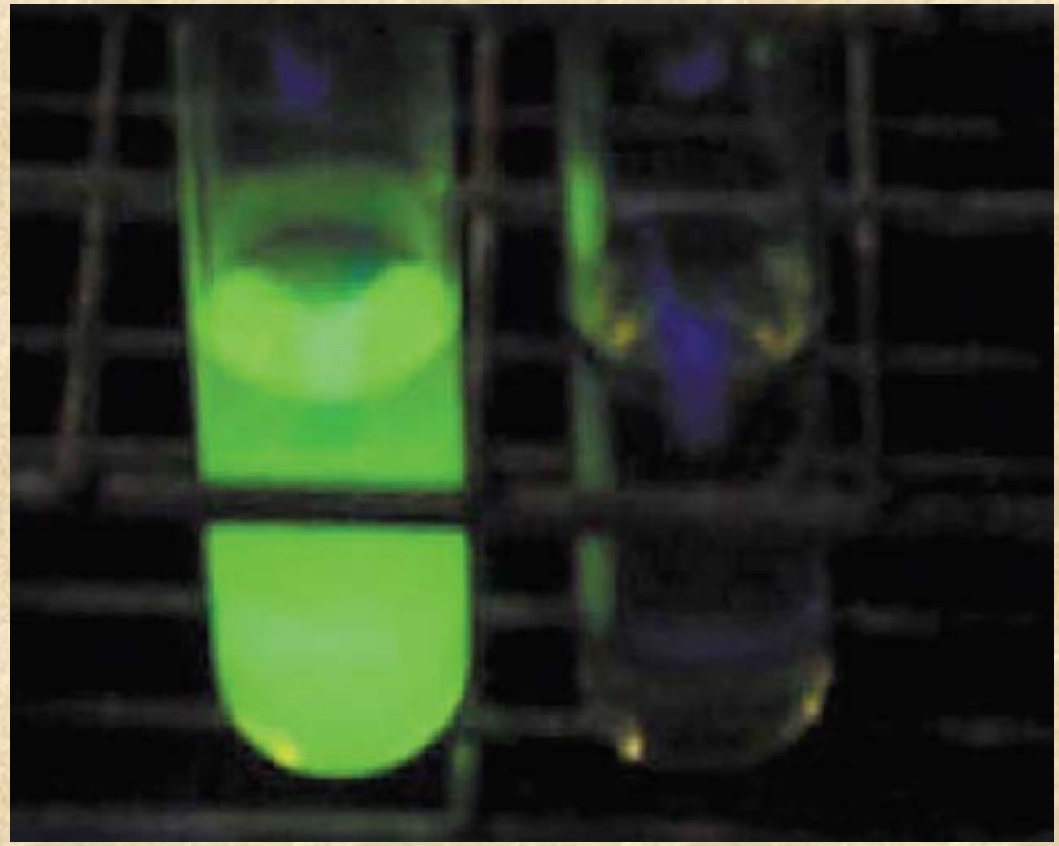

**FIGURE 7.2** Photo of fluorescein solution, illuminated using a UV handlamp, in the absence (left) and presence (right) of potassium iodide. (From Croney et al., 2001. *Bio Chem.* and *Mol. Biol. Ed.* 29:60.)

A Stern-Volmer plot, is shown below for the case of fluorescein quenched by iodide ion ($I^-$).

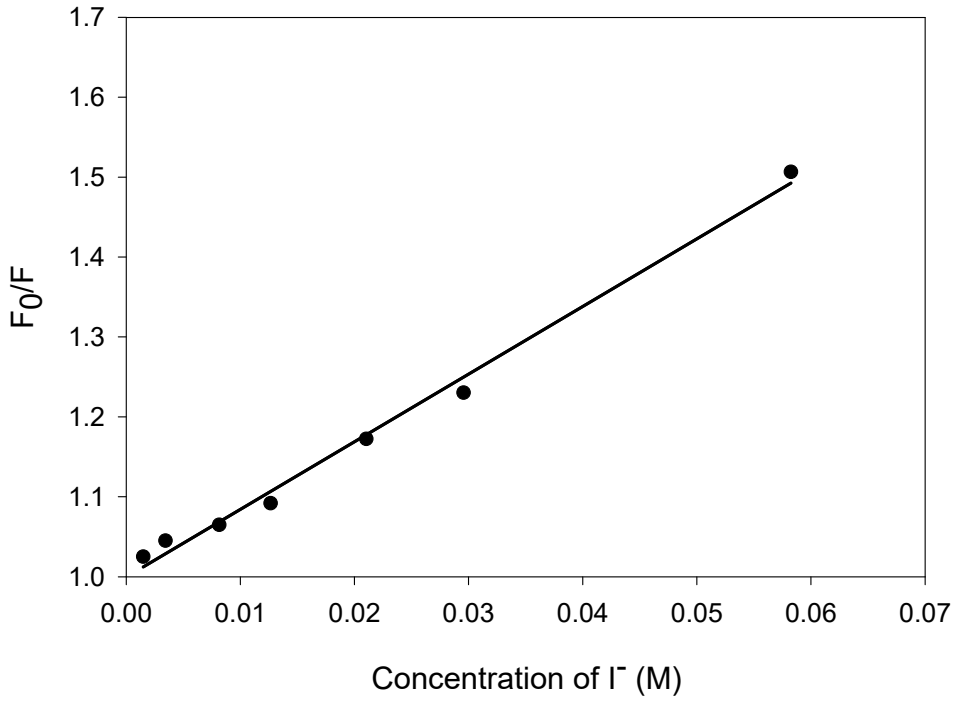


In this case, $K_{SV}$ ~ 8 L-mol$^{-1}$

$K_{SV} = k_q \tau_0$ where **$k_q$ is the bimolecular quenching rate constant** (proportional to the sum of the diffusion coefficients for fluorophore and quencher) and **$\tau_0$ is the excited state lifetime** in the absence of quencher.

In the case of purely collisional quenching, also known as ***dynamic*** quenching,:

$$\mathbf{F_0/F = \tau_0/ \tau.}$$

Hence in this case: $\mathbf{\tau_0/ \tau = 1 + k_q \tau[Q]}$

In the fluorescein/iodide system, $\tau$ = 4ns and $k_q$ ~ 2 x 10$^9$ M$^{-1}$ sec$^{-1}$

Why does dynamic quenching reduce the lifetime?

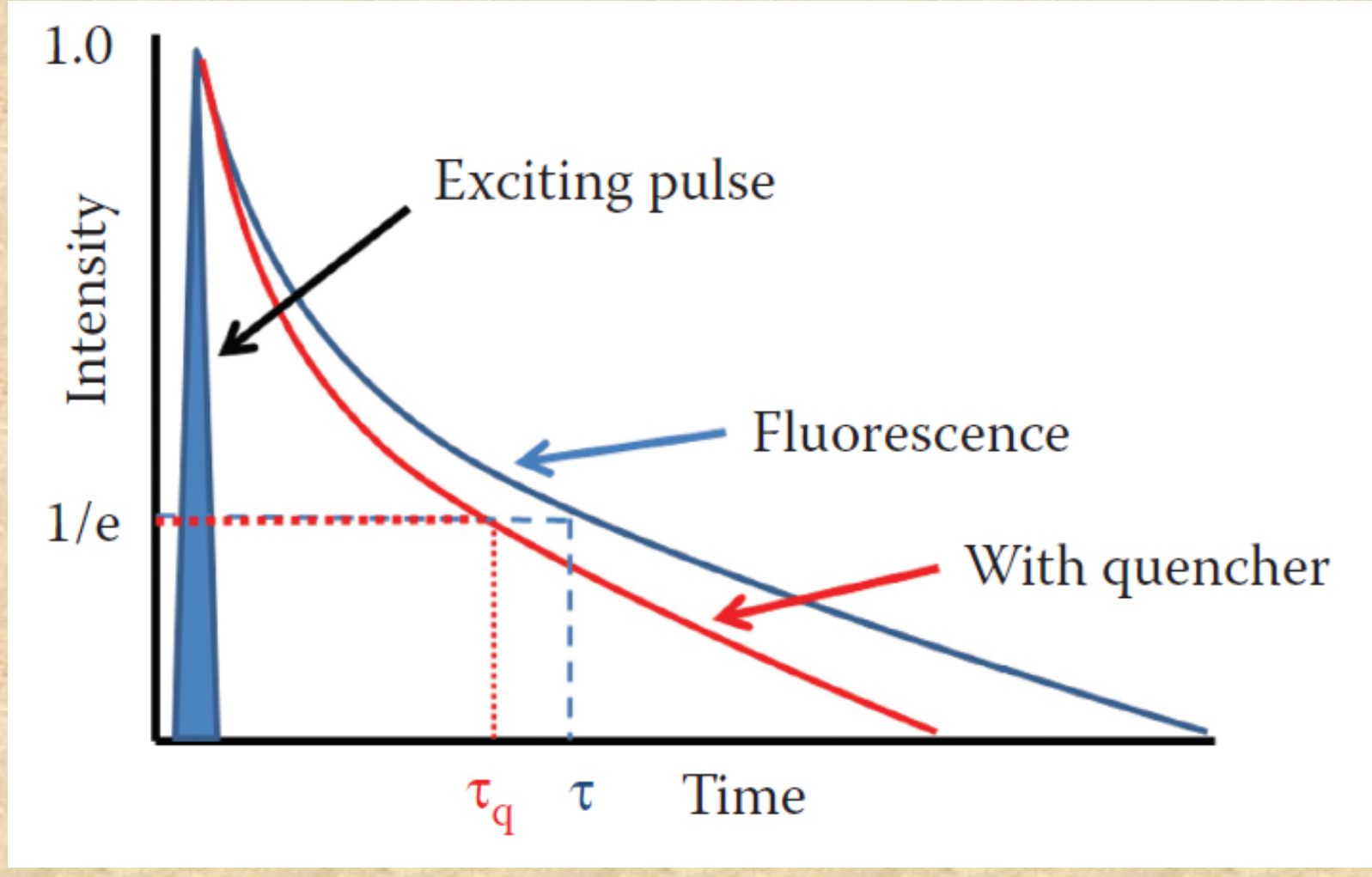

## Static Quenching

In some cases, the fluorophore can form a stable complex with another molecule. If this *ground-state* is non-fluorescent then we say that the fluorophore has been statically quenched.

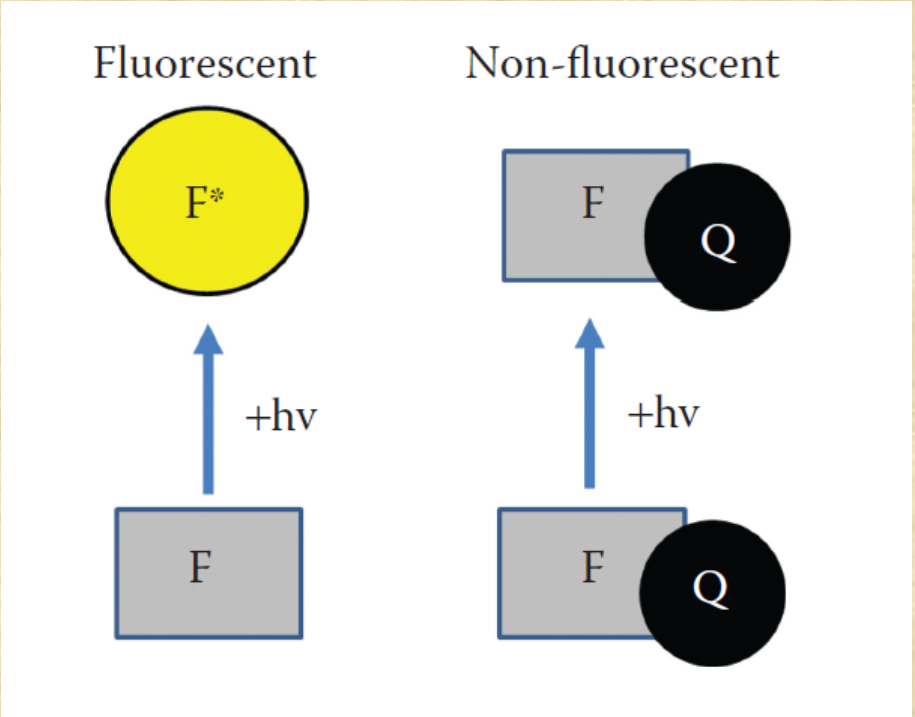


In such a case, the dependence of the fluorescence as a function of the quencher concentration follows the relation:

$$F0/F = 1 + Ka[Q]$$

where Ka is the association constant of the complex. Such cases of quenching via complex formation were first described by Gregorio Weber.

If both static and dynamic quenching are occurring in the sample then the following relation holds:

$$F_0/F = (1 + k_q \tau[Q]) (1 + K_a[Q])$$

In such a case then a plot of $F_0/F$ versus [Q] will give an upward curving plot

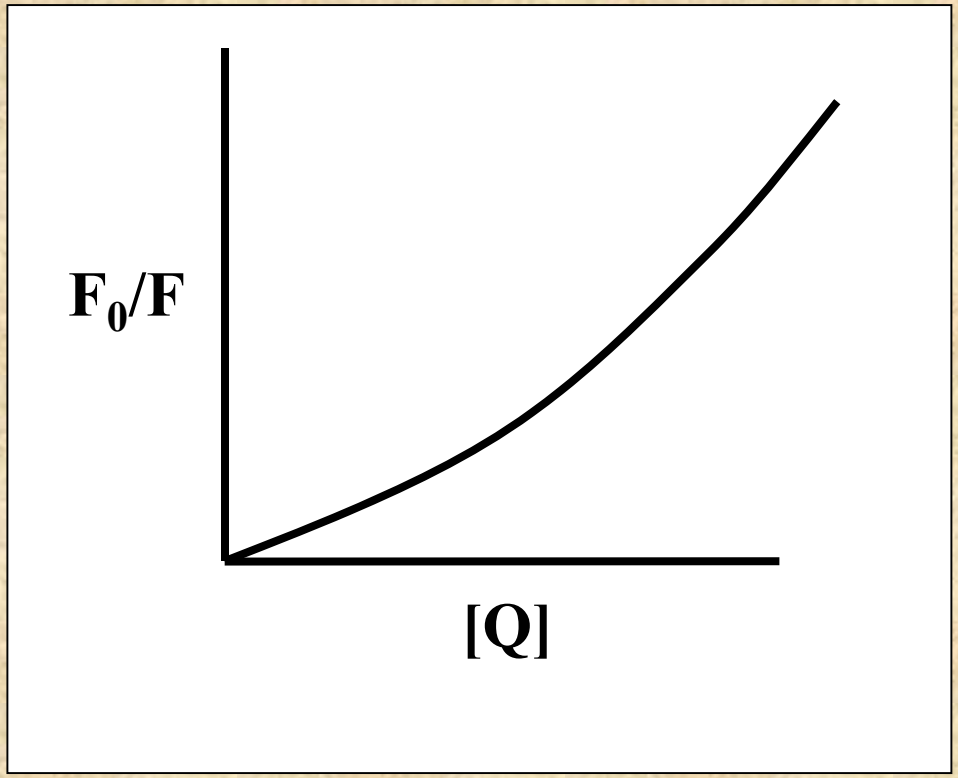


The upward curvature occurs because of the $[Q]^2$ term in the equation

However, since the lifetime is unaffected by the presence of quencher in cases of pure static quenching, a plot of $\tau_0/\tau$ versus [Q] would give a straight line

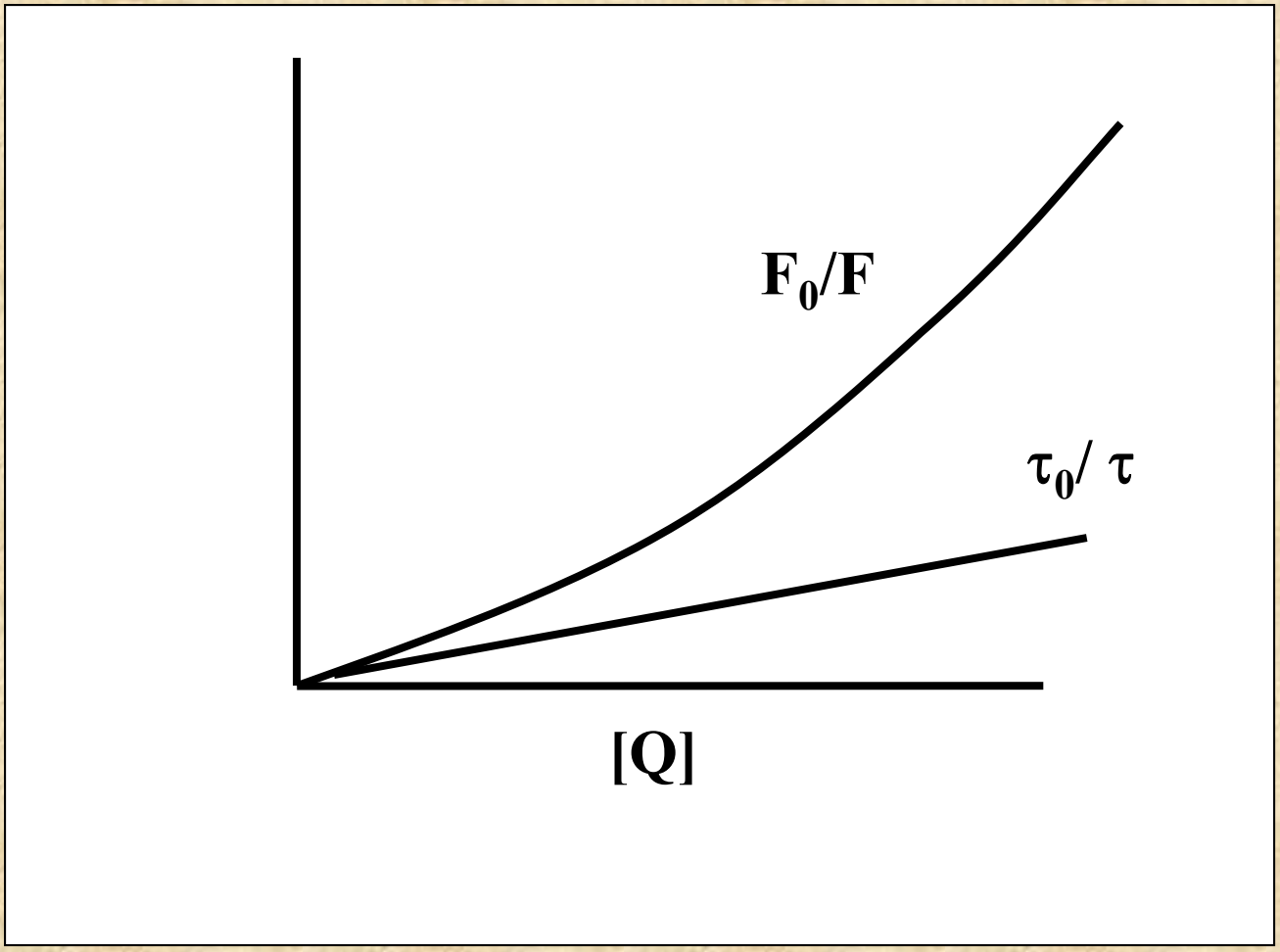

Sometimes you will see the equation for simultaneous static and dynamic quenching given as:

$$F_0/F = (1 + K_{SV}[Q])\mathbf{e}^{\mathbf{V[Q]}}$$

where the term $\mathbf{e}^{\mathbf{V[Q]}}$ is used as a phenomological descriptor of the quenching process. The term V in this equation represents an *active volume* element around the fluorophore such that any quencher within this volume at the time of fluorophore excitation is able to quench the excited fluorophore.

Non-linear Stern-Volmer plots can also occur in the case of purely collisional quenching if some of the fluorophores are less accessible than others. Consider the case of multiple tryptophan residues in a protein – one can easily imagine that some of these residues would be more accessible to quenchers in the solvent than other.

In the extreme case, a Stern-Volmer plot for a system having accessible and inaccessible fluorophores could look like this:

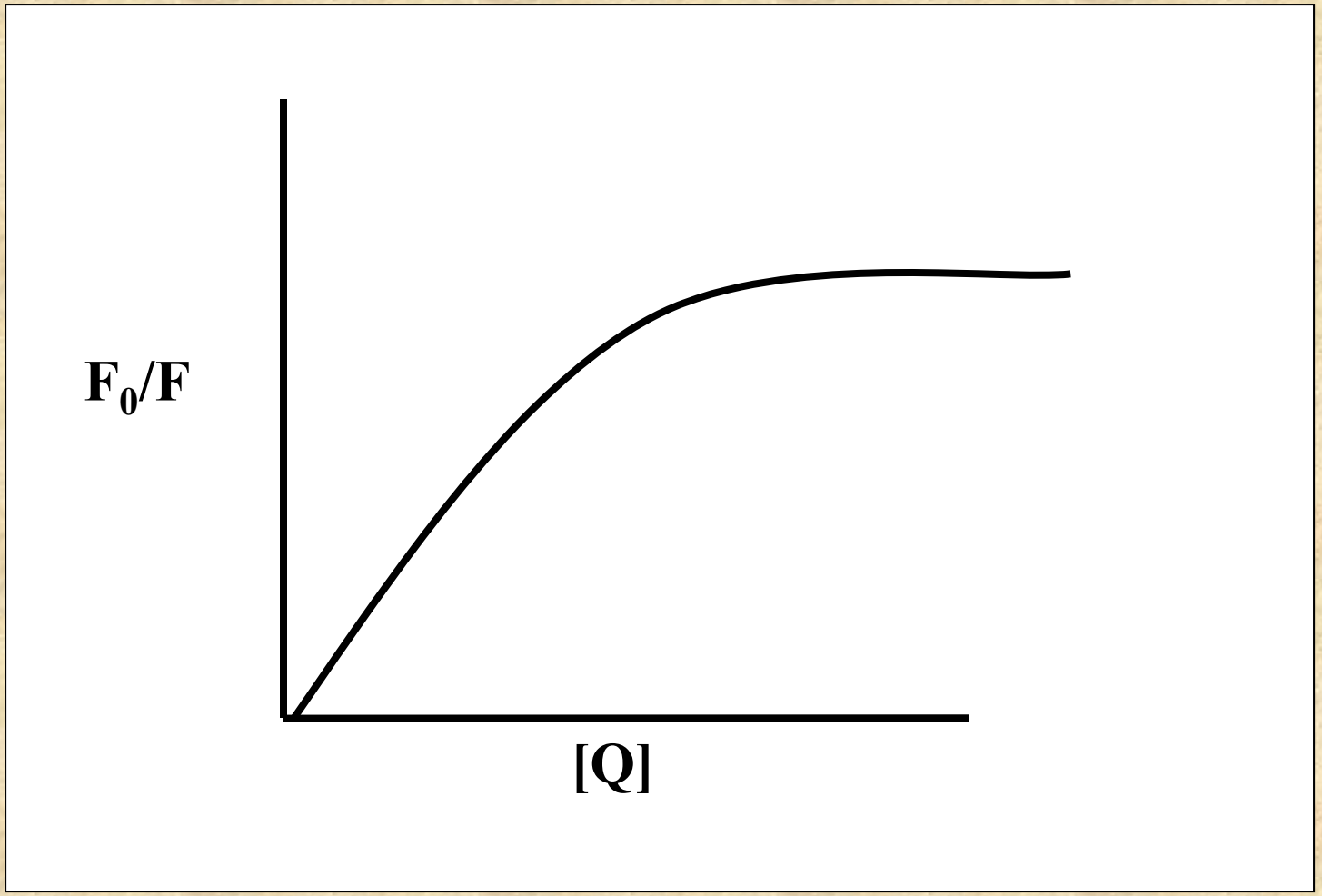

The quenching of LADH intrinsic protein fluorescence by iodide gives, in fact, just such a plot. LADH is a dimer with 2 tryptophan residues per identical monomer. One residue is buried in the protein interior and is relatively inaccessible to iodide while the other tryptophan residue is on the protein's surface and is more accessible.

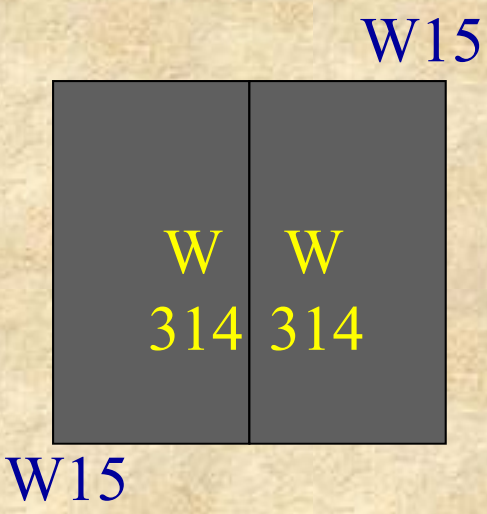


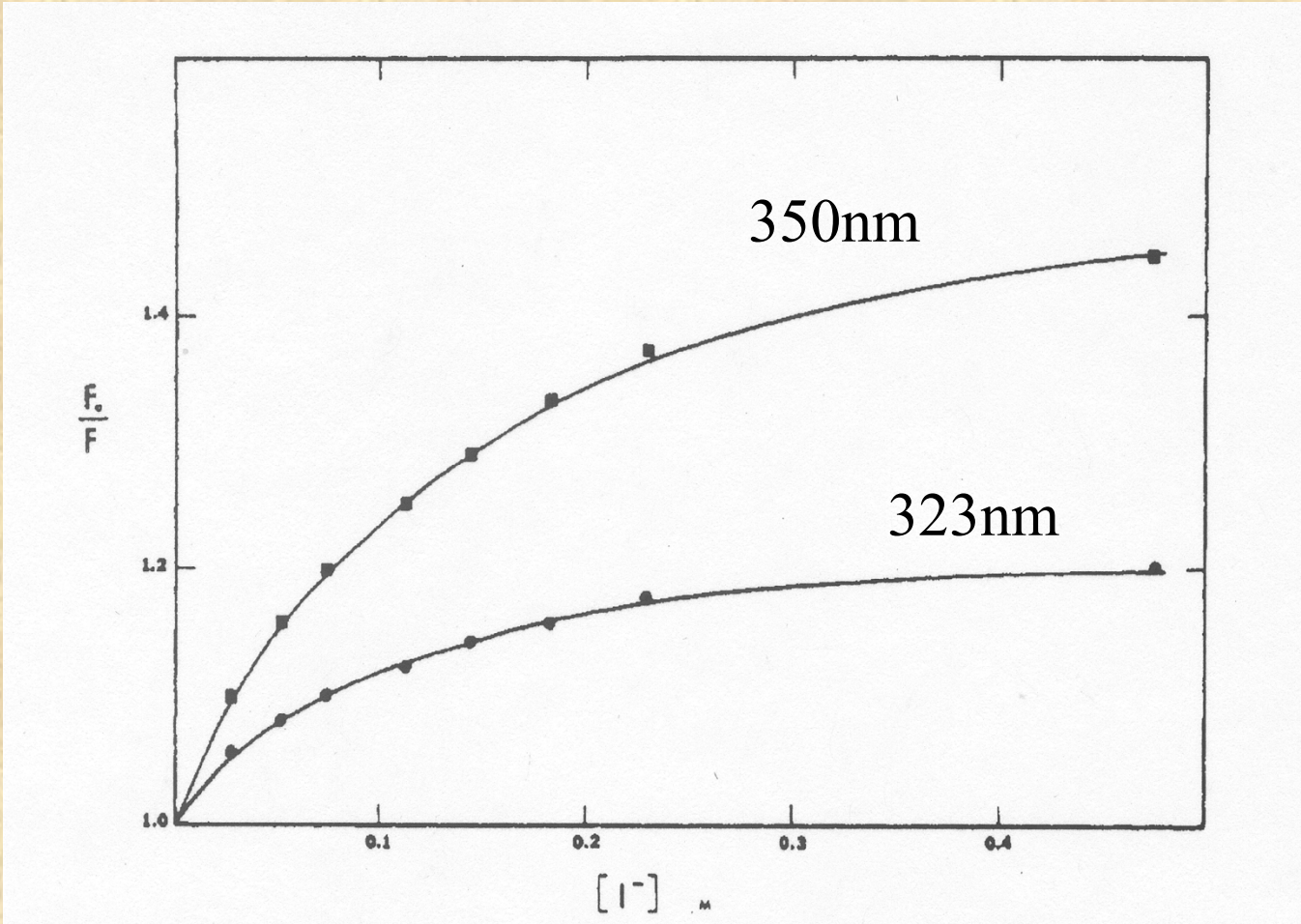


In this case (from Eftink and Selvidge, Biochemistry 1982, 21:117) the different emission wavelengths preferentially weigh the buried (323nm) or solvent exposed (350nm) tryptophans.

Sam Lehrer modified the Stern–Volmer equation to take into account such situations wherein two populations of fluorophores exist—one that is accessible (a) to quencher, and the other that is buried and is not accessible (b). The observed fluorescence is then the fractional fluorescence due to *a*, or *fa*. Rearrangement of the Stern–Volmer equation leads to:

$$F_o/\Delta F = 1/([Q]\, f_a\, K_{SV}) + 1/f_a$$

where $\Delta F$ is the observed decrease in the fluorescence and $K_{SV}$ is the Stern–Volmer quenching constant of the accessible tryptophans. A plot of *F*o/Δ*F* versus1/[*Q*], has a Y-axis intercept of 1/*fa*. In his original work of iodide quenching of lysozyme (which has multiple tryptophan residues), Lehrer showed that for lysozyme in pH 7.5 buffer, *fa* was 0.38 whereas this value increased to unity for lysozyme in 6 M guanidinium chloride.

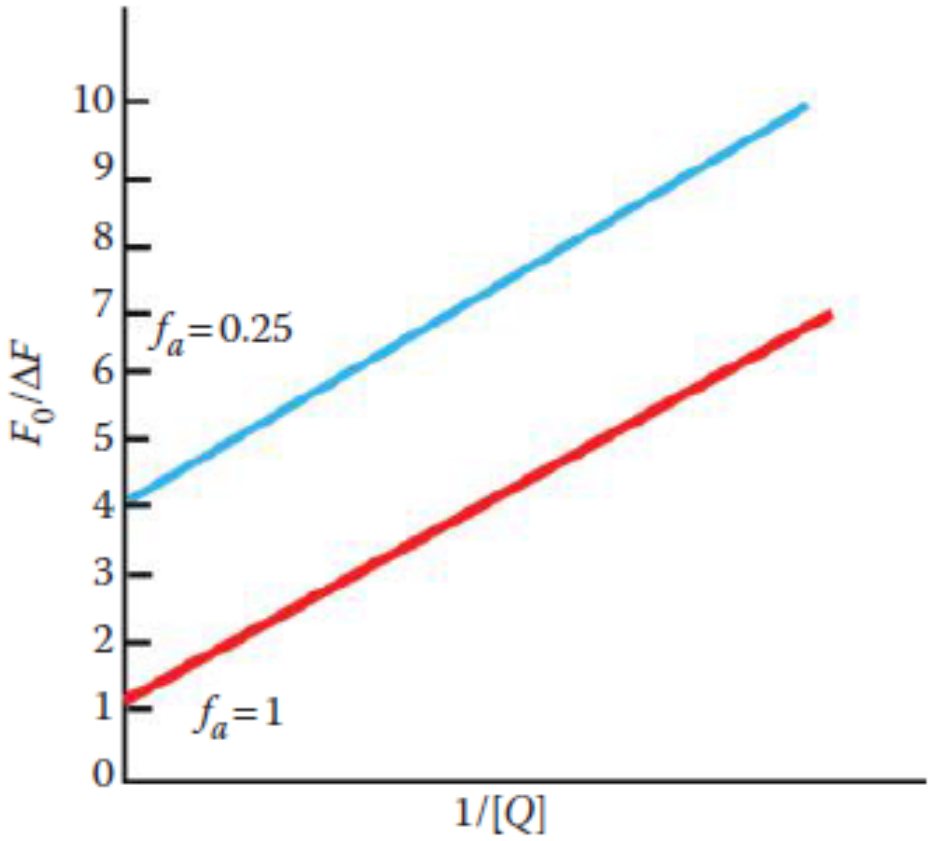


**FIGURE 7.9** Illustration of Lehrer plot for fluorescence quenching for the cases of 100% accessible fluorescence (red) and 25% accessible fluorescence (blue).